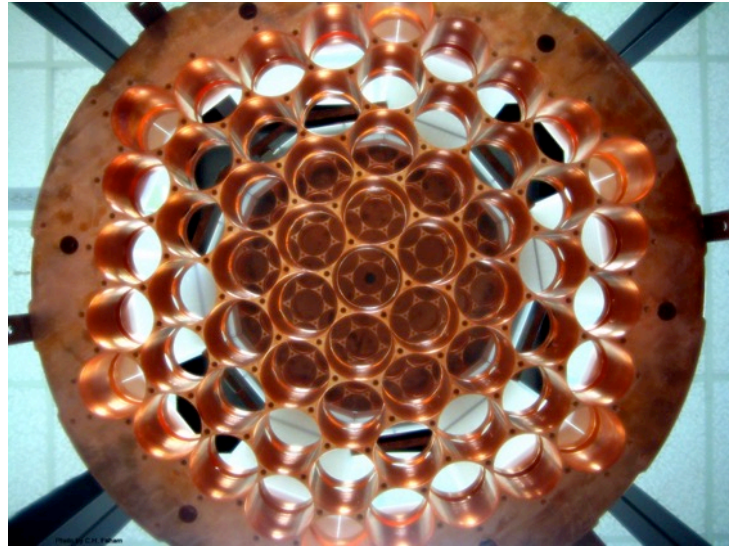


Recent developments in two-phase xenon detector technology



Daniel N. McKinsey

LUX Co-Spokesperson

Professor, University of California, Berkeley

Faculty Senior Scientist, Lawrence Berkeley National Laboratory

Brown Bag Instrumentation Seminar
Lawrence Berkeley National Laboratory
October 12, 2016

Liquified Noble Gases: Basic Properties

Dense and homogeneous

Do not attach electrons, heavier noble gases give high electron mobility

Easy to purify (especially lighter noble gases)

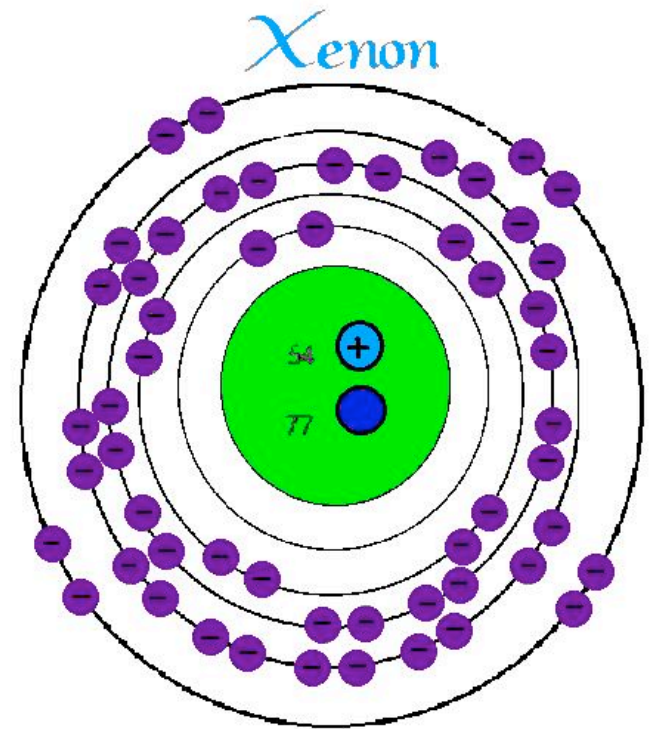
Inert, not flammable, very good dielectrics

Bright scintillators

	Liquid density (g/cc)	Boiling point at 1 bar (K)	Electron mobility (cm ² /Vs)	Scintillation wavelength (nm)	Scintillation yield (photons/MeV)	Long-lived radioactive isotopes	Triplet molecule lifetime (μs)
LHe	0.145	4.2	low	80	19,000	none	13,000,000
LNe	1.2	27.1	low	78	30,000	none	15
LAr	1.4	87.3	400	125	40,000	³⁹ Ar, ⁴² Ar	1.6
LKr	2.4	120	1200	150	25,000	⁸¹ Kr, ⁸⁵ Kr	0.09
LXe	3.0	165	2200	175	42,000	¹³⁶ Xe	0.03

The appeal of liquid xenon

- ✓ Density = 3 g/cc – efficient stopping and capture of gamma rays.
 - Photoabsorption dominates Compton scattering up to 300 keV ($Z = 54$)
 - Strong gamma stopping power: 6 cm attenuation length at 1 MeV
- ✓ High scintillation and ionization yields
 - Bright and fast scintillation yield from gammas: 42 photons / keV; 4 and 27 ns components.
- ✓ Ratio of scintillation and ionization is different for gamma rays versus neutrons
- ✓ High purity attainable
 - Long (> 1 m) electron drift lengths readily achievable
 - Electrons drift at 2 mm / microsecond under ~ 1 kV / cm drift fields
- ✓ 'Easy' cryogenics
 - Detectors typically operate at 178 K and 2 bar pressure.
 - Liquid nitrogen or mechanical coolers



“Emission Detectors”, now usually called “two-phase detectors”

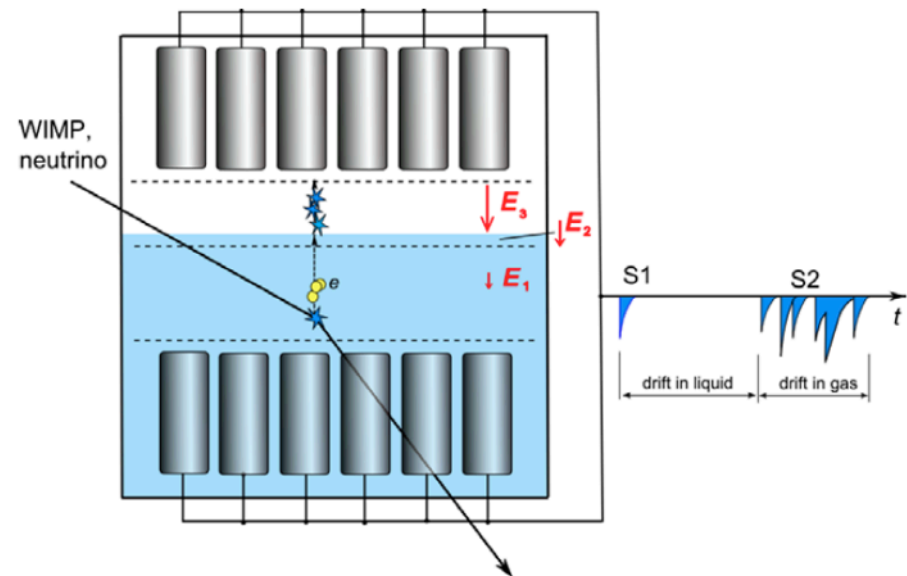
Proposed in B.A. Dolgoshein, V.N. Lebedenko, B.U. Rodionov, JETP Lett. 11 (1970) 513, with subsequent development in the USSR.

The currently favored method of charge detection from a liquid target relies on using electroluminescence to convert the ionization signal into a proportional photon signal in the gas phase.

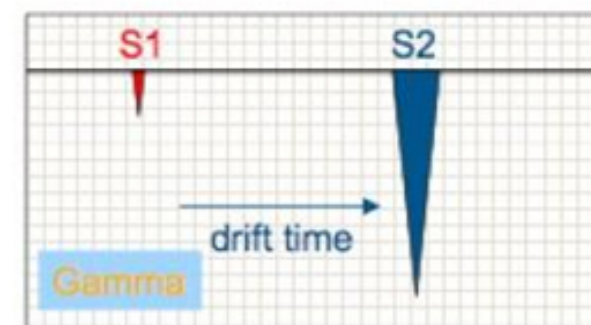
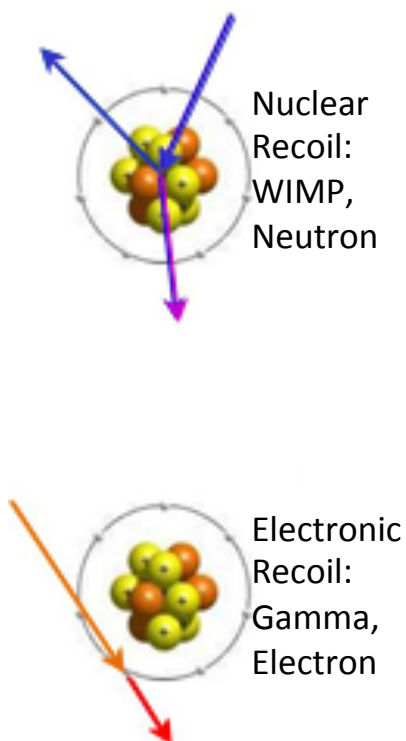
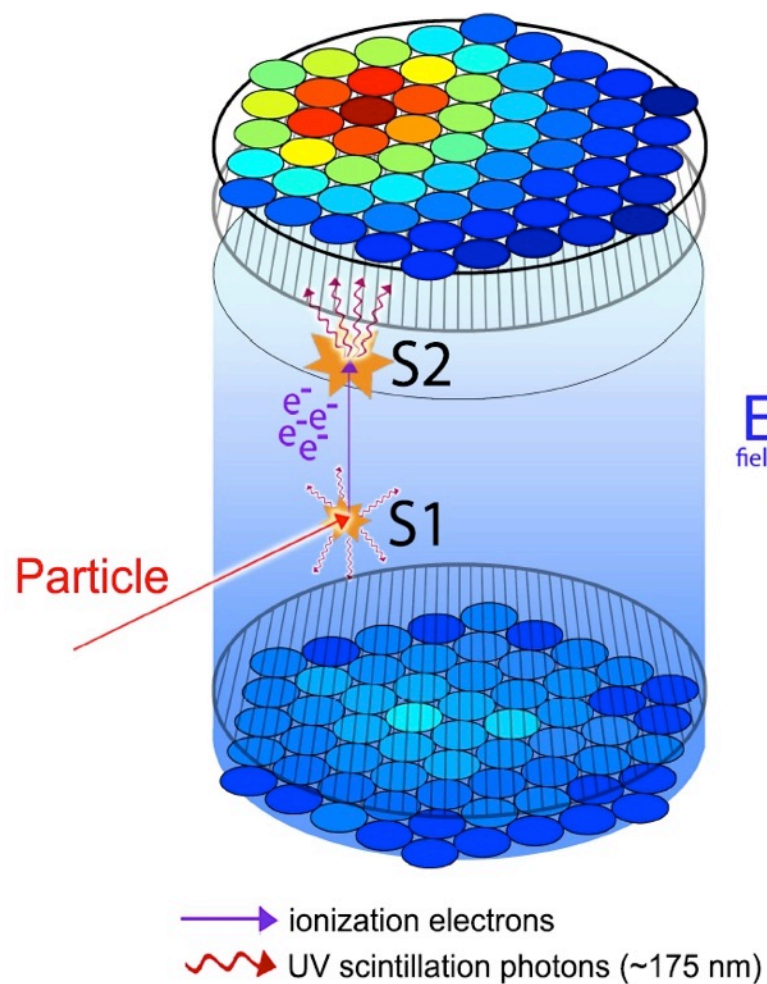
Upon reaching the liquid surface, electrons can be emitted into the gas phase with near unity efficiency at 5 kV/cm liquid field E_2 .

Once in the gas, they are accelerated by the stronger field there, collisionally exciting atoms to produce many VUV photons through secondary scintillation. to be detected with the same array of photon detectors.

Best of both worlds: liquid for target mass, and gas for charge amplification!



Two-Phase Xenon TPCs

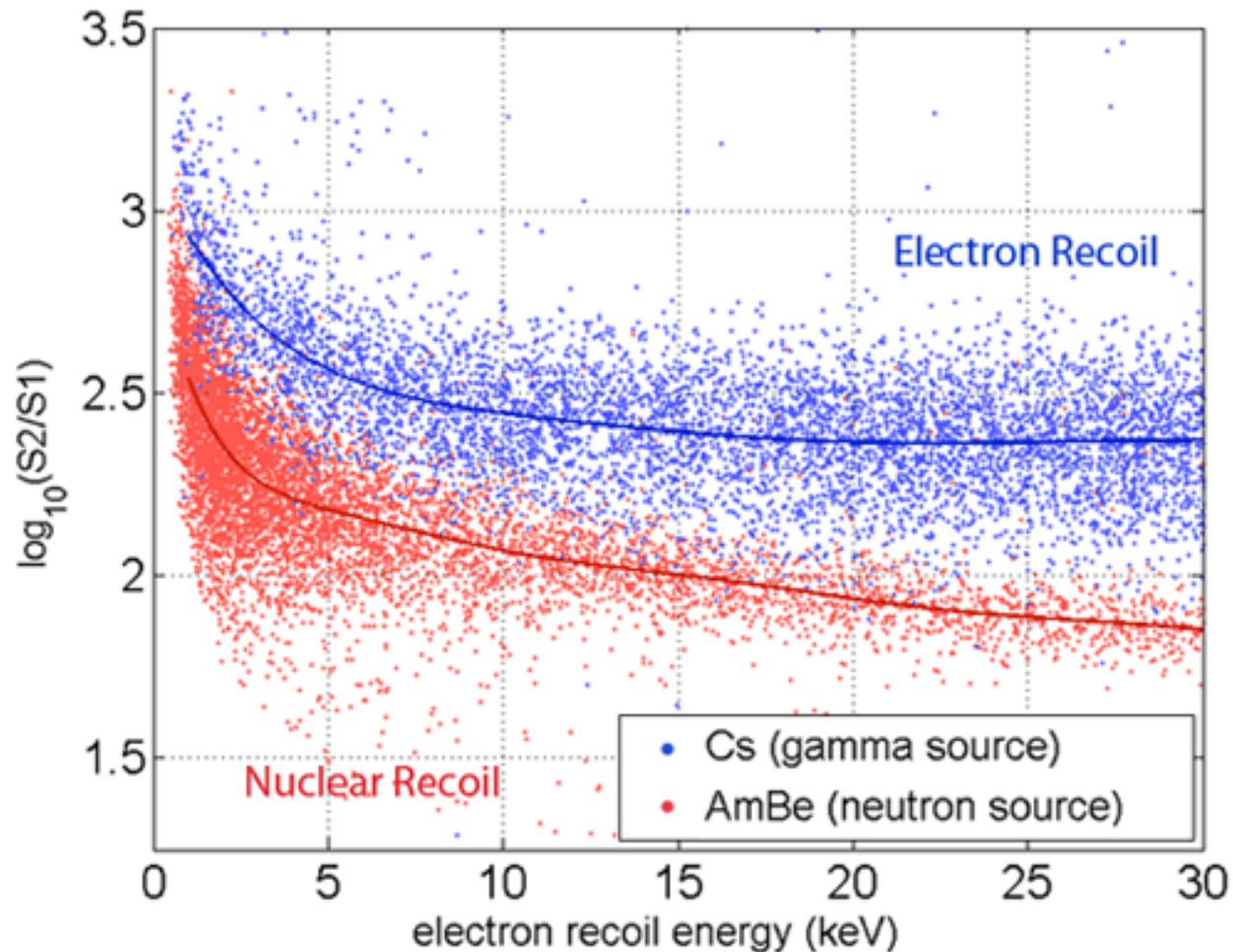


$$(S2/S1)_{\text{wimp}} \ll (S2/S1)_{\text{gamma}}$$

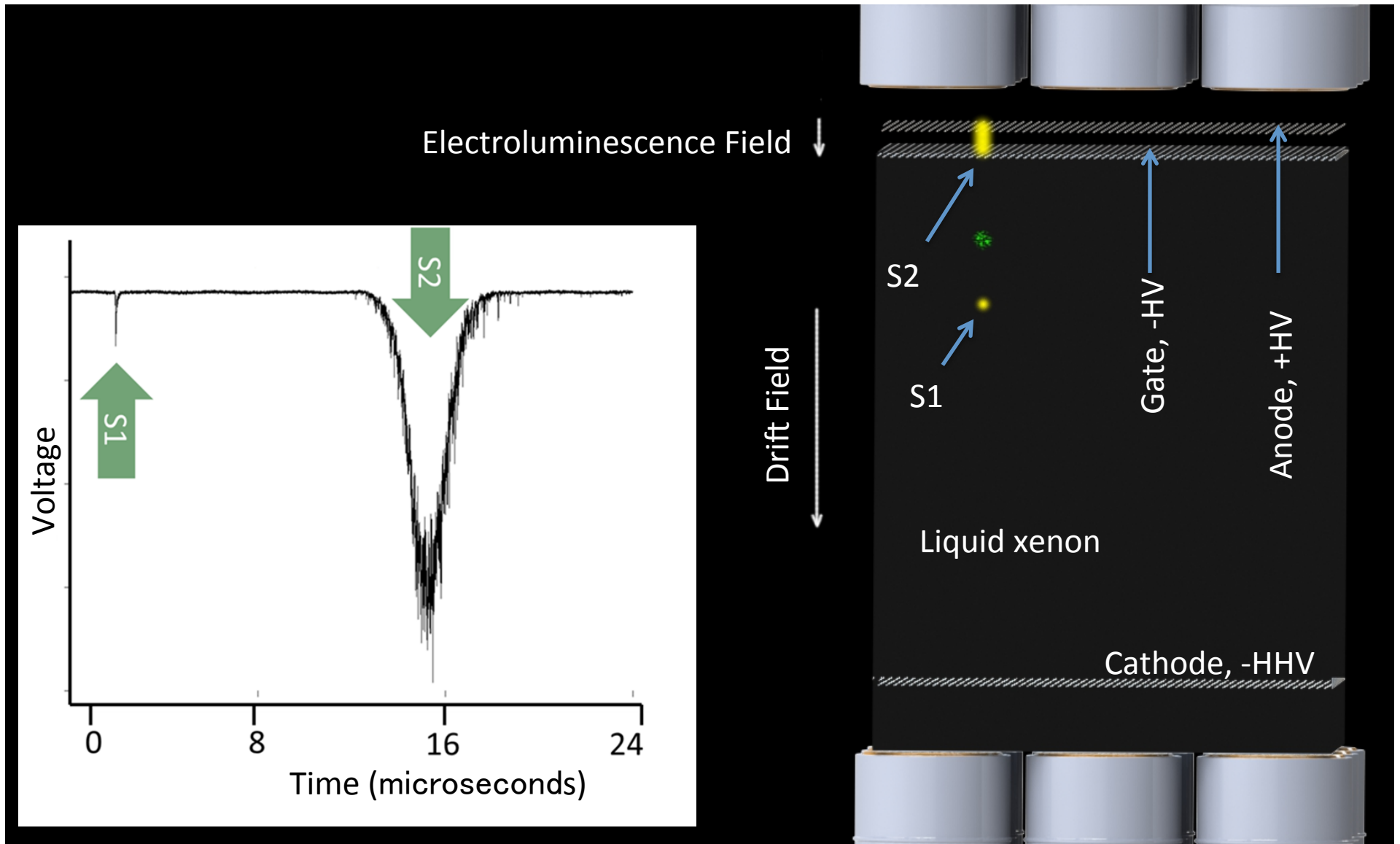


Charge to light ratio gives electron recoil/nuclear recoil discrimination

- ER/NR discrimination + excellent position reconstruction leads to killer application: the direct detection of dark matter with ZEPLIN, XENON, PandaX, LUX, LUX-ZEPLIN experiments.



Two-Phase Xenon TPC Operation



The LUX Collaboration



Brown

Richard Gaitskell	PI, Professor
Simon Fiorucci	Research Associate
Monica Pangilinan	Postdoc
Jeremy Chapman	Graduate Student
David Malling	Graduate Student
James Verbus	Graduate Student
Samuel Chung Chan	Graduate Student
Dongqing Huang	Graduate Student



Case Western

Thomas Shutt	PI, Professor
Dan Akerib	PI, Professor
Karen Gibson	Postdoc
Tomasz Biesiadzinski	Postdoc
Wing H To	Postdoc
Adam Bradley	Graduate Student
Patrick Phelps	Graduate Student
Chang Lee	Graduate Student
Kati Pech	Graduate Student



Imperial College London

Henrique Araujo	PI, Reader
Tim Sumner	Professor
Alastair Currie	Postdoc
Adam Bailey	Graduate Student



Lawrence Berkeley + UC Berkeley

Bob Jacobsen	PI, Professor
Murdock Gilchriese	Senior Scientist
Kevin Lesko	Senior Scientist
Carlos Hernandez Faham	Postdoc
Victor Gehman	Scientist
Mia Ihm	Graduate Student



Lawrence Livermore

Adam Bernstein	PI, Leader of Adv. Detectors Group
Dennis Carr	Mechanical Technician
Kareem Kazkaz	Staff Physicist
Peter Sorensen	Staff Physicist
John Bower	Engineer



LIP Coimbra

Isabel Lopes	PI, Professor
Jose Pinto da Cunha	Assistant Professor
Vladimir Solovov	Senior Researcher
Luiz de Viveiros	Postdoc
Alexander Lindote	Postdoc
Francisco Neves	Postdoc
Claudio Silva	Postdoc



SD School of Mines

Xinhua Bai	PI, Professor
Tyler Liebsch	Graduate Student
Doug Tiedt	Graduate Student



SDSTA

David Taylor	Project Engineer
Mark Hanhardt	Support Scientist



Texas A&M

James White †	PI, Professor
Robert Webb	PI, Professor
Rachel Mannino	Graduate Student
Clement Sofka	Graduate Student



UC Davis

Mani Tripathi	PI, Professor
Bob Svoboda	Professor
Richard Lander	Professor
Britt Holbrook	Senior Engineer
John Thomson	Senior Machinist
Ray Gerhard	Electronics Engineer
Aaron Manalaysay	Postdoc
Matthew Szydagis	Postdoc
Richard Ott	Postdoc
Jeremy Mock	Graduate Student
James Morad	Graduate Student
Nick Walsh	Graduate Student
Michael Woods	Graduate Student
Sergey Uvarov	Graduate Student
Brian Lenardo	Graduate Student



UC Santa Barbara

Harry Nelson	PI, Professor
Mike Witherell	Professor
Dean White	Engineer
Susanne Kyre	Engineer
Carmen Carmona	Postdoc
Curt Nehrhorn	Graduate Student
Scott Haselschwardt	Graduate Student



University College London

Chamkaur Ghag	PI, Lecturer
Lea Reichhart	Postdoc



Collaboration Meeting,
Sanford Lab, April
2013



University of Edinburgh

Alex Murphy	PI, Reader
Paolo Beltrame	Research Fellow
James Dobson	Postdoc



University of Maryland

Carter Hall	PI, Professor
Attila Dobi	Graduate Student
Richard Knoche	Graduate Student
Jon Balajthy	Graduate Student



University of Rochester

Frank Wolfs	PI, Professor
Wojtek Skutski	Senior Scientist
Eryk Druszkiewicz	Graduate Student
Mongkol Moongweluwan	Graduate Student



University of South Dakota

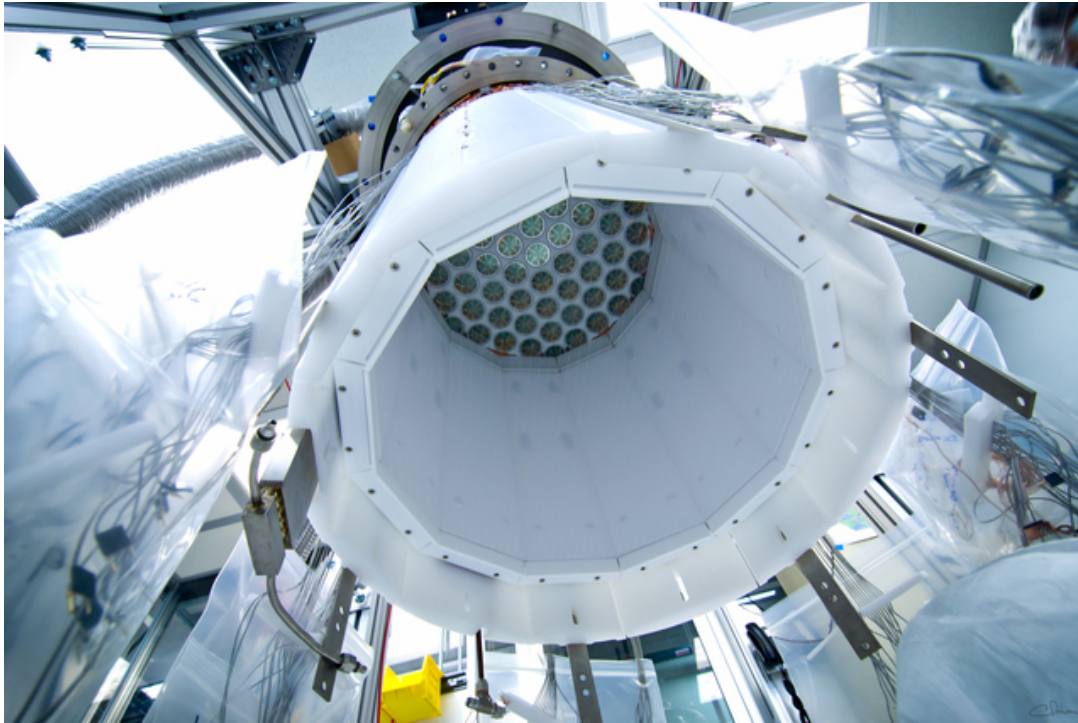
Dongming Mei	PI, Professor
Chao Zhang	Postdoc
Angela Chiller	Graduate Student
Chris Chiller	Graduate Student
Dana Byram	*Now at SDSTA



Yale -> UC Berkeley

Daniel McKinsey	PI, Professor
Peter Parker	Professor
Sidney Cahn	Lecturer/Research Scientist
Ethan Bernard	Postdoc
Markus Horn	Postdoc
Blair Edwards	Postdoc
Scott Hertel	Postdoc
Kevin O'Sullivan	Postdoc
Nicole Larsen	Graduate Student
Evan Pease	Graduate Student
Brian Tennyson	Graduate Student
Ariana Hackenburg	Graduate Student
Elizabeth Boulton	Graduate Student

Xenon for Physics – The LUX Detector

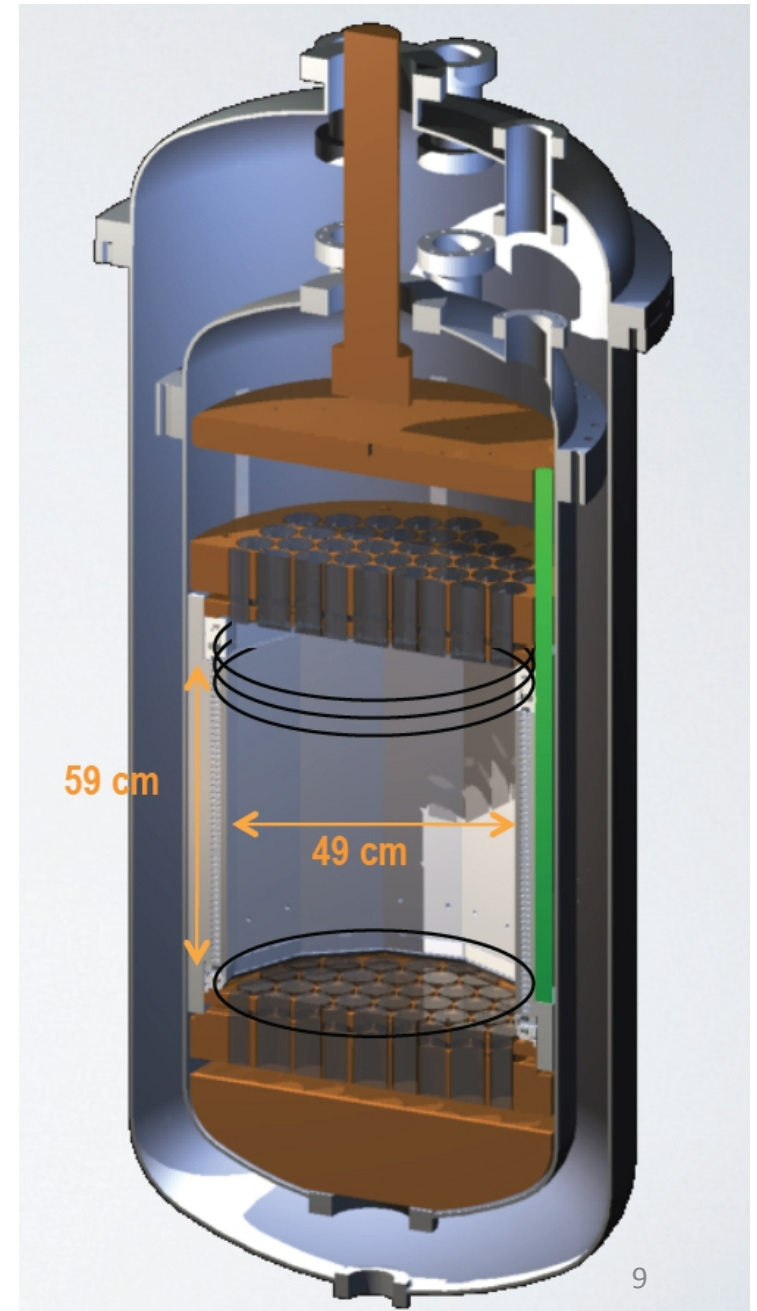


Searches for extremely rare “WIMP” dark matter particle interactions.

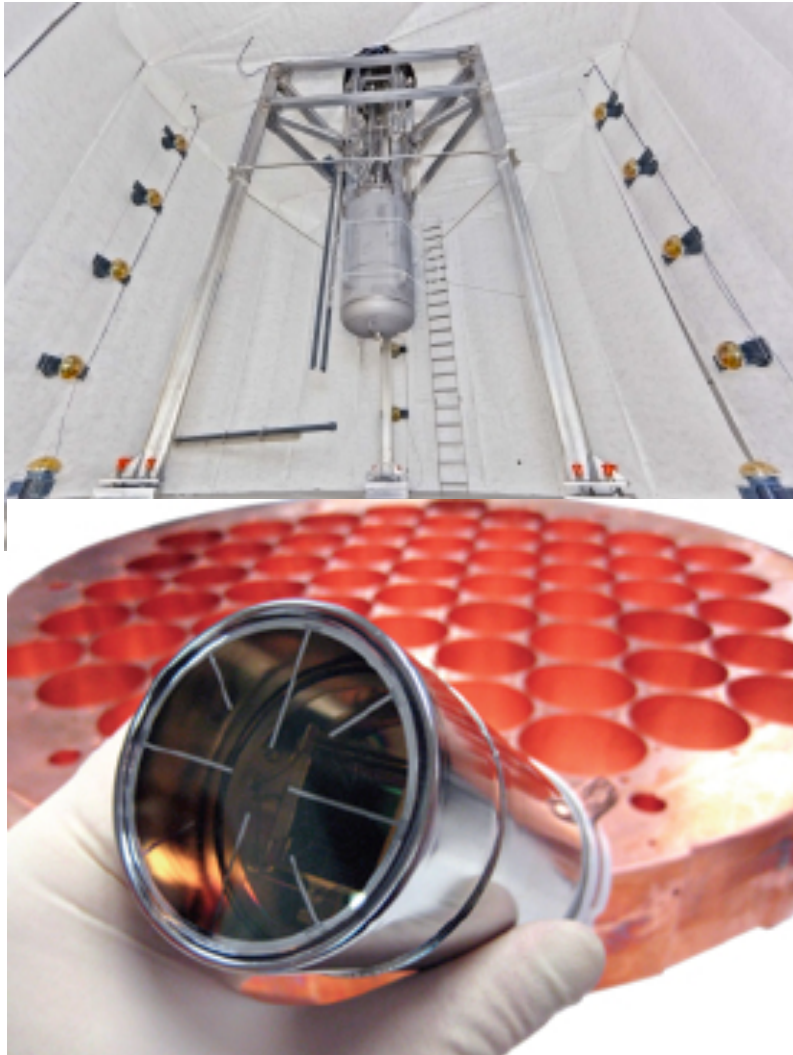
Deployed inside a large water tank at the Sanford Underground Laboratory, 4850 foot depth.

Currently the most sensitive WIMP detector, for masses above 4 GeV.

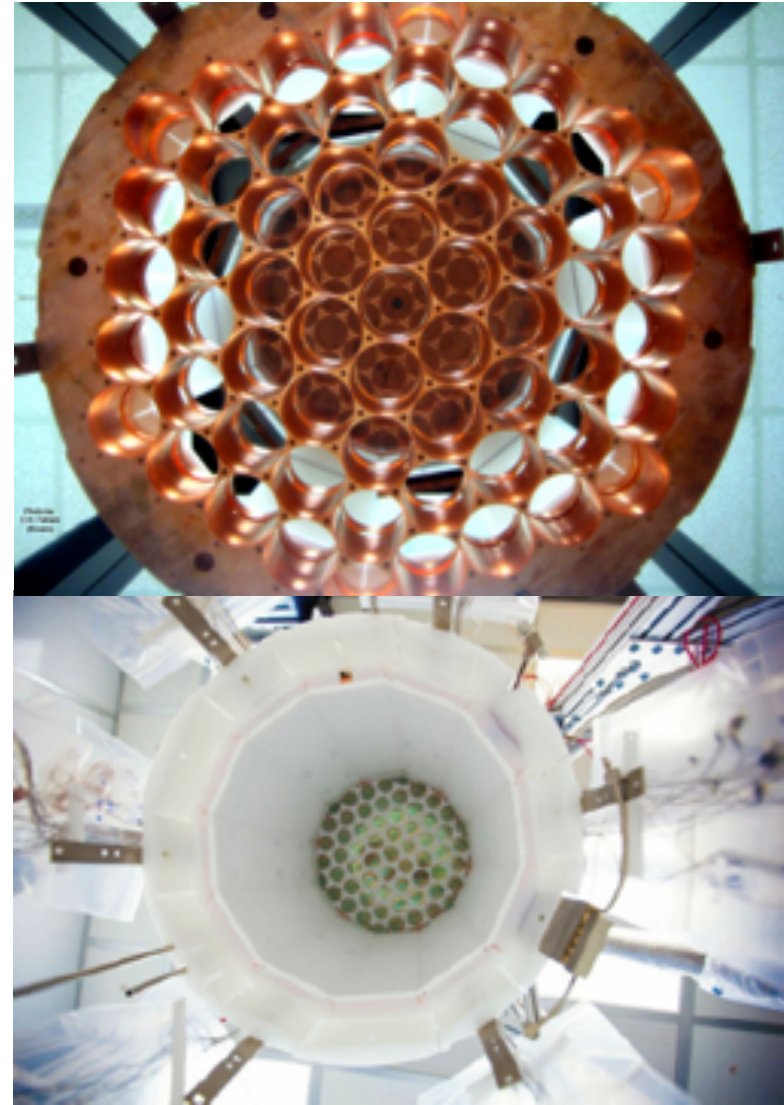
Energy threshold < 1 keV within 350 kg of xenon.



LUX – the Instrument



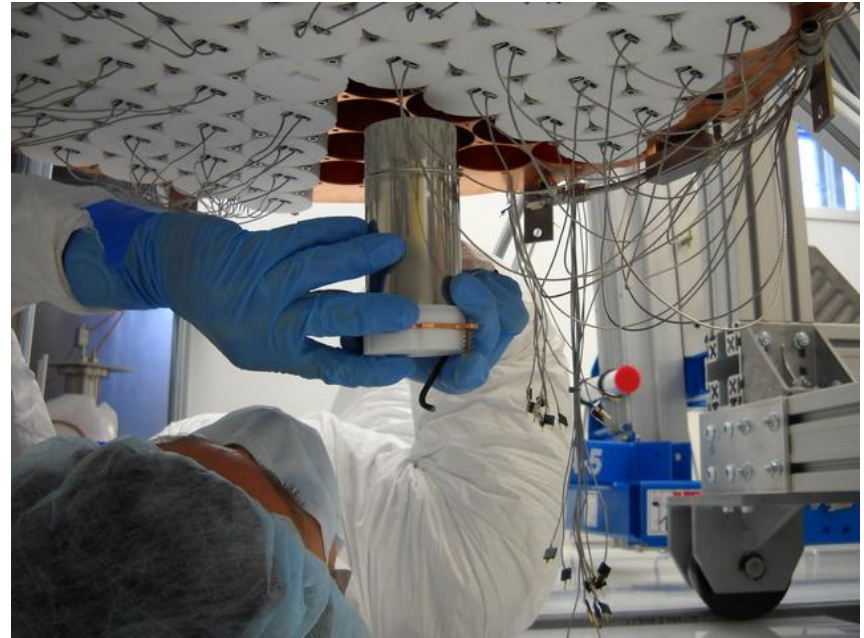
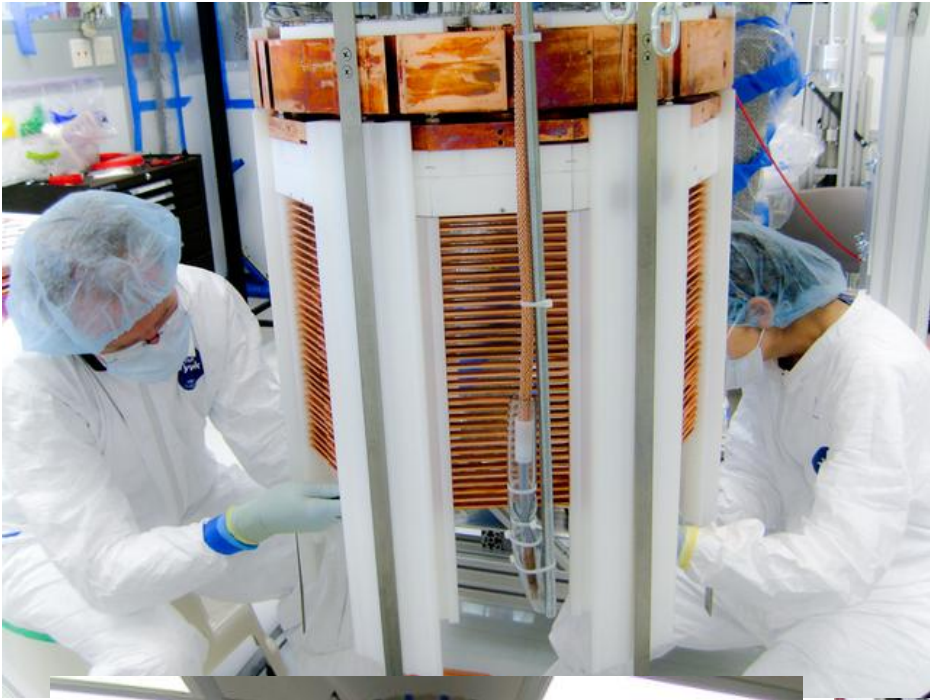
10/12/16



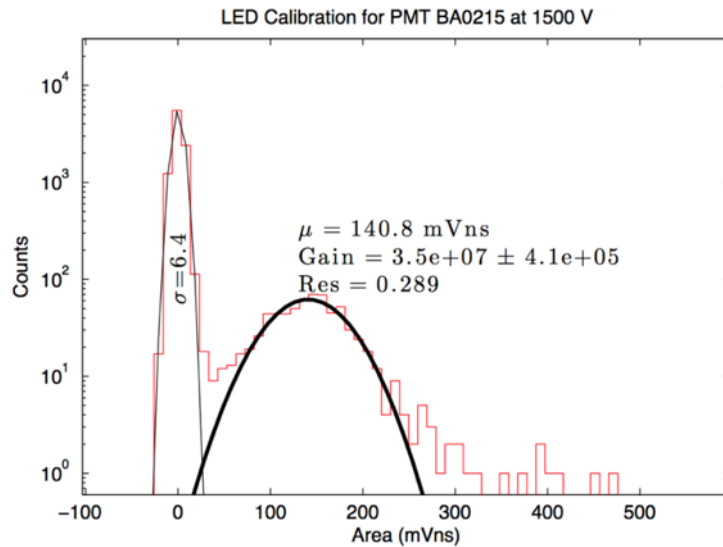
D. McKinsey

10

Construction

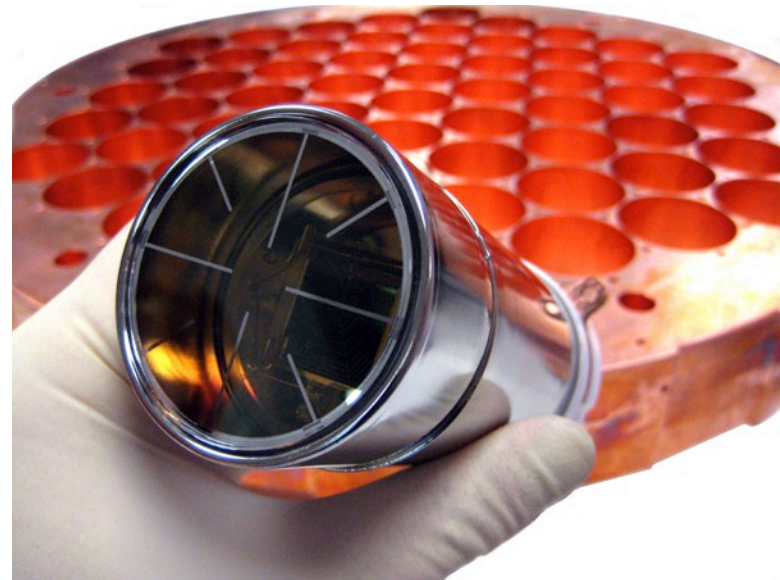


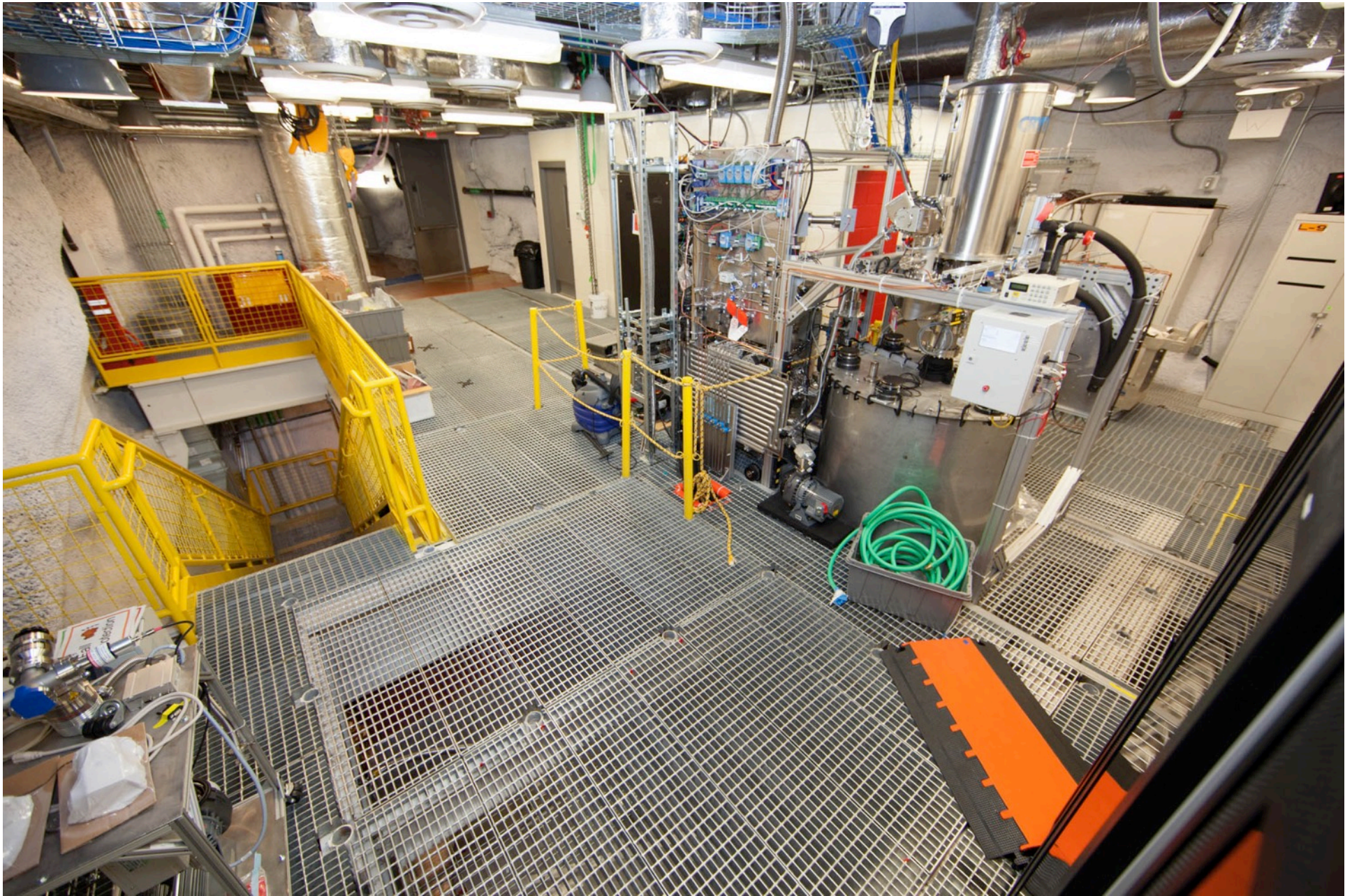
Hamamatsu R8778 PMTs (used in LUX)



- Extremely low radioactivity:
 - $< 9.5 \text{ mBq } ^{238}\text{U} / \text{PMT}$
 - $< 2.7 \text{ mBq } ^{232}\text{Th} / \text{PMT}$
 - $< 66 \text{ mBq } ^{40}\text{K} / \text{PMT}$
- 33% quantum efficiency; 90% collection efficiency
- Gain = 3.3×10^6

- 2" diameter provides high surface area coverage
- Efficient detection of 178 nm light
- Operates in the LXe temperature range (165 - 180 K)





10/12/16

D. McKinsey

13

LUX installed in its water tank shield, a mile underground at SURF



10/12/16

D. McKinsey

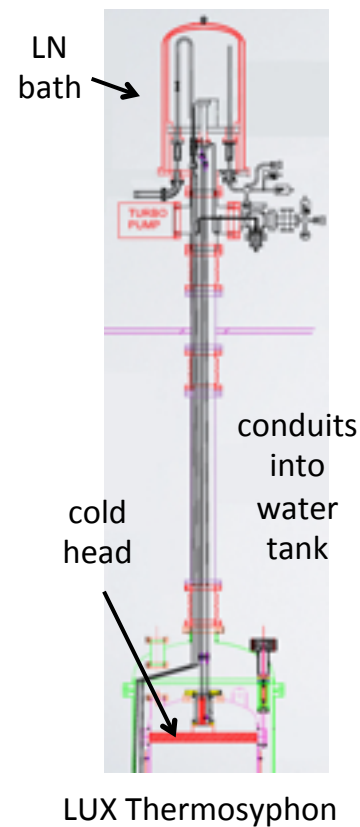
14

LUX – Supporting Systems

Xenon gas handling and sampling



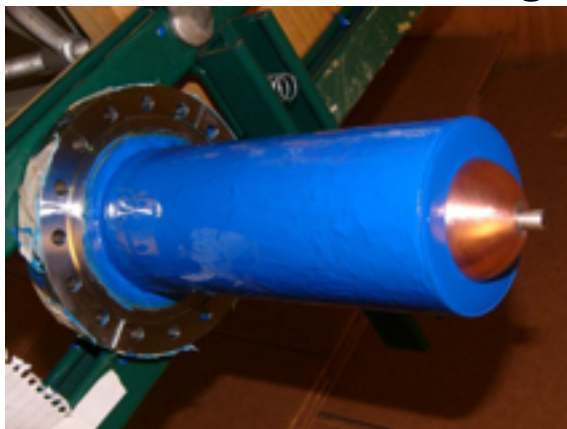
Thermosyphon cryogenics



Xe storage and recovery

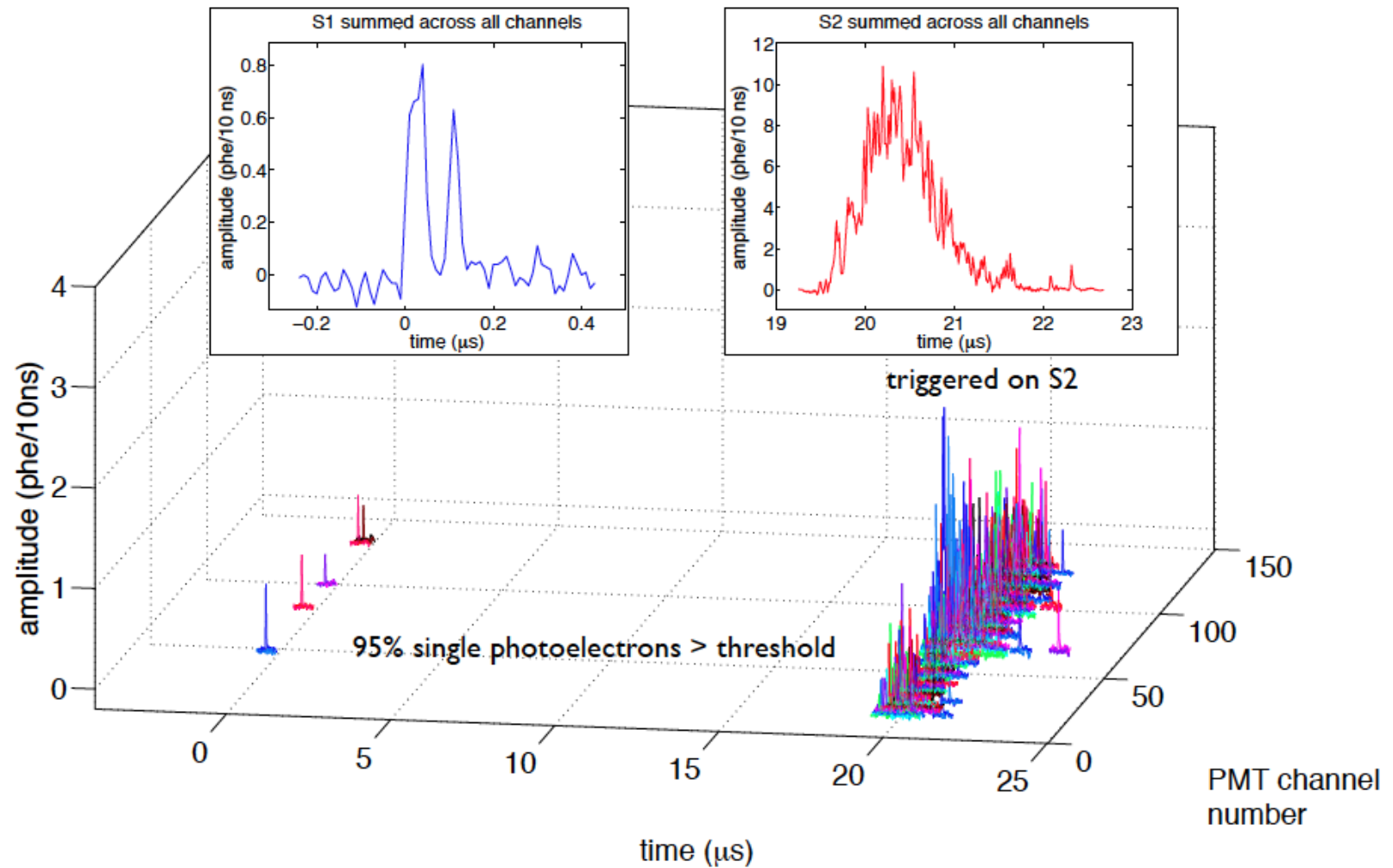


Cathode HV feedthrough



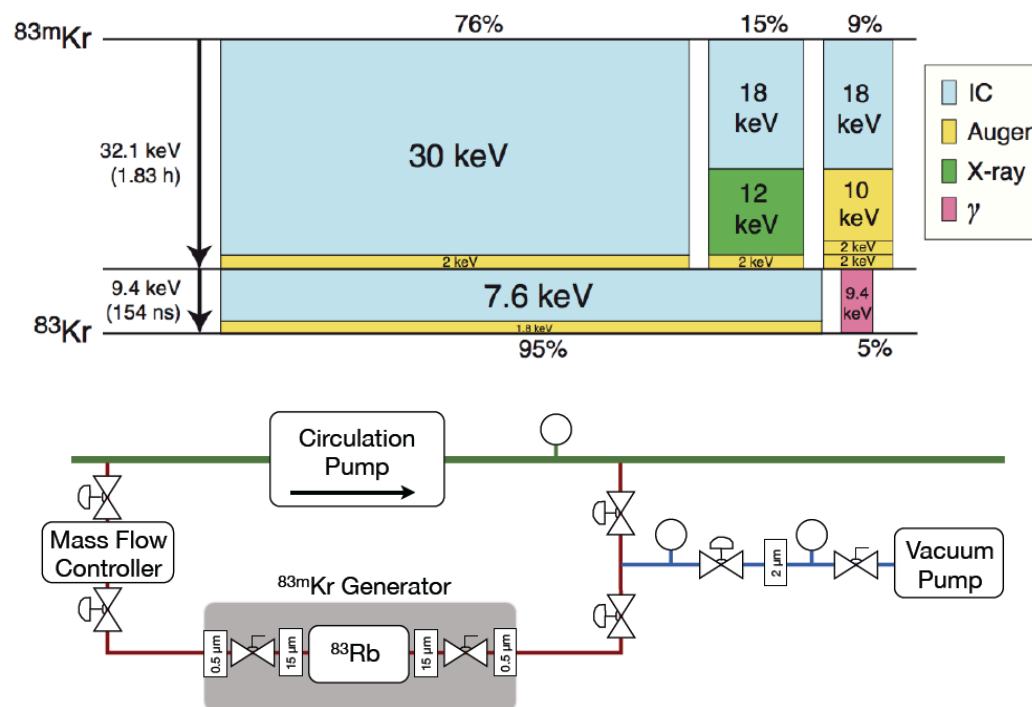
Typical Event in LUX

1.5 keV gamma ray scattering event



Kr-83m Calibration

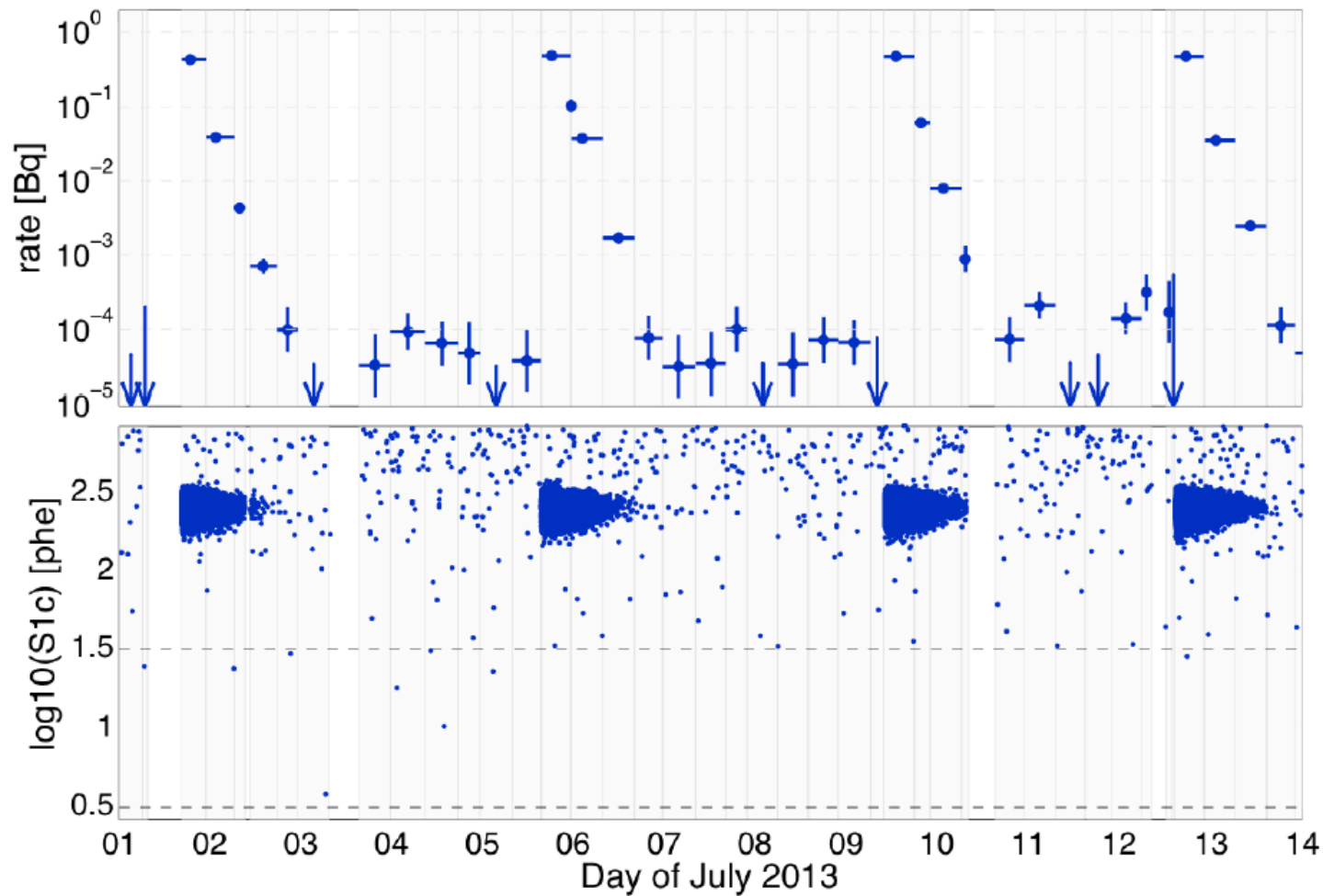
- Rb-83 produces Kr-83m when it decays; this krypton gas can then be flushed into the LUX gas system to calibrate the detector as a function of position.
- Provides reliable, efficient, homogeneous calibration of both S1 and S2 signals, which then decays away in a few hours, restoring low-background operation.
- First used in liquid nobles by the McKinsey group:
 - see L. Kastens et al, Phys. Rev. C **80**, 045809 (2009) and Journal of Instrumentation **5**, P05006



Kr-83m source (Rb-83 coated on charcoal, within xenon gas plumbing)



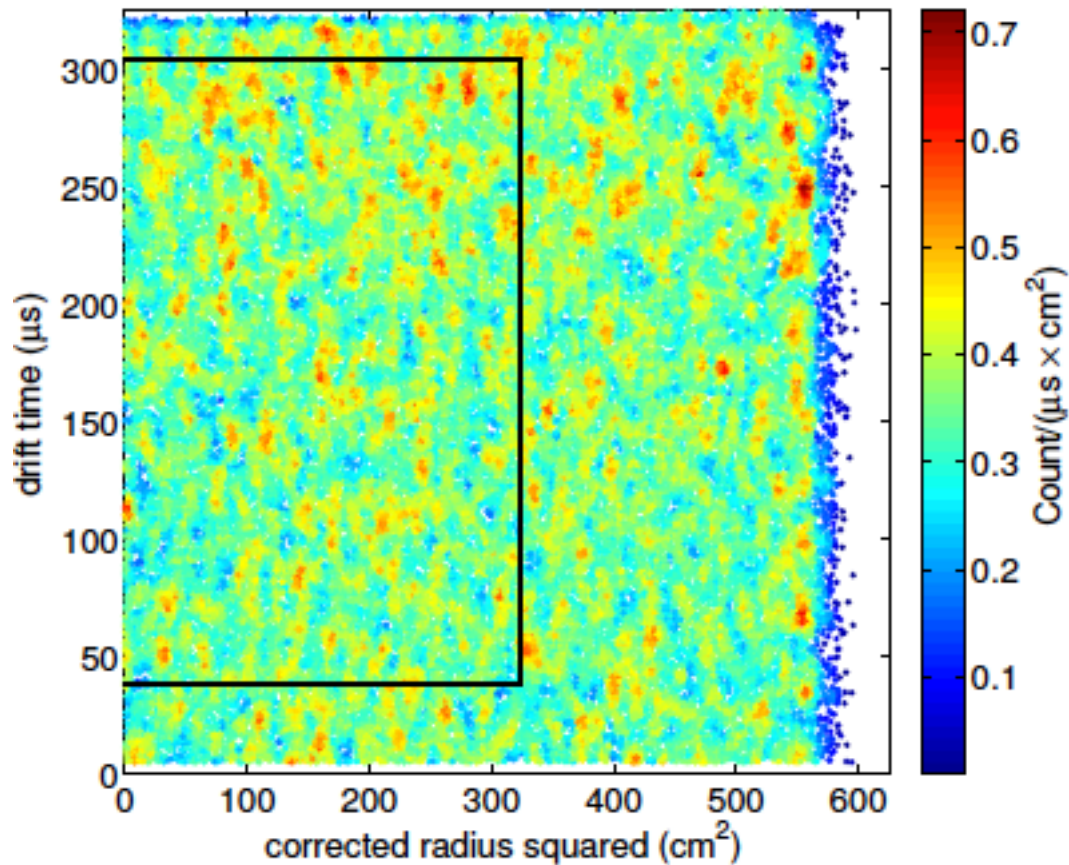
Repeated, frequent use of Kr-83m



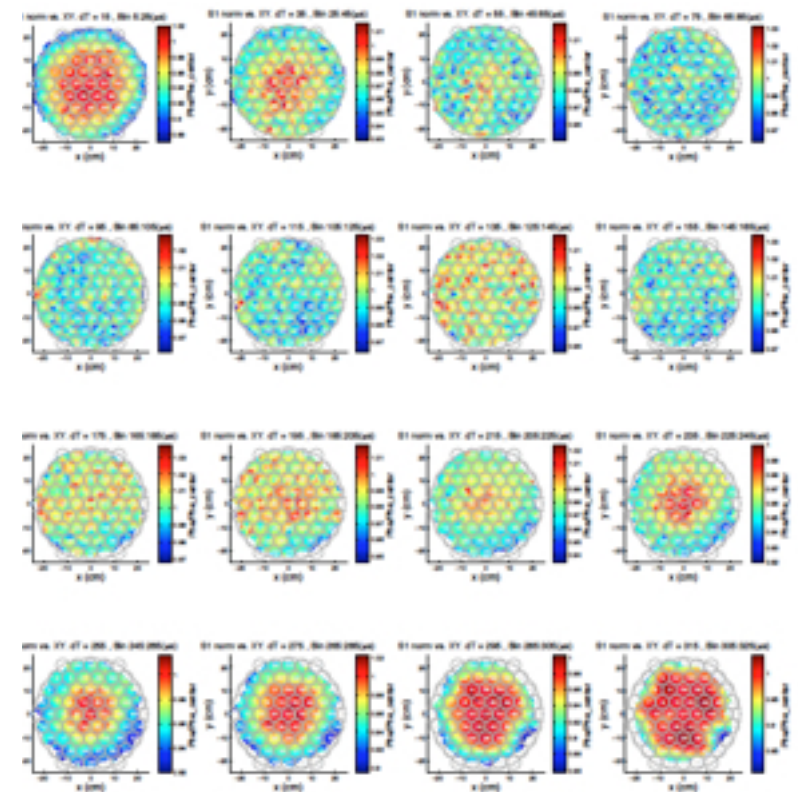
Kr-83m Calibration

- Over 1 million Kr-83m events, spread uniformly through the detector.

Fiducial volume determination



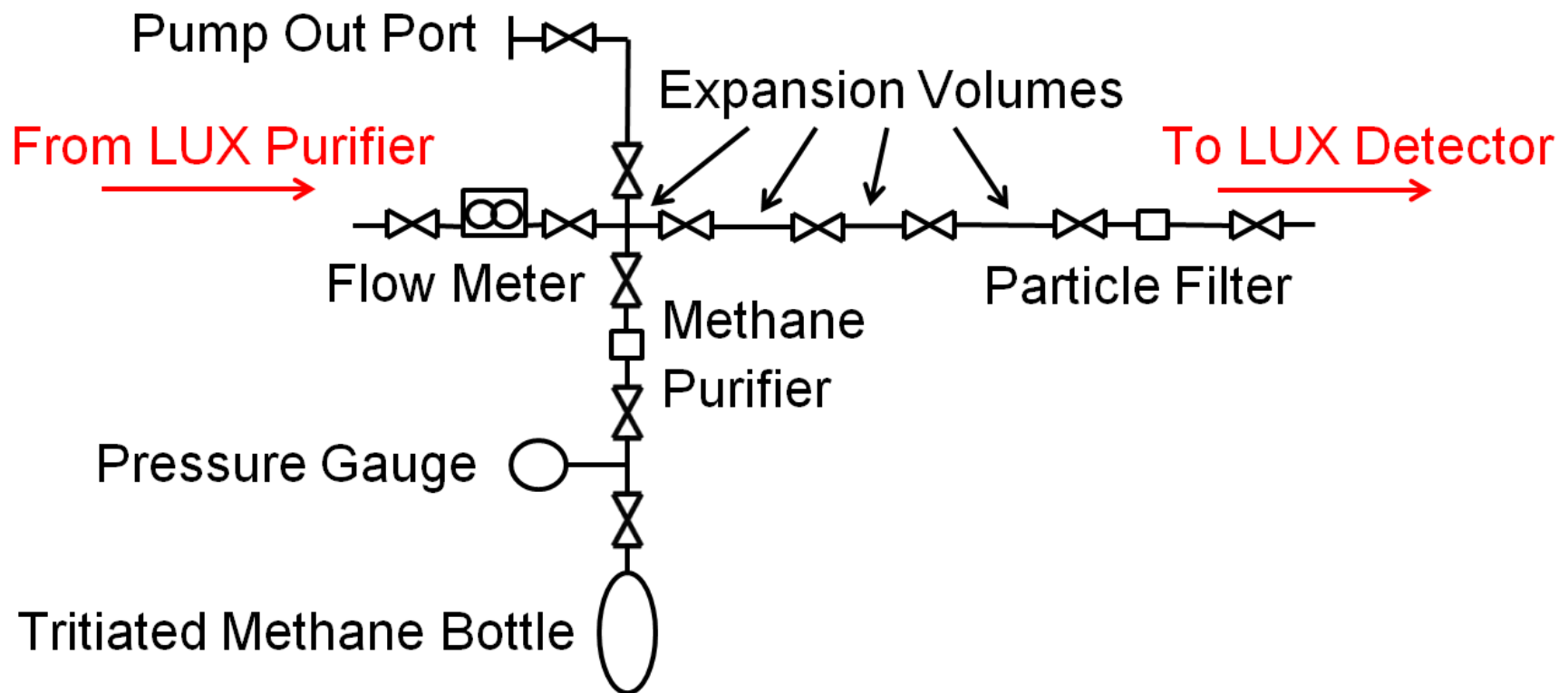
Position-based S1 corrections



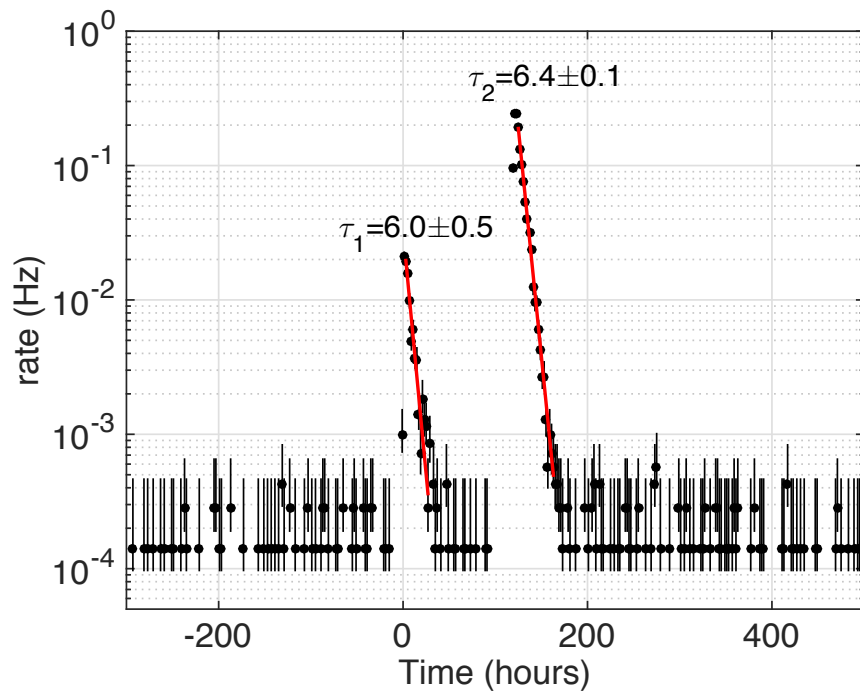
Tritiated Methane Calibration

- LUX uses tritiated methane, doped into the detector, to accurately calibrate the efficiency of background rejection.
- This beta source (endpoint energy 18 keV) allows electron recoil S2/S1 band calibration with unprecedented accuracy
- The tritiated methane is then fully removed by circulating the xenon through the getter
- Parametrization of the electron recoil band from the high-statistics tritiated methane data is then used to characterize the background model.

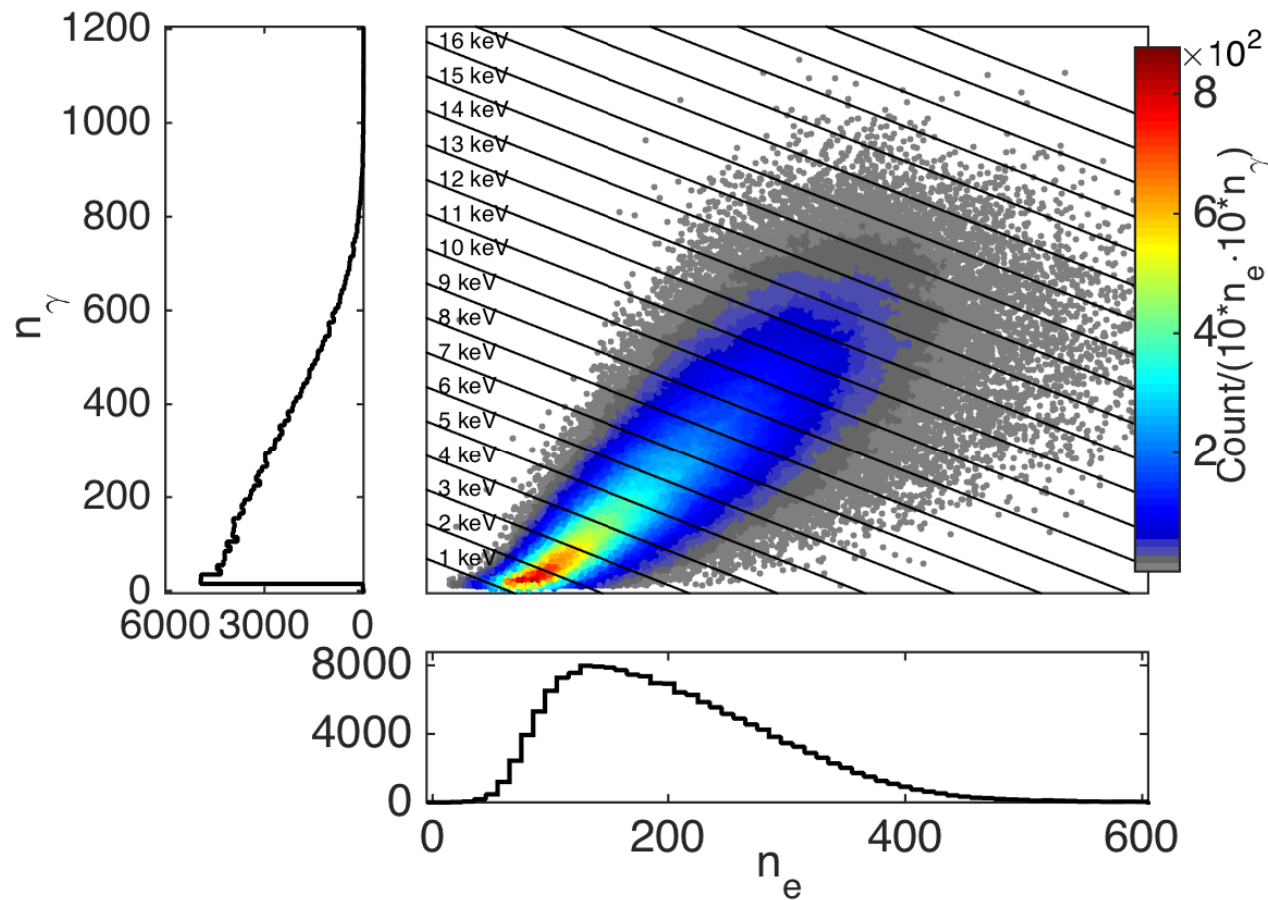
Tritiated Methane injection system



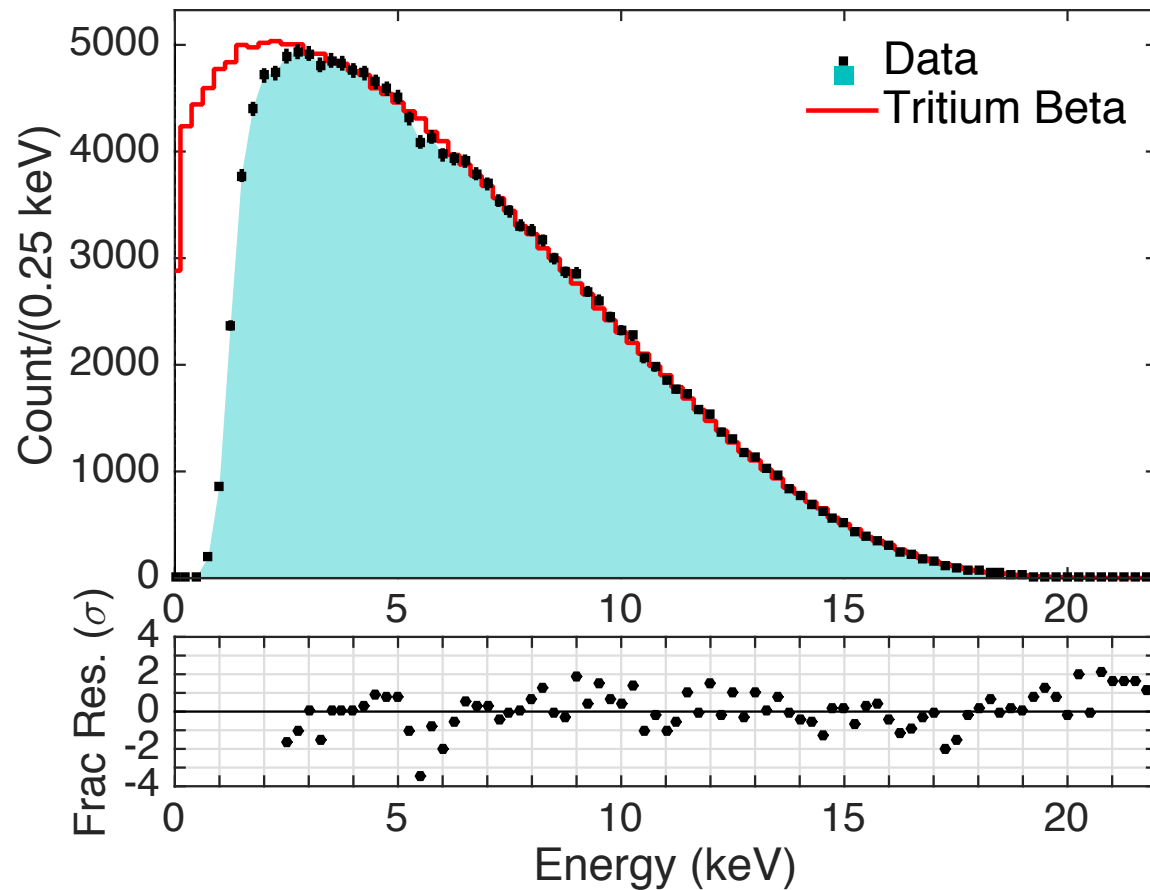
Tritiated Methane injection



Tritium beta decay measured in both light and charge

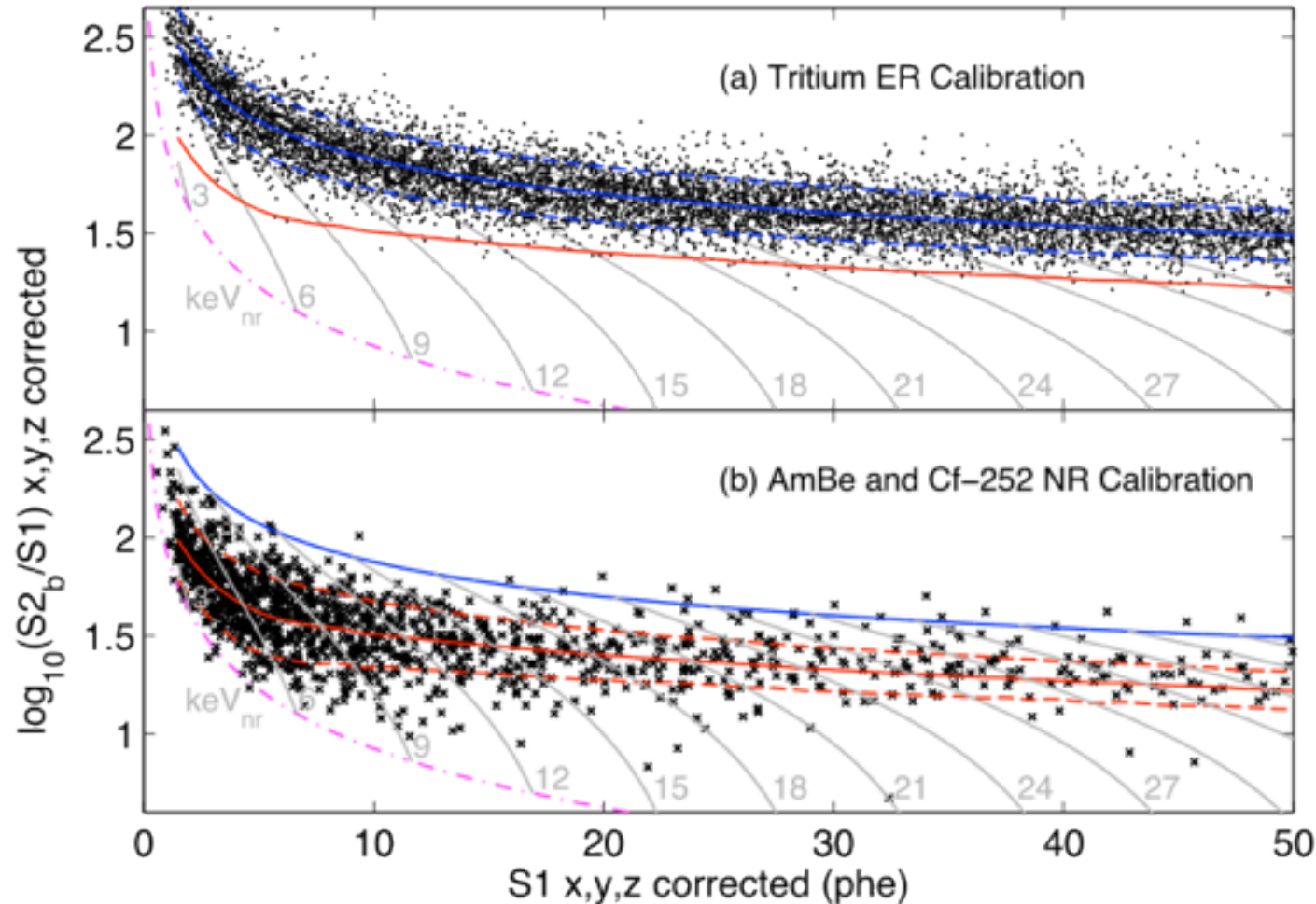


Tritium combined energy spectrum



Electron Recoil and Nuclear Recoil Bands

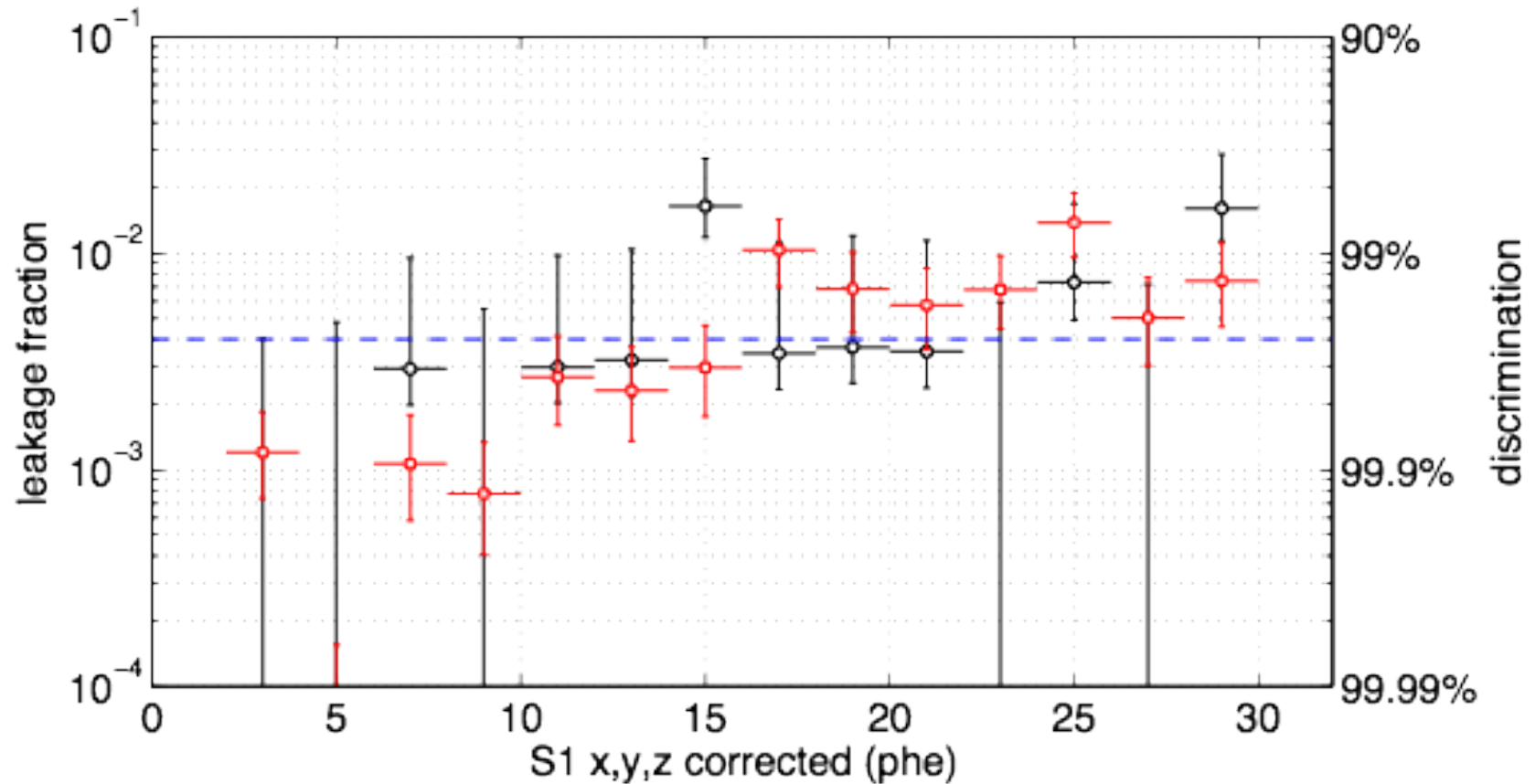
Tritium provides very high statistics electron recoil calibration (200 events/phe)
Neutron calibration is consistent with NEST + simulations



Gray contours indicate constant energies using a S1-S2 combined energy scale

Electron Recoil Discrimination

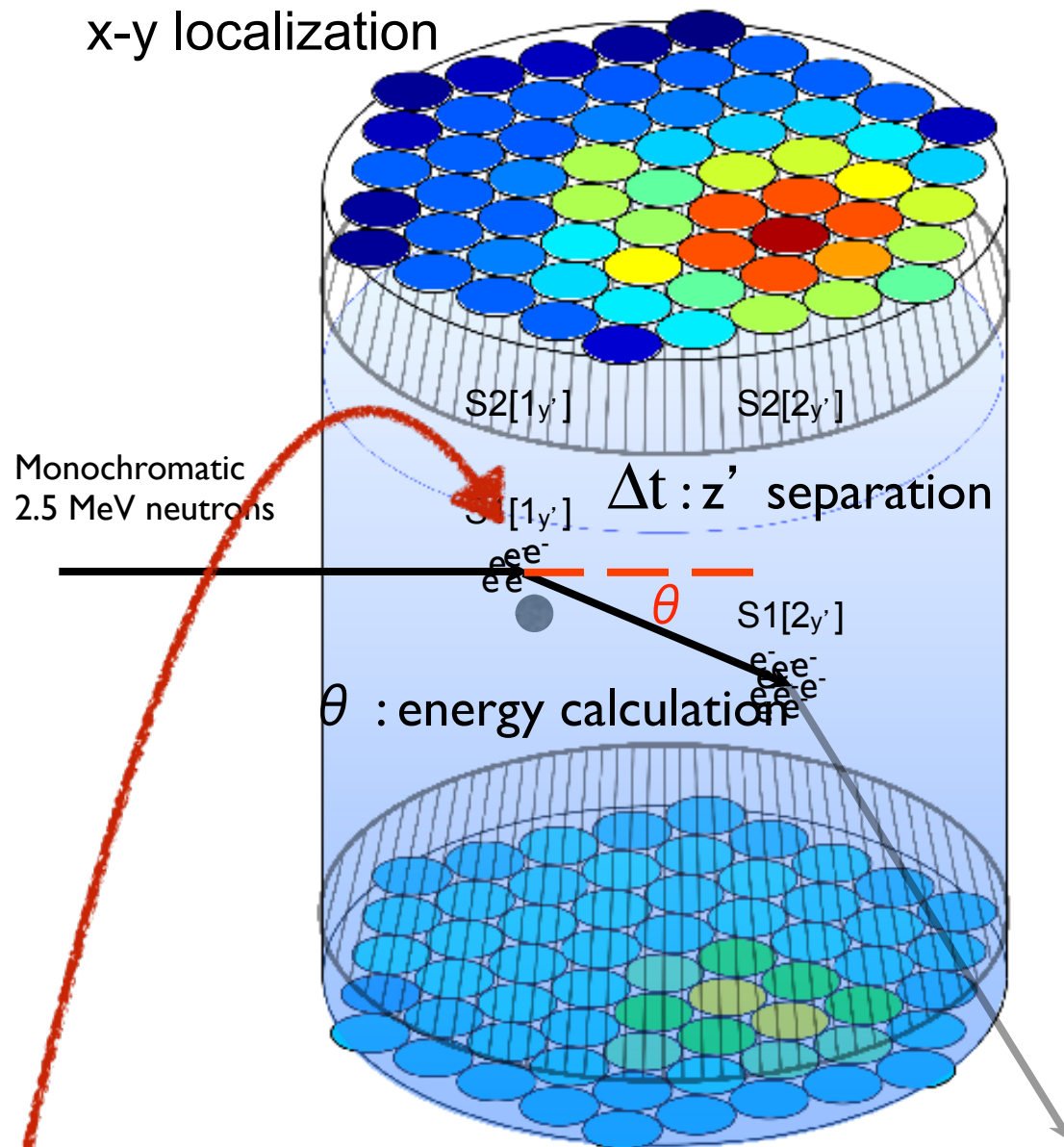
Average discrimination from 2-30 S1 photoelectrons
measured to be 99.6% (with 50% nuclear recoil acceptance)



Black circles show leakage from counting events from the dataset

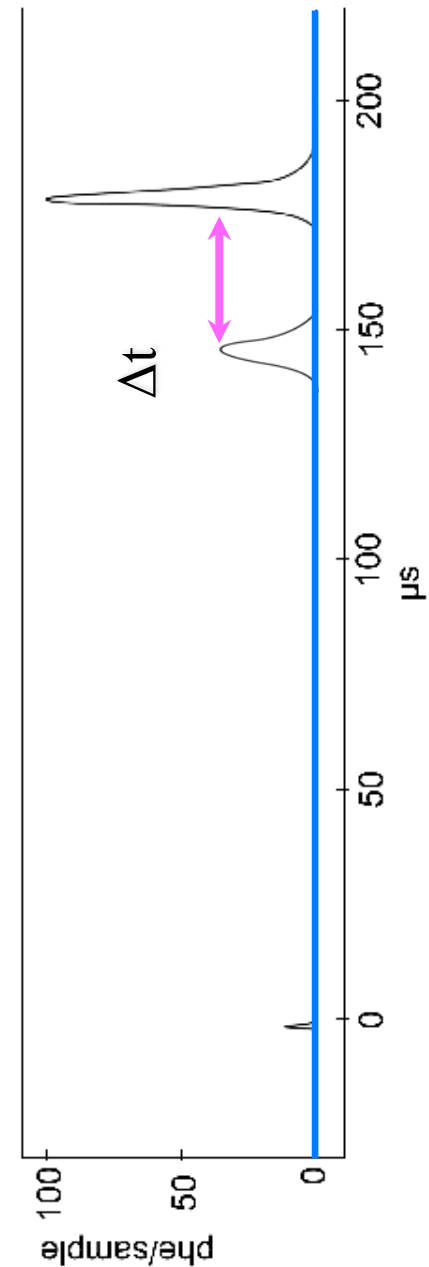
Red circles show projections of Gaussian fits below the nuclear recoil band mean

top hit pattern:
x-y localization

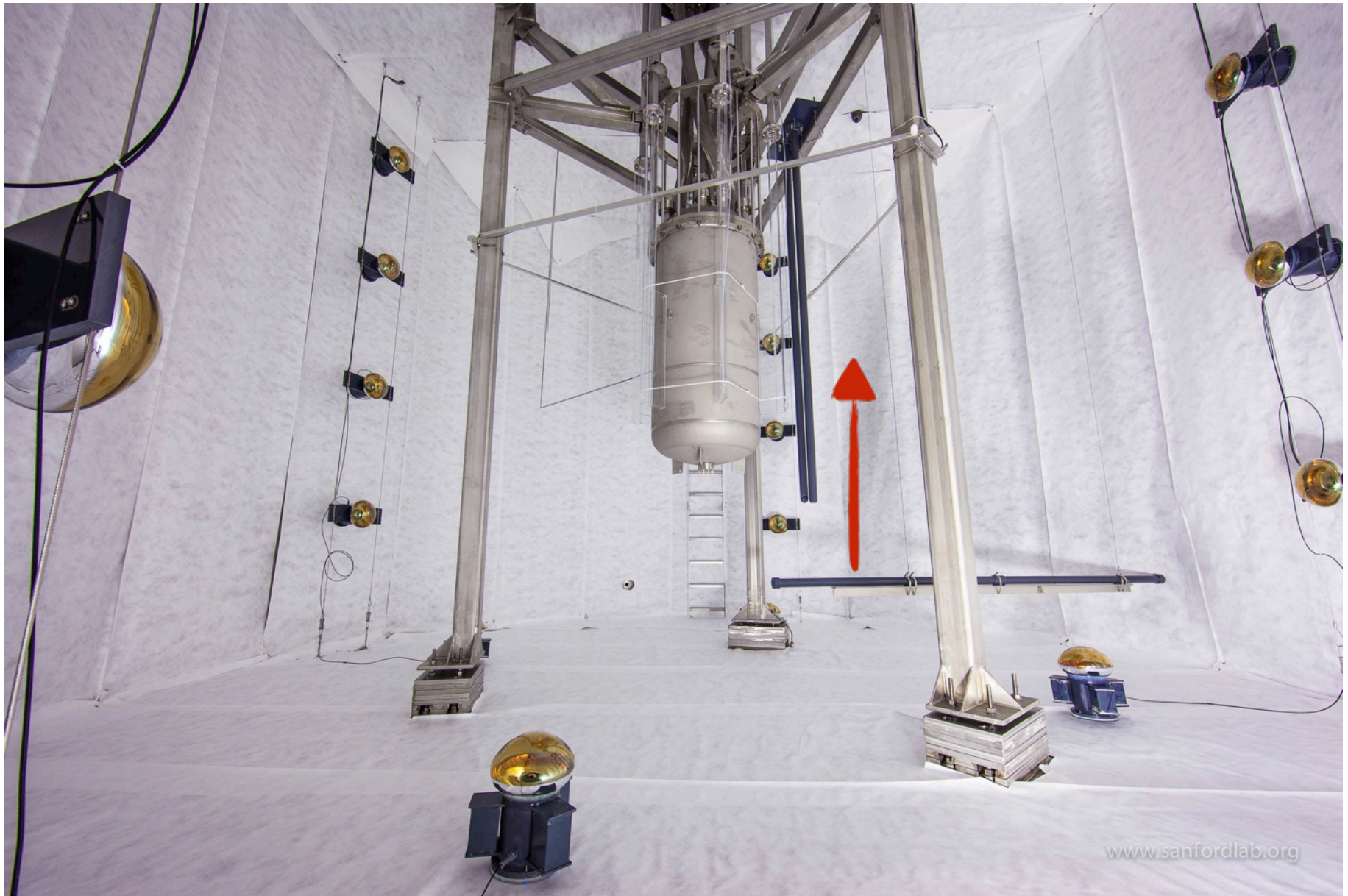


$$E_r = E_n \frac{4m_n m_{Xe}}{(m_n + m_{Xe})^2} \frac{1 - \cos \theta}{2}$$

D. McKinsey



Neutron Conduit Installed in the LUX Water Tank - Fall 2012



10/12/16

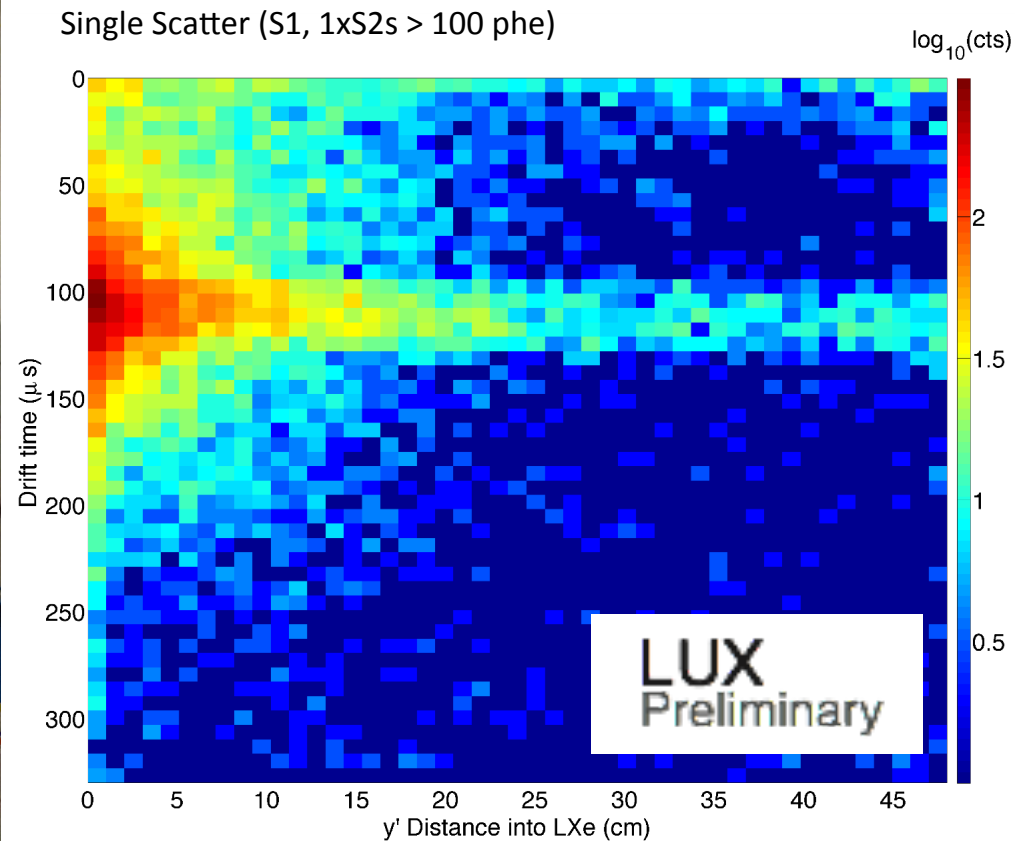
D. McKinsey
28

28

Adelphi DD108 Neutron Generator Installed Outside LUX Water Tank - Fall 2013



10/12/16



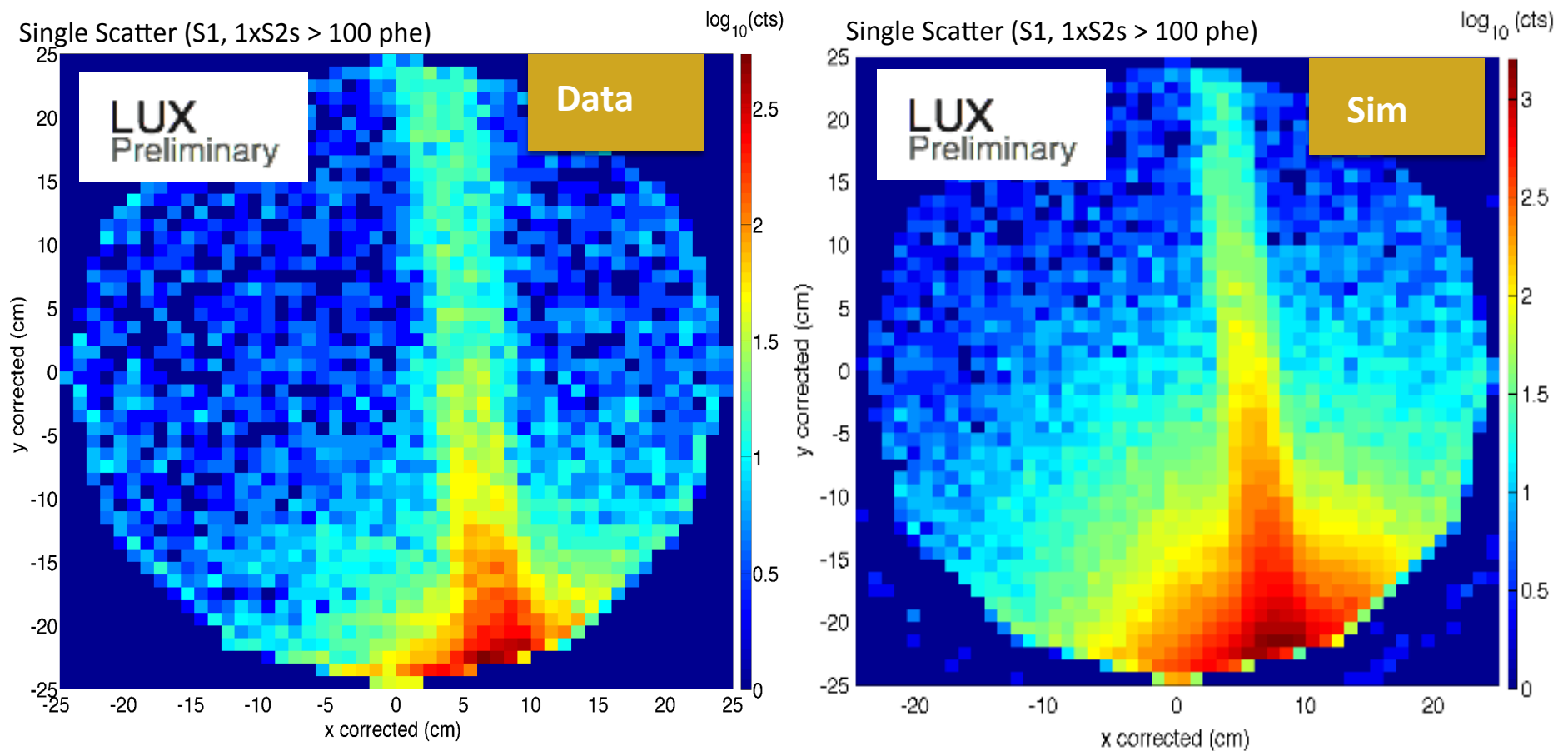
- Neutron generator/beam pipe assembly aligned 15.5 cm below liquid level in LUX active region to maximize usable single / double scatters
- Beam leveled to ~ 1 degree
- 105.5 live hours of neutron tube data used for analysis

D. McKinsey
29

29

Reconstructed Neutron Beam Event X-Y Positions

Complete Geant4 LUXSim + NEST simulation of D-D neutron calibration



10/12/16

D. McKinsey

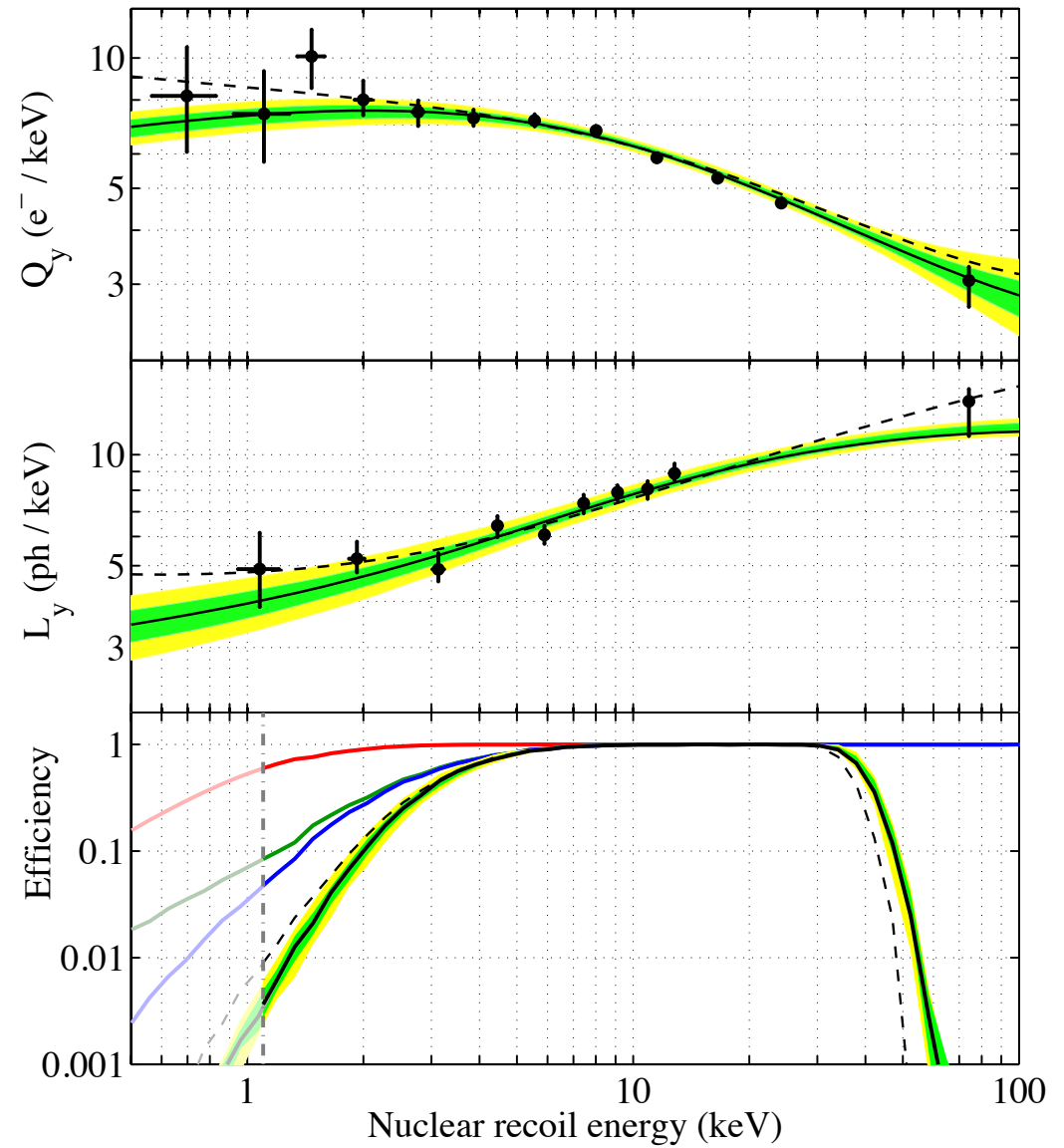
30

Charge and Light Yields for Nuclear Recoils, Measured Using DD Neutron Calibration in LUX

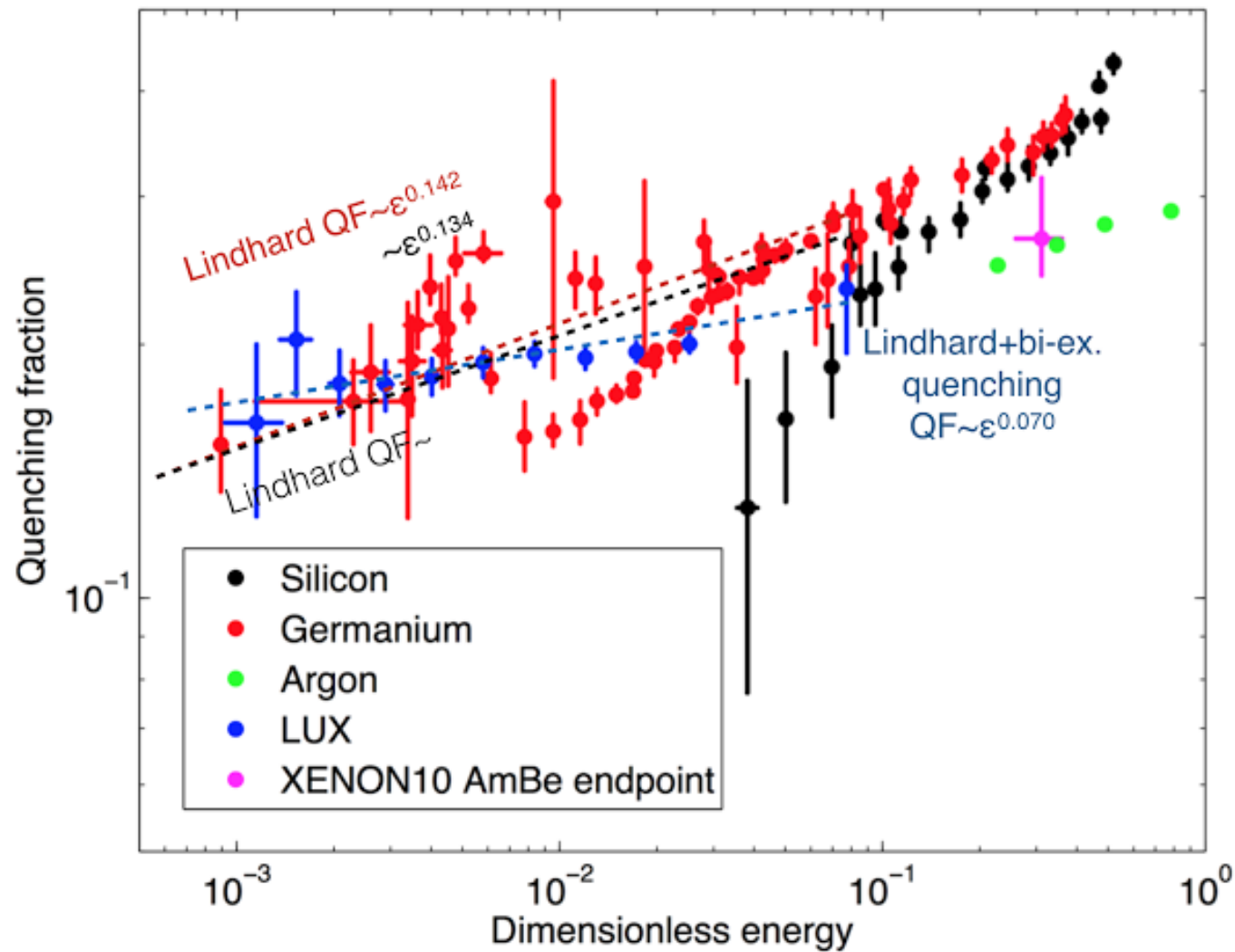
Charge Yield

Light Yield

WIMP signal efficiency



The Lindhard Quenching Factor in Liquid Xenon



LUX installed in its water tank shield, a mile underground in Lead, South Dakota
LUX ran stably since early 2013 through September 2016.



LUX removed from its water tank shield, September 28, 2016.



The newest LUX paper

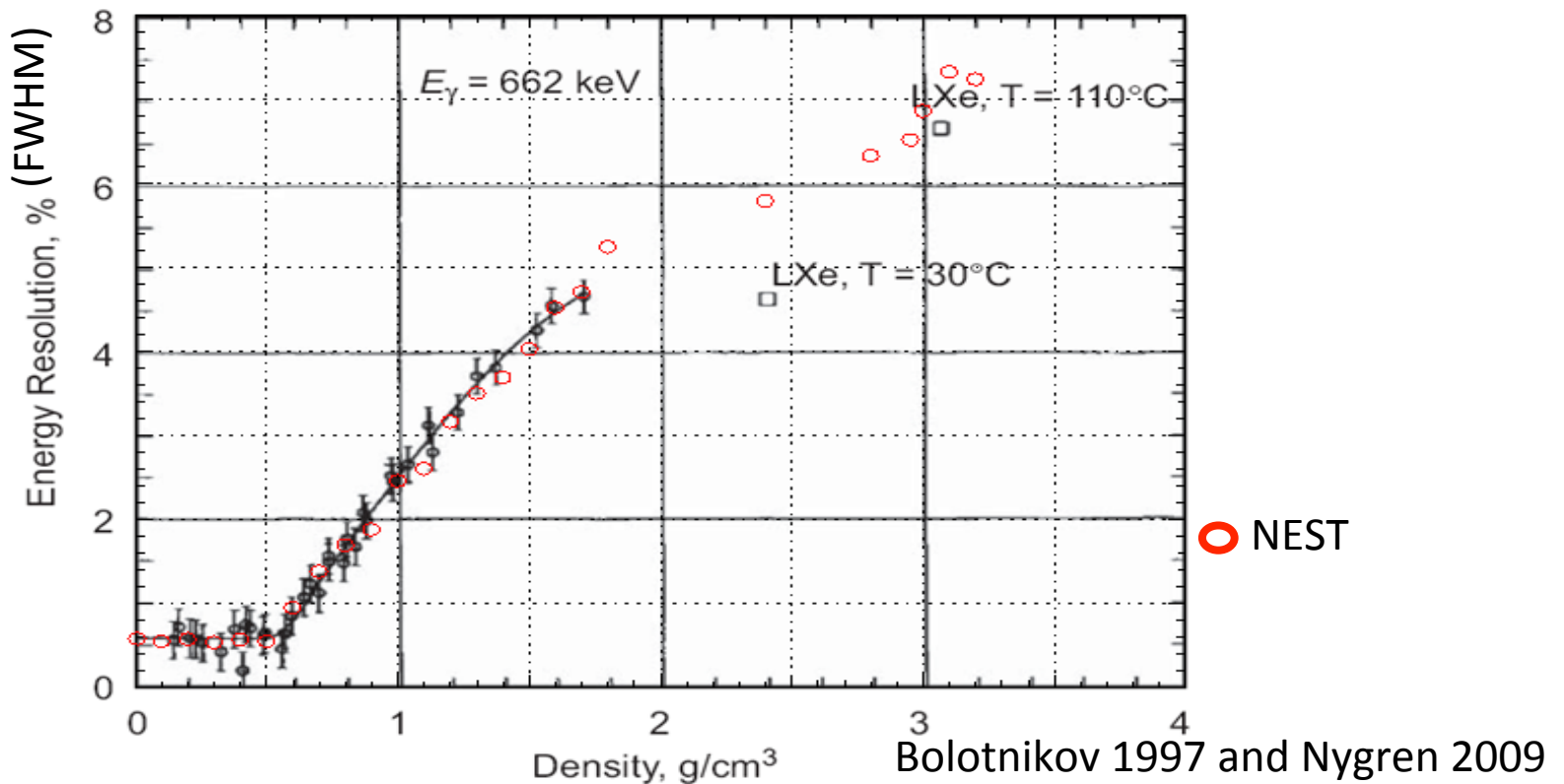
Signal yields, energy resolution, and recombination fluctuations in liquid xenon (arXiv:1610.02076)

Follows upon past studies of ion-electron recombination:

- E. Conti et al., Phys. Rev. B 68, 054201 (2003).
- E. Aprile, K. Giboni, P. Majewski, K. Ni, and M. Yamashita, Phys. Rev. B 76, 014115 (2007).
- D. S. Akerib et al. (LUX Collaboration), Phys. Rev. D 93, 072009 (2016).

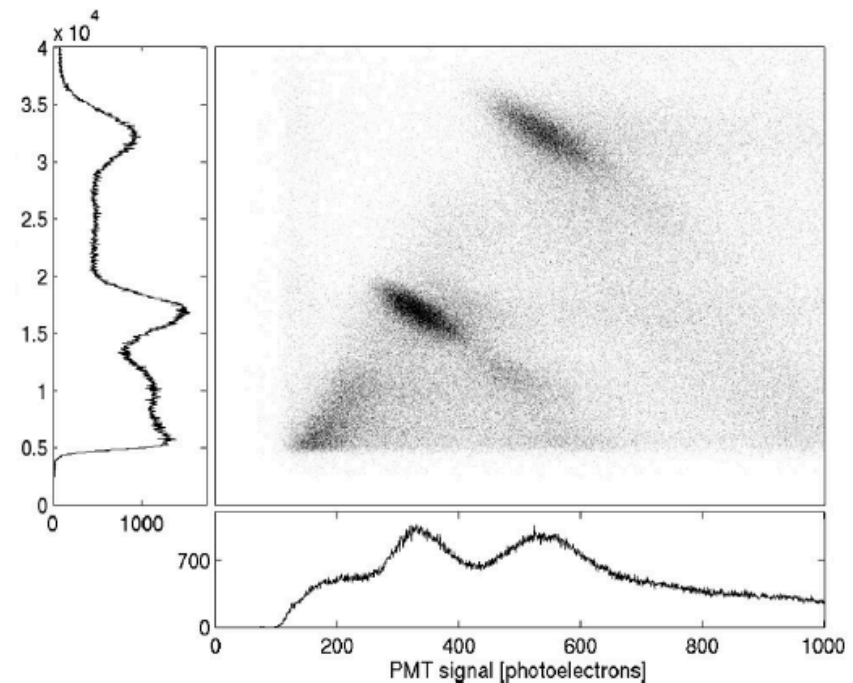
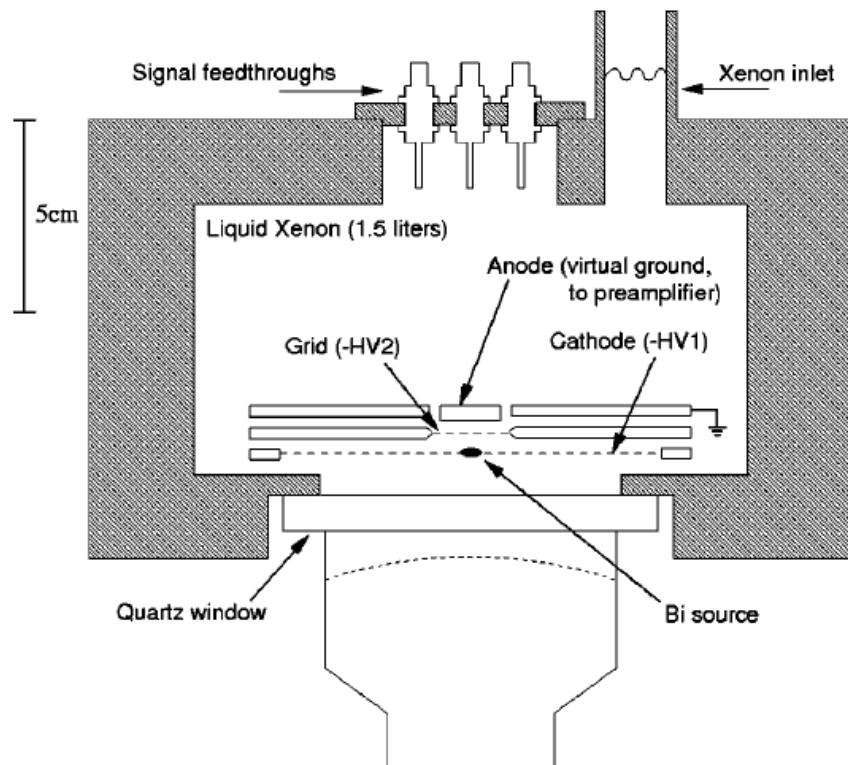
Charge-only energy resolution

Because of recombination fluctuations, energy resolution is poor above 0.5 g/cc, if based on charge alone or light alone.



Anti-correlation between charge and light in LXe

E.Conti et al, Correlated fluctuations between luminescence and ionization in liquid xenon, Phys. Rev. B 68, 054201 (2003).





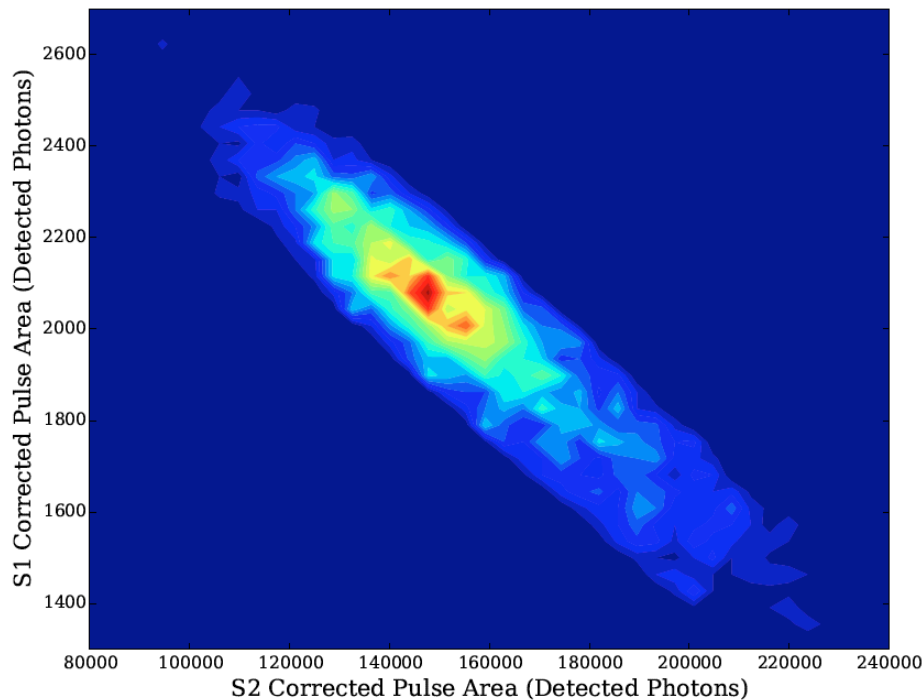
Energy resolution in LUX

Event energy is determined using a linear combination of charge and light signals

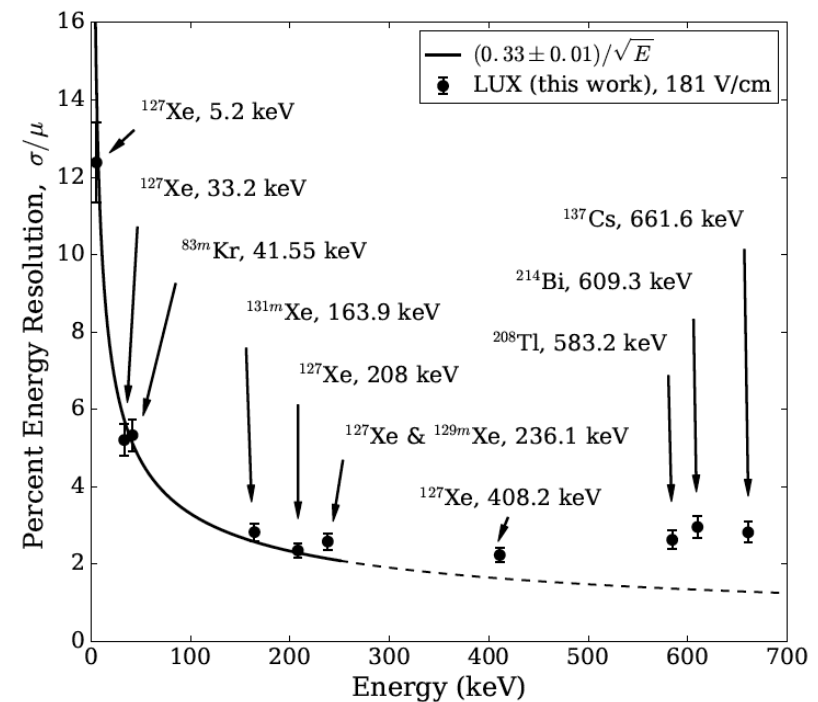
Because the correctly weighted charge and light signals add to a constant for a given event energy, they are anticorrelated.

Recombination fluctuations cause “sloshing” between charge and light production

Cs-137 events



$$E = W \cdot (n_{ph} + n_e) = W \cdot \left(\frac{S1}{g_1} + \frac{S2}{g_2} \right)$$

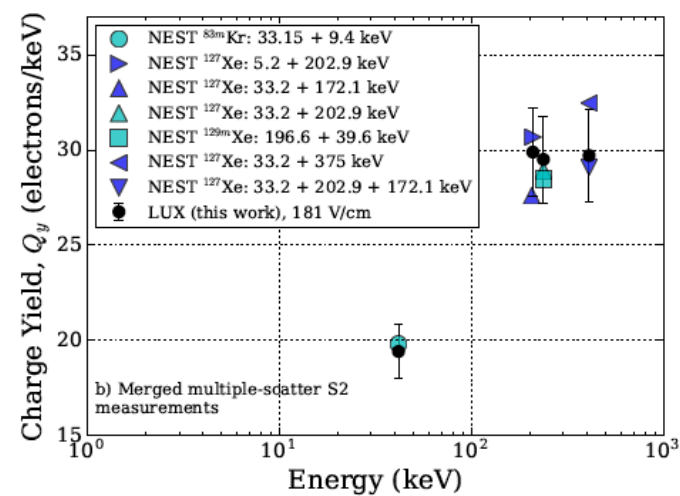
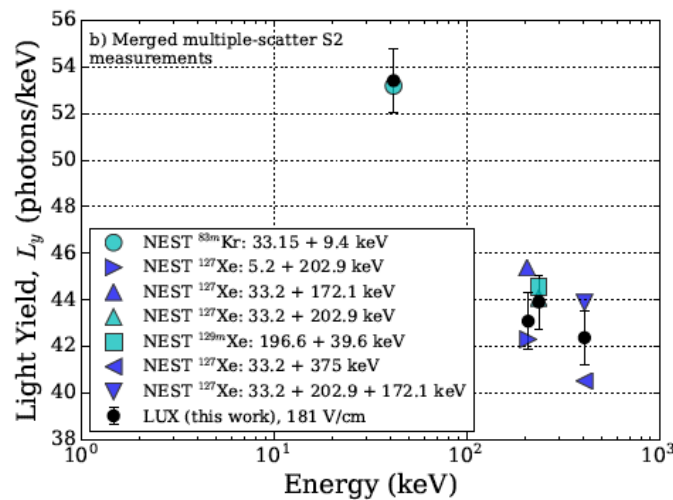
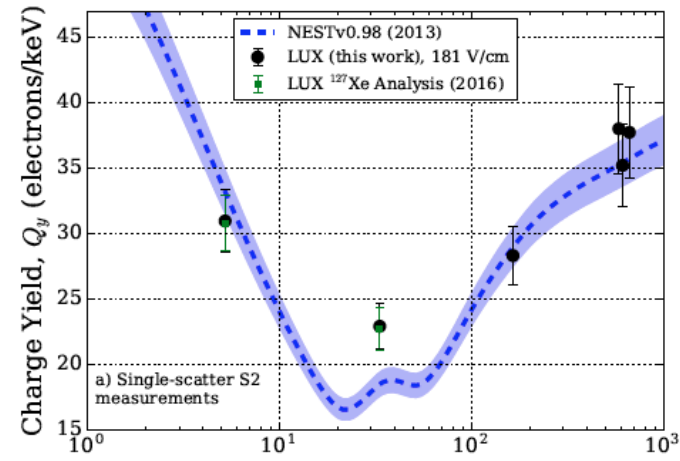
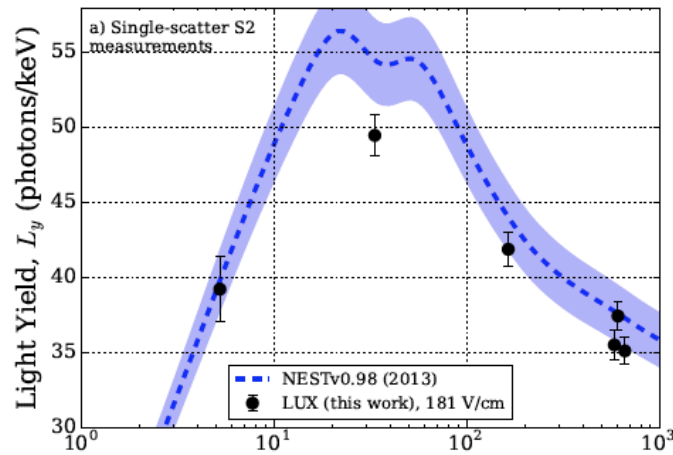




Run 3 - ER charge and light yields

Observed charge and light yields are well matched by NEST model, which uses a “Thomas-Imel box model” at low energies and a “Doke model” at high energies..

$$n_{ph} = (\alpha + r)n_i \text{ and } n_e = (1 - r)n_i$$





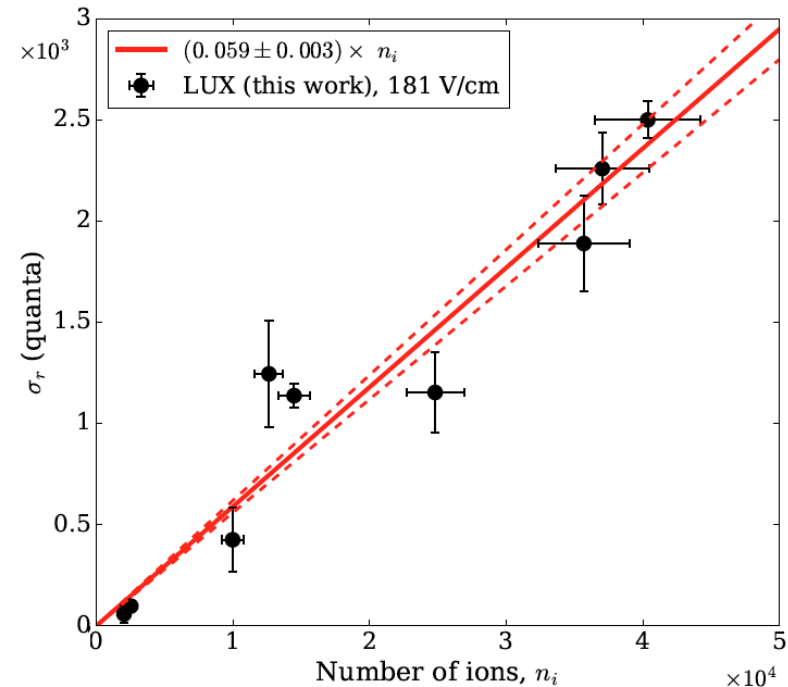
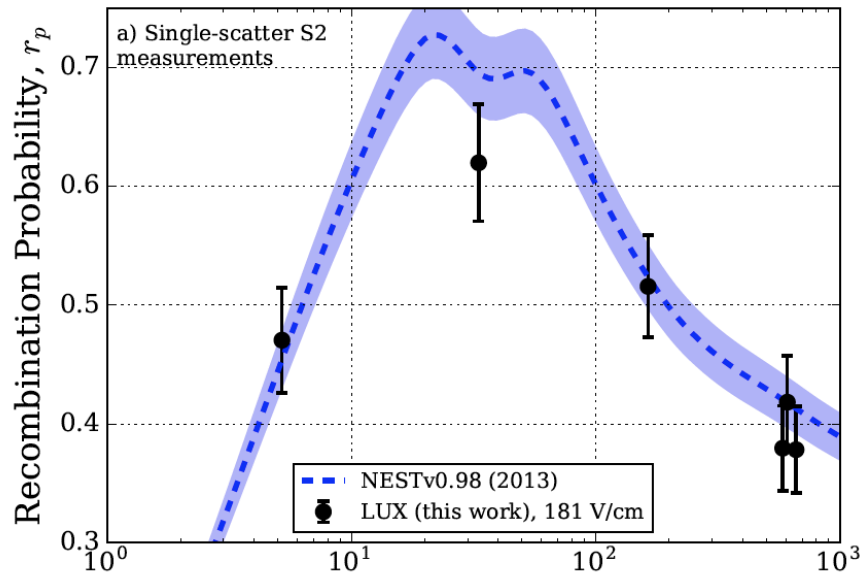
Electron Recombination

Question: How much does electron-ion recombination vary from event to event in LXe?

How does this depend on event type and event energy?

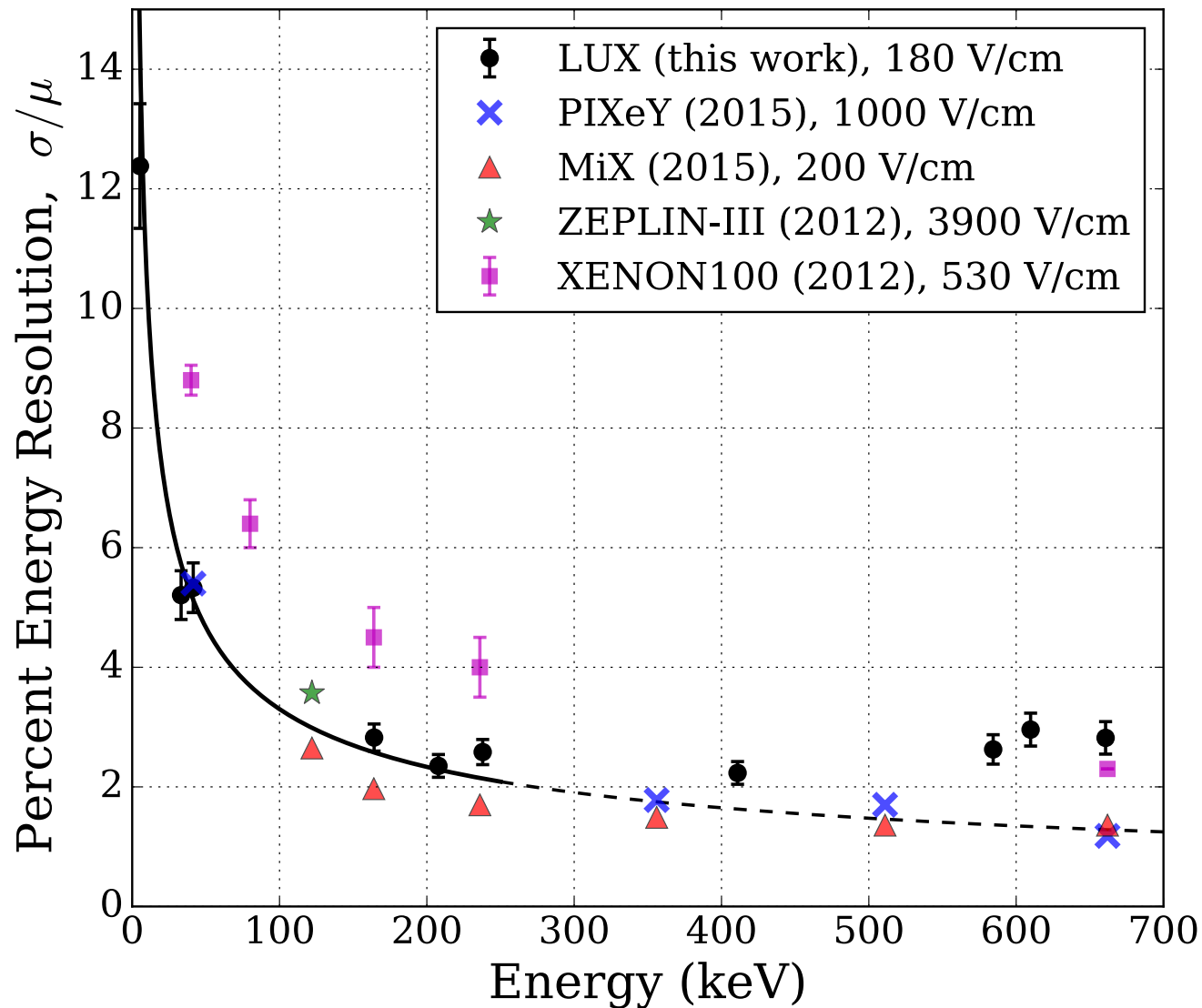
Motivation: Recombination physics is key for modeling energy resolution, S2/S1 discrimination

We find that recombination peaks at ~ 30 keVee, and that fluctuations scale linearly with the number of ions in the initial event.





Energy resolution in two-phase Xe detectors



The PIXeY Team



Undergraduate Students:

Andreas Biekert, Anastasia Salova,
Brian Tien-Street, Chris Kachulis,
Humaira Taz

Graduate Students:

Elizabeth Boulton, Nicholas DeStefano,
Ariana Hackenberg, Nicole Larsen
Brian Tennyson

Postdocs:

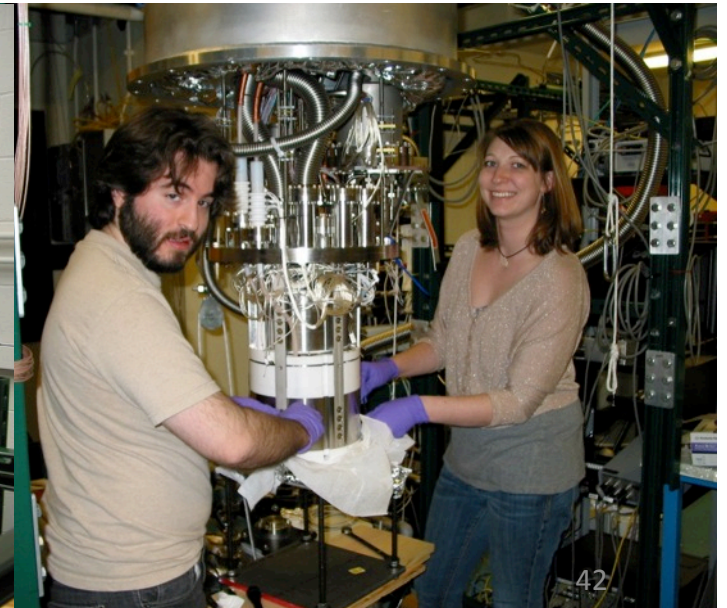
Blair Edwards, Scott Hertel

Research Scientists:

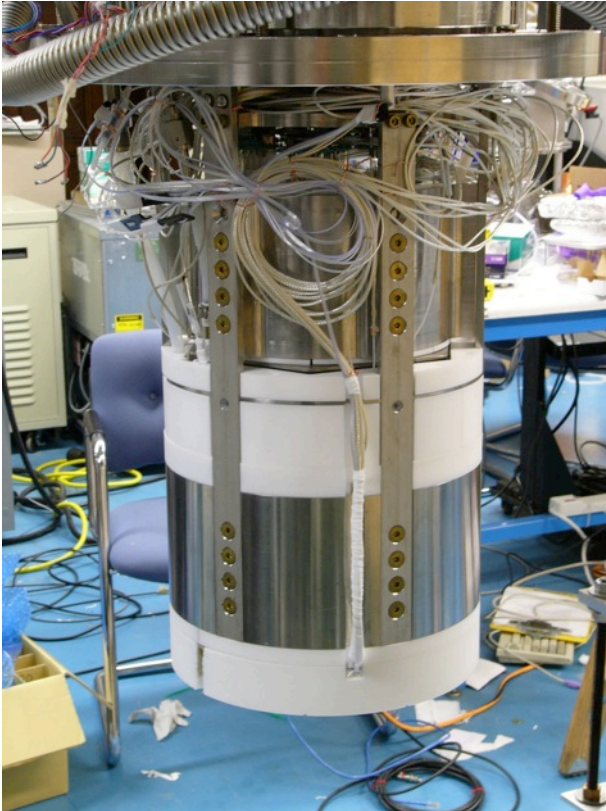
Ethan Bernard, Markus Horn

Professors:

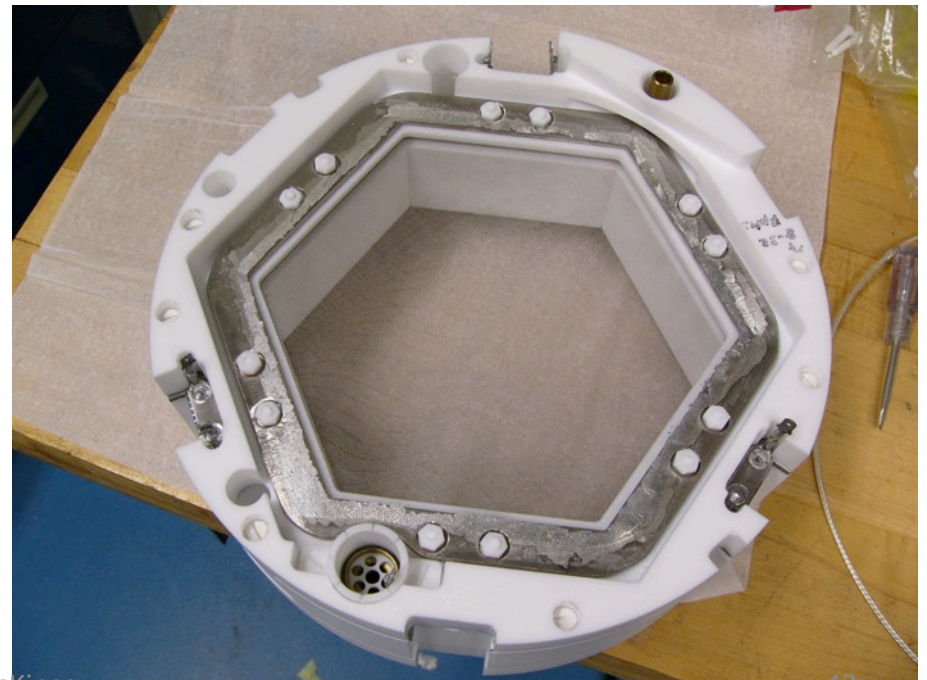
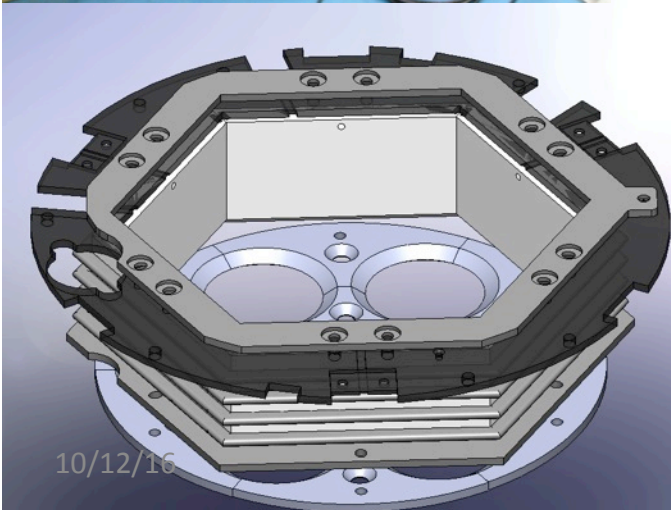
Daniel McKinsey, Moshe Gai



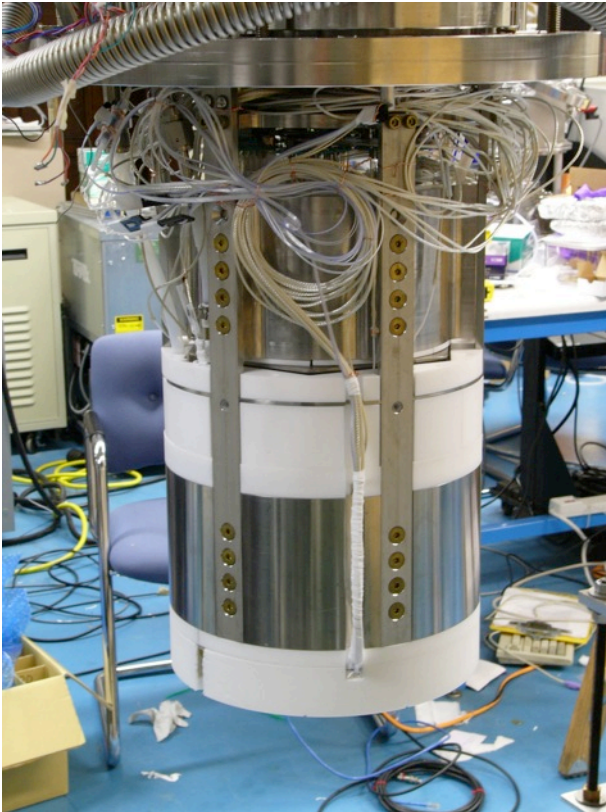
PIXeY – Particle Identification in Xenon at Yale



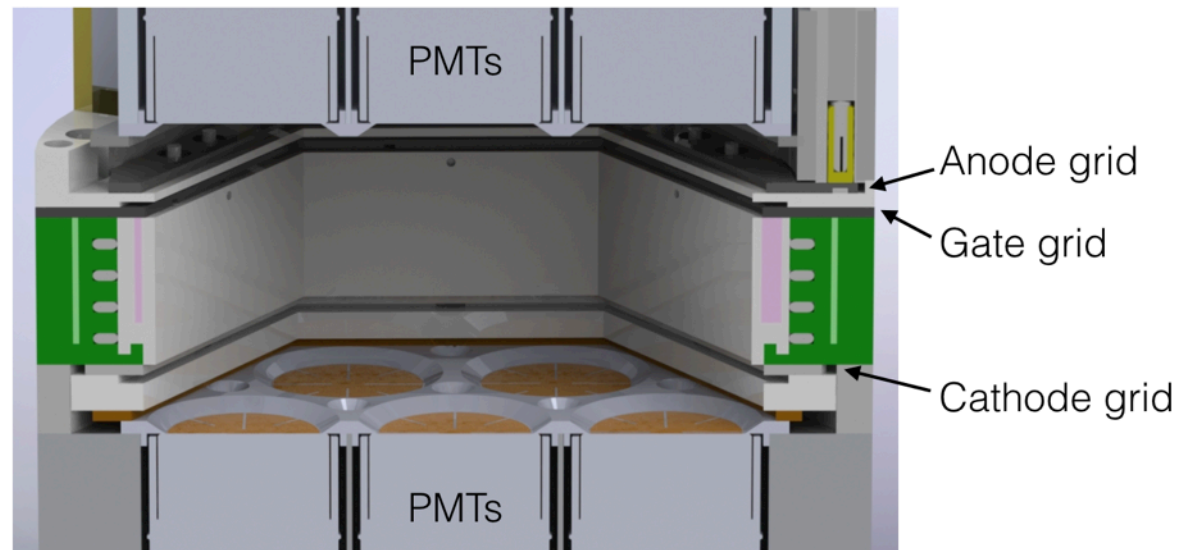
- Two-phase Xe detector; 4 kg active xenon volume.
- 5 cm tall by 18 cm across corners.
- Designed for optimal light collection and strong drift field.
- Ran at Yale from June 2014 through April 2015.
- Test platform for technologies supporting Compton imaging:
 - Uniform, transparent grids.
 - Cryogenic and xenon circulation platform.
 - PMT readout and data processing software.



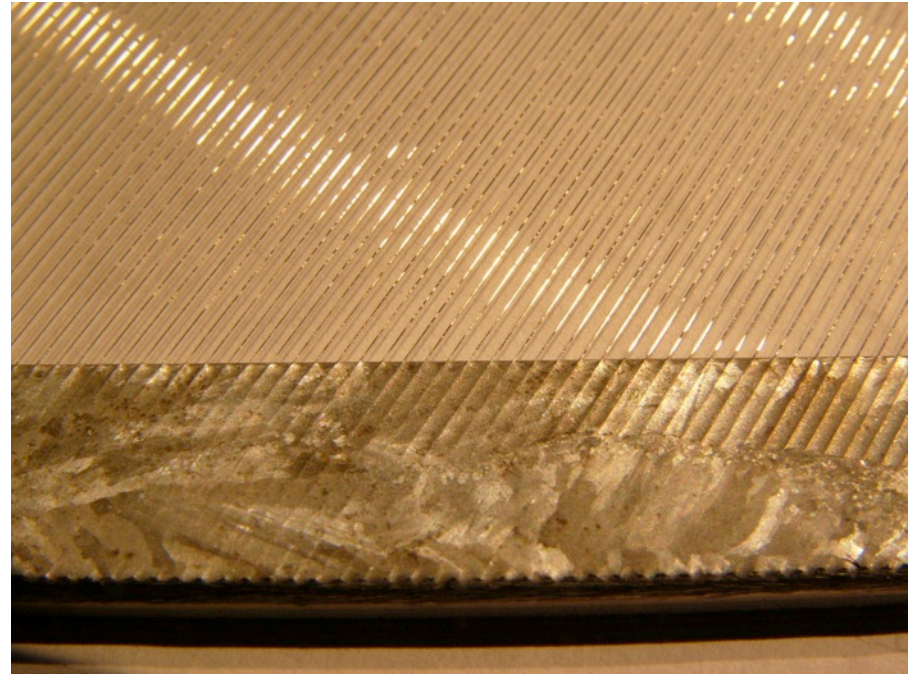
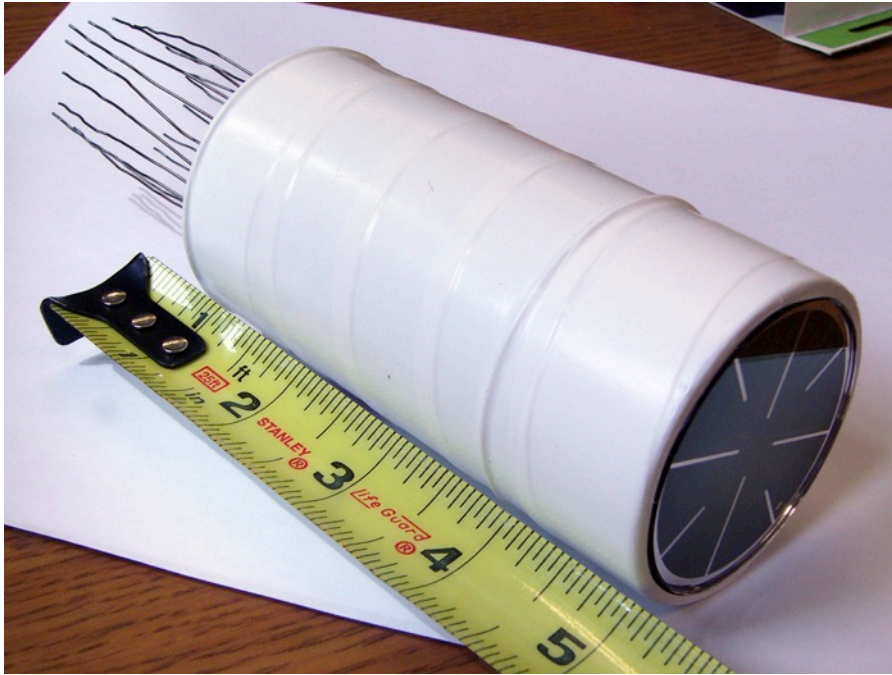
PIXeY – Particle Identification in Xenon at Yale



- Two-phase Xe detector; 4 kg active xenon volume.
- 5 cm tall by 18 cm across corners.
- Designed for optimal light collection and strong drift field.
- Ran at Yale from June 2014 through April 2015.
- Test platform for technologies supporting Compton imaging:
 - Uniform, transparent grids.
 - Cryogenic and xenon circulation platform.
 - PMT readout and data processing software.



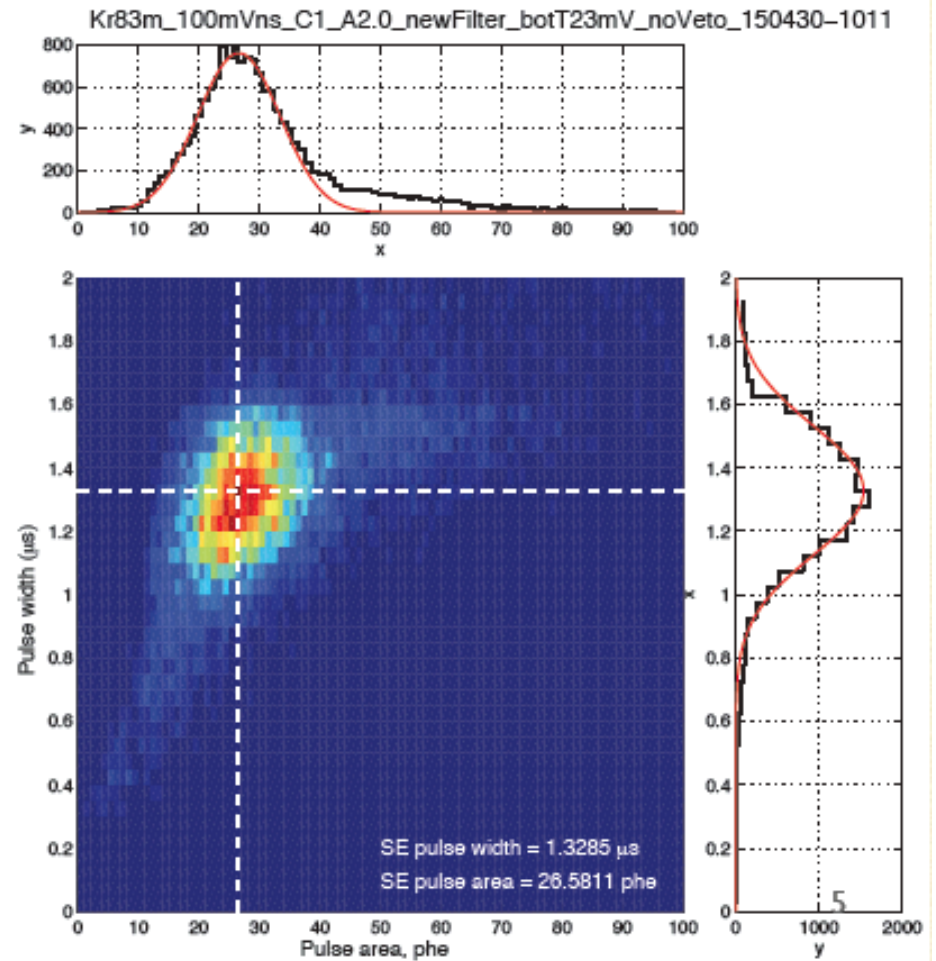
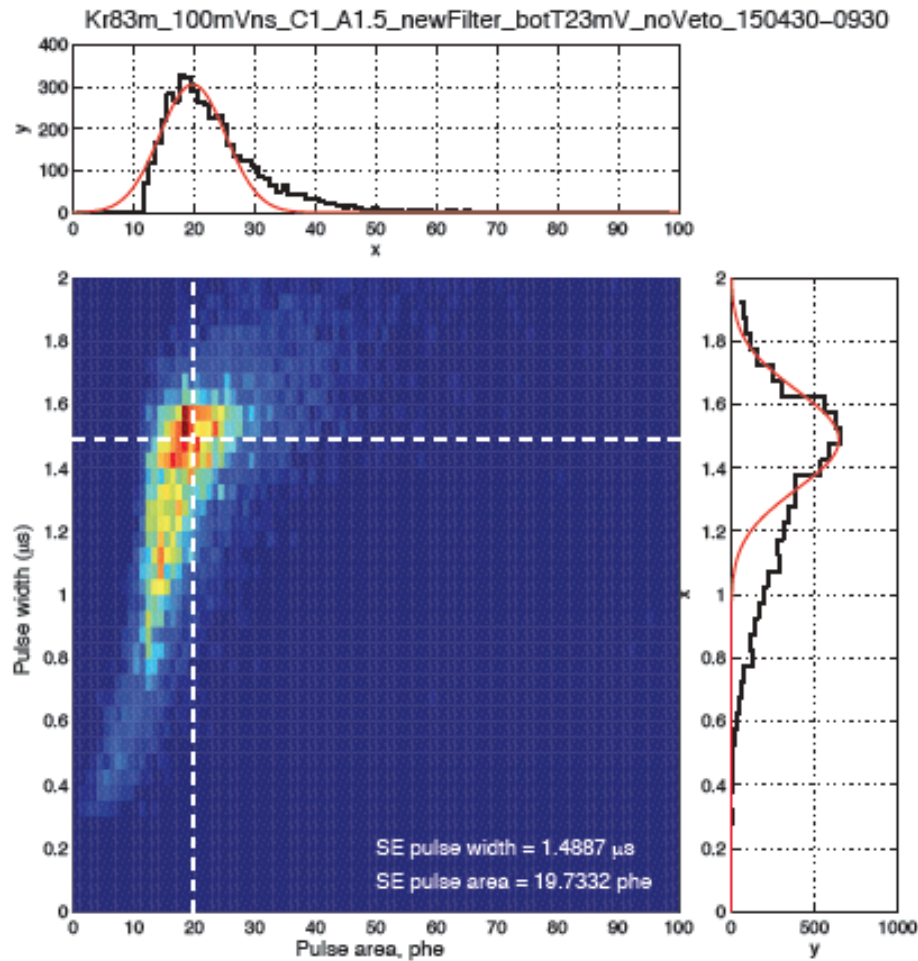
PIXEY Hardware: PMTs and Grids



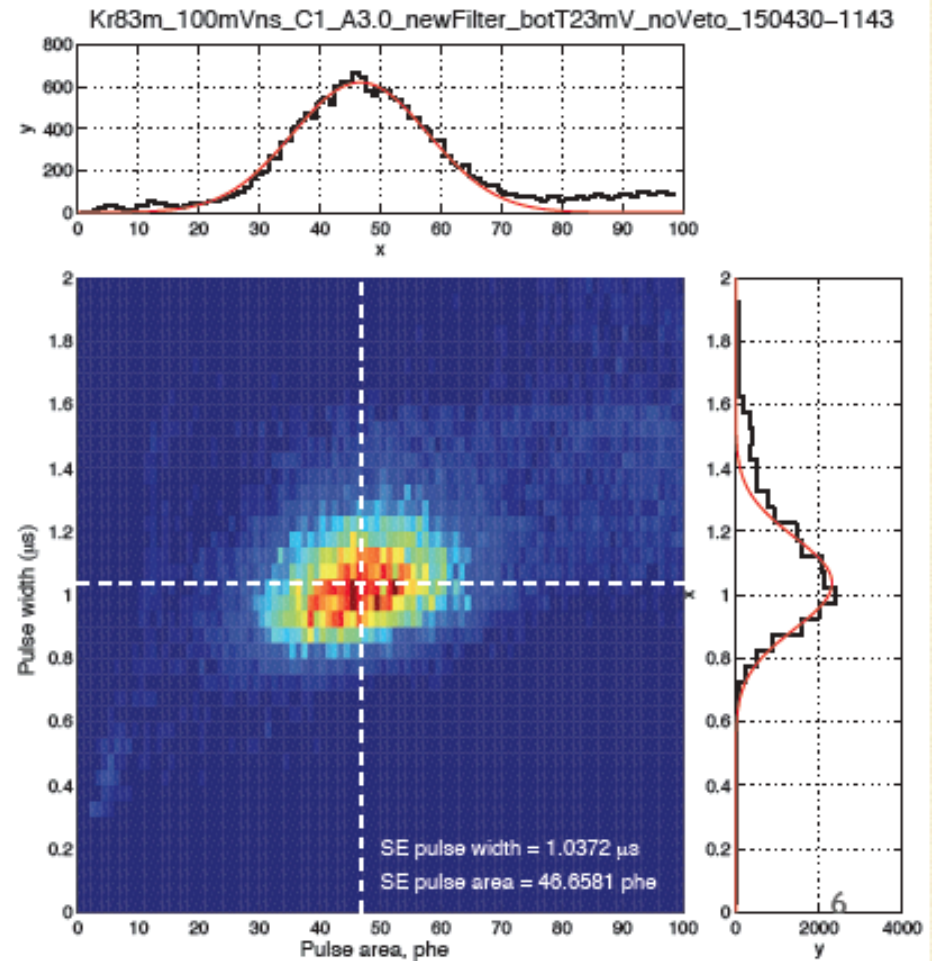
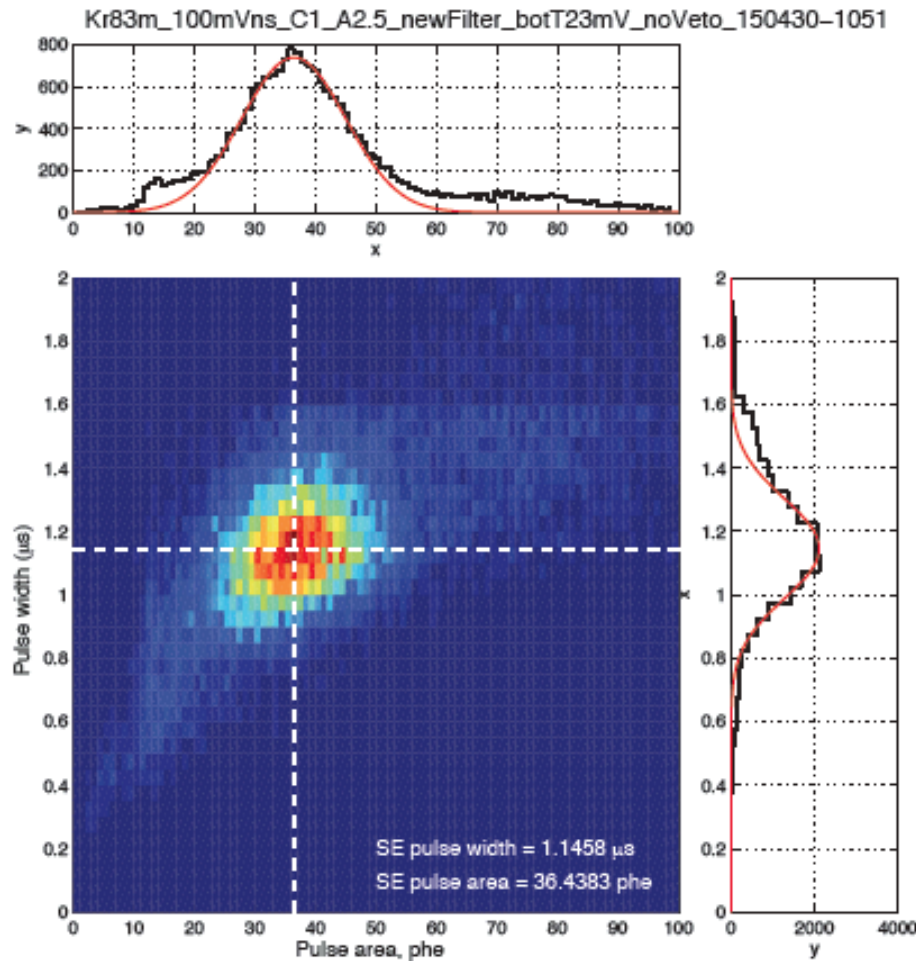
- Direct collection of 175 nm Xe scintillation light through quartz window.
- Bialkali Photocathode; 35% quantum efficiency; gain $10^5 - 10^7$
- Operate immersed in liquid xenon.
- Used in the LUX and XMASS LXe dark matter experiments.

- Wire and frame are monel alloy 400
 - 92% open field establishing grids
 - 80 μm wire, 1 mm pitch
 - 250 g/wire tension
 - Can fabricate to arbitrary pitch
- Maintain uniform tension while cold

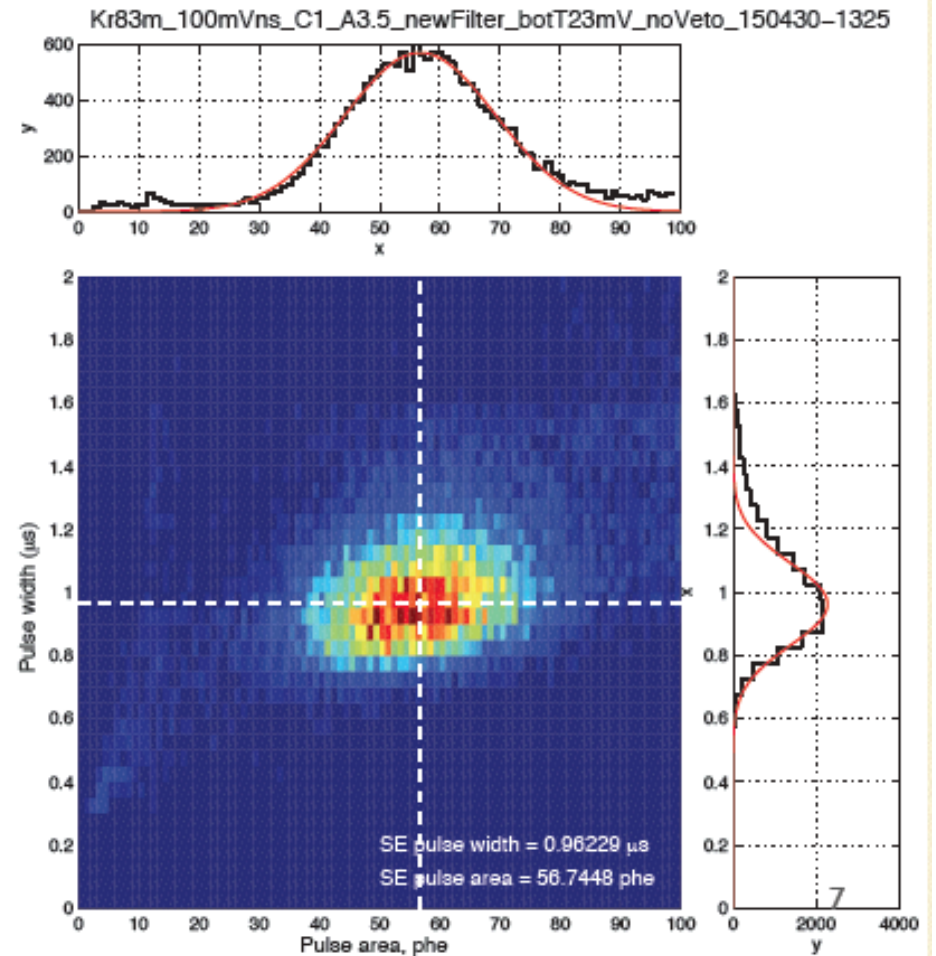
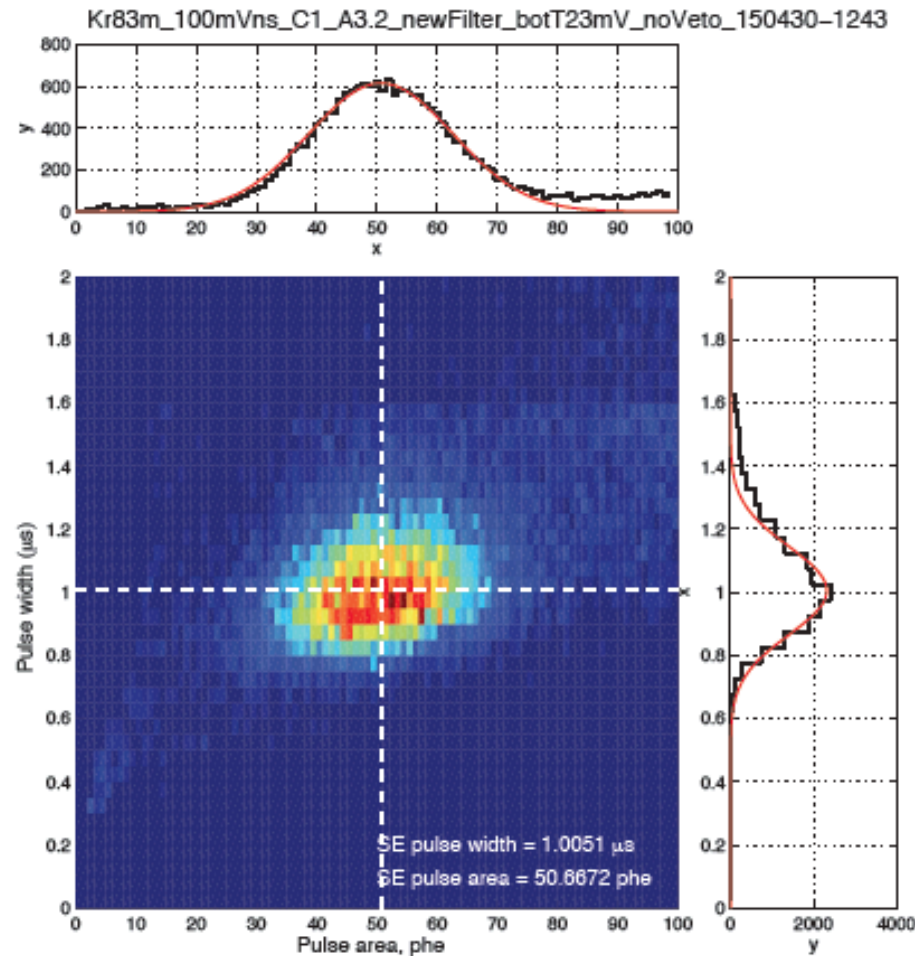
Single electrons in PIXeY



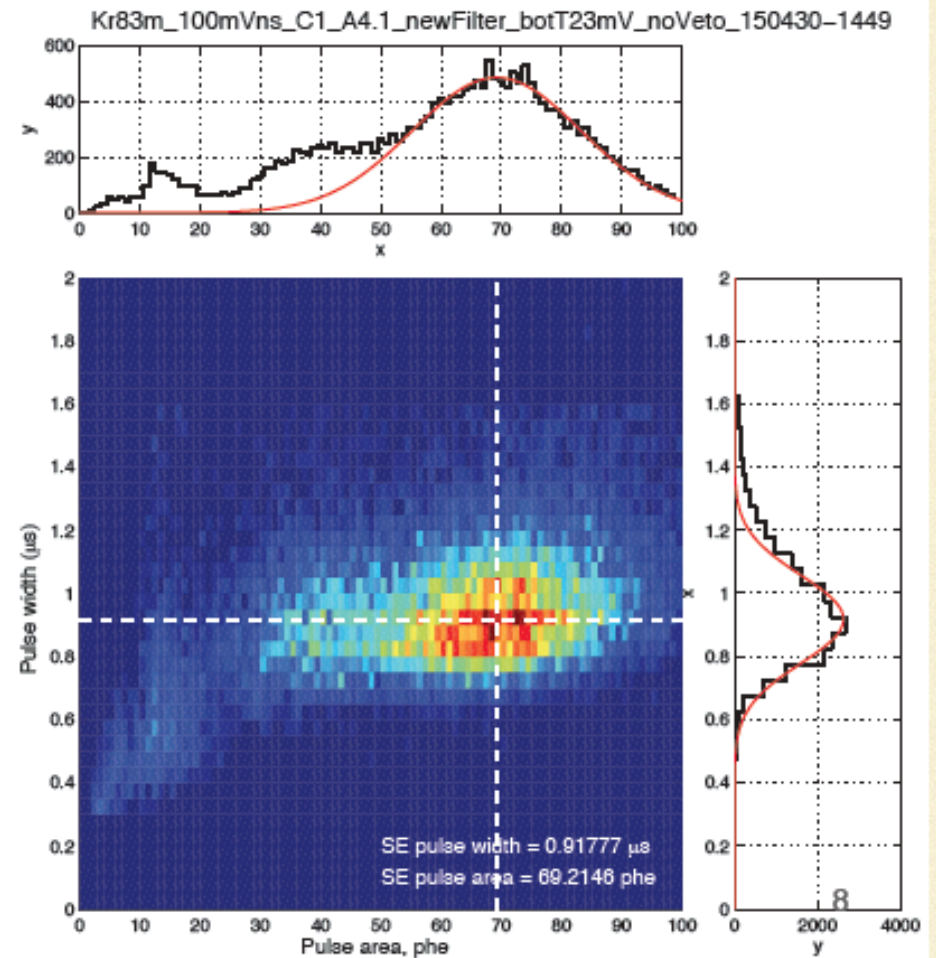
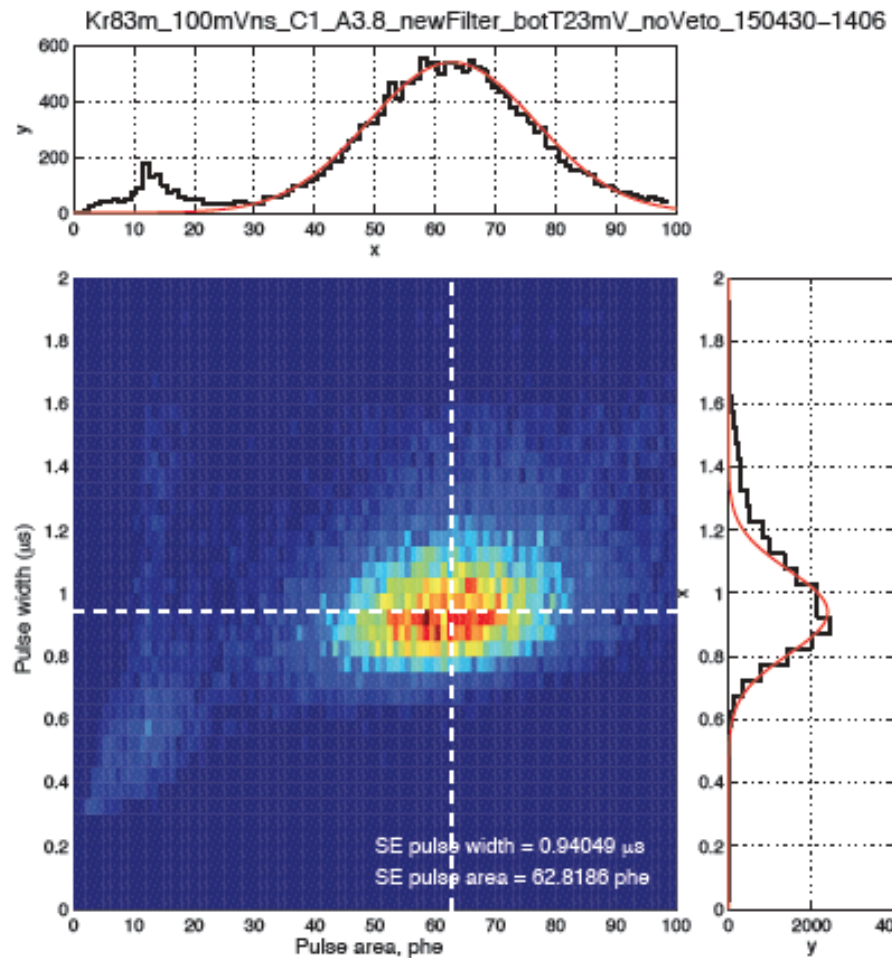
Single electrons in PIXeY



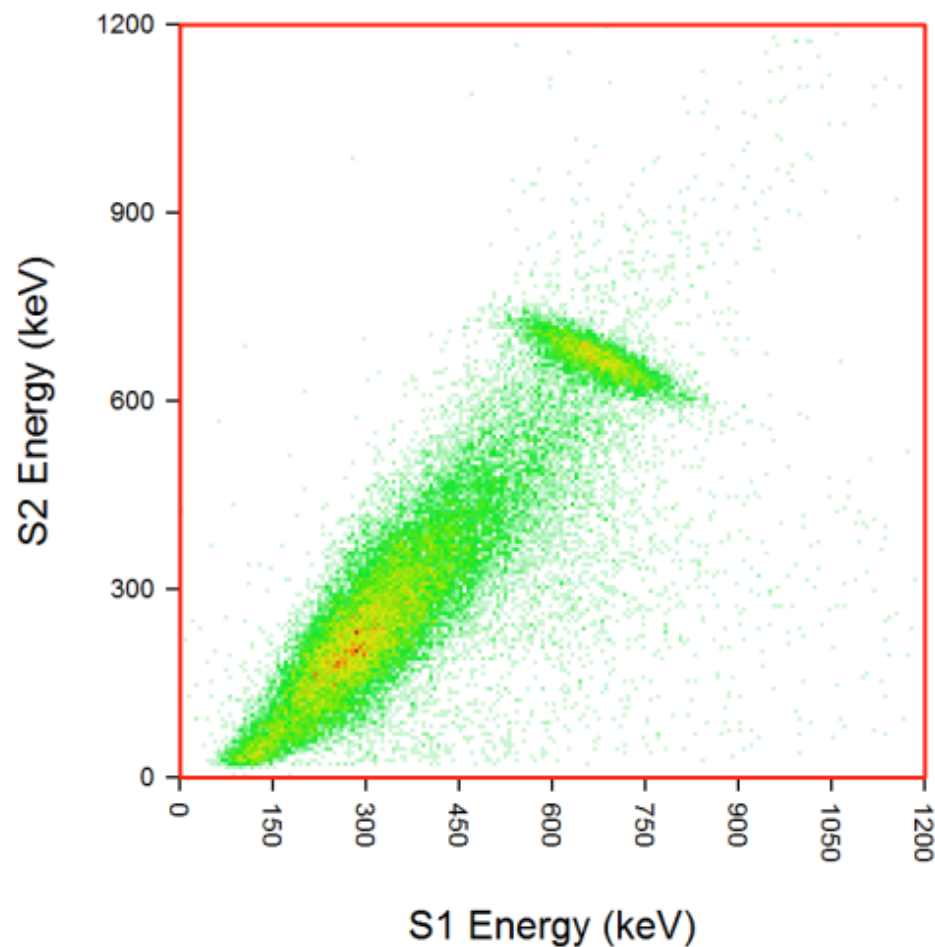
Single electrons in PIXeY



Single electrons in PIXeY

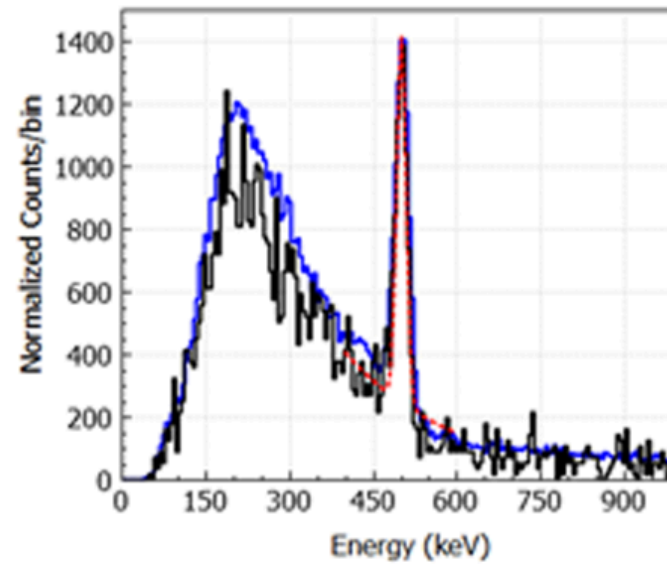
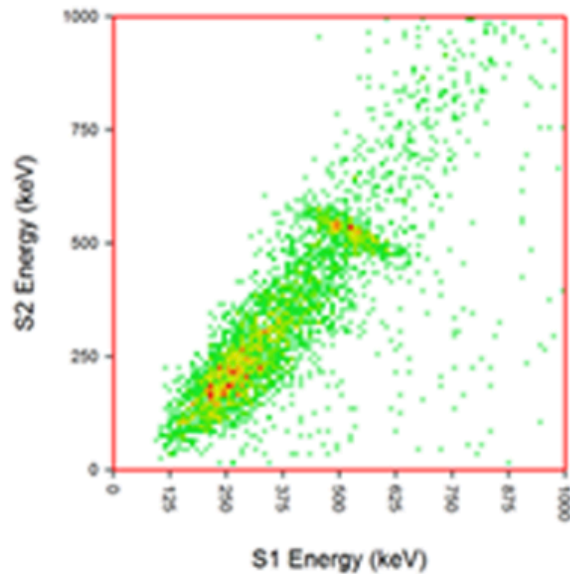


Anticorrelation in S1 and S2 Signals

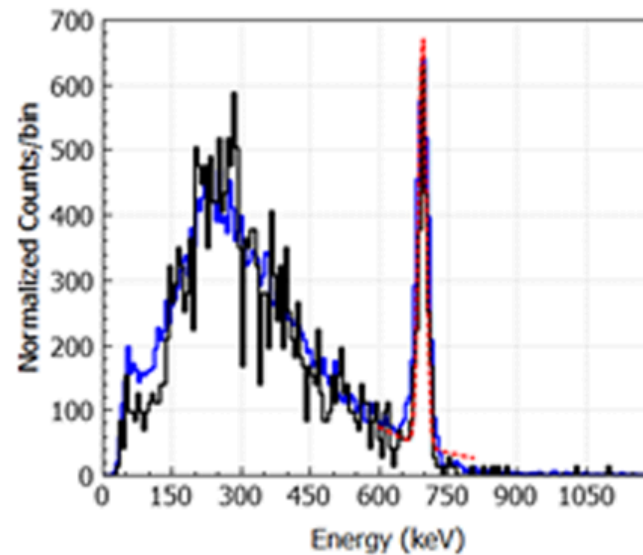
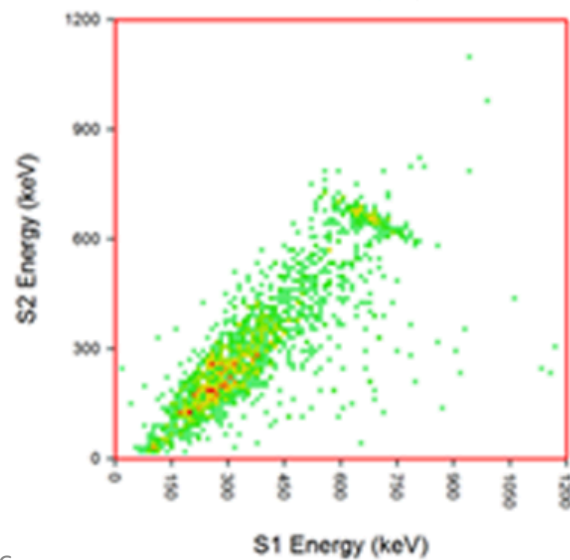


Gamma-ray data from Cs-137 as measured in the PIXeY detector. Monoenergetic gamma ray absorption events in LXe produce both light (S1) and charge (S2) signals, which are anticorrelated.

Energy resolution measurements in PIXeY, with 1 kV/cm drift field

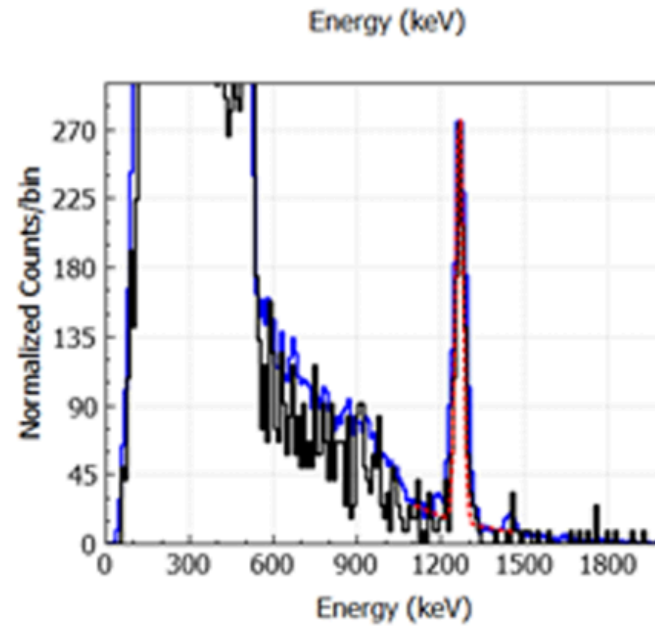
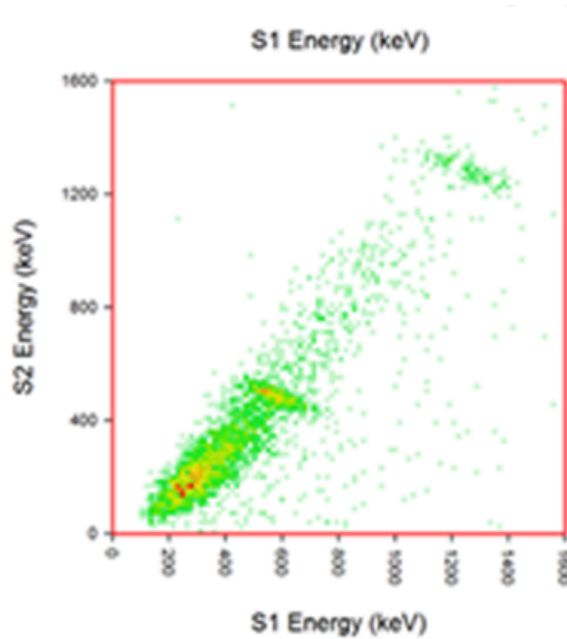


^{22}Na (511 keV)
3.9% FWHM

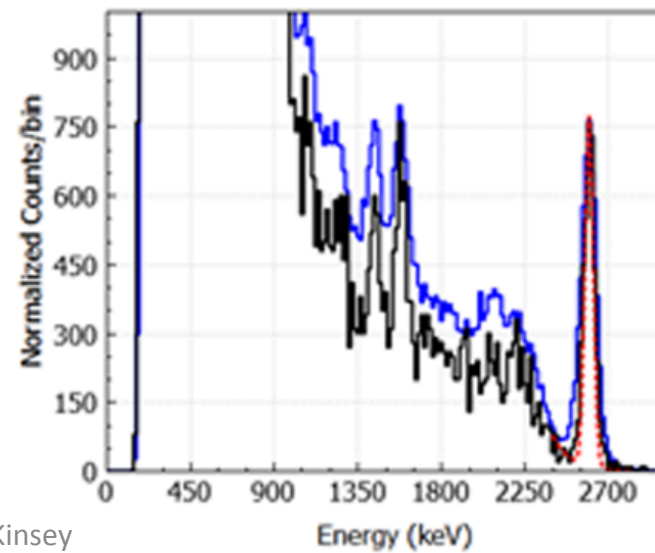
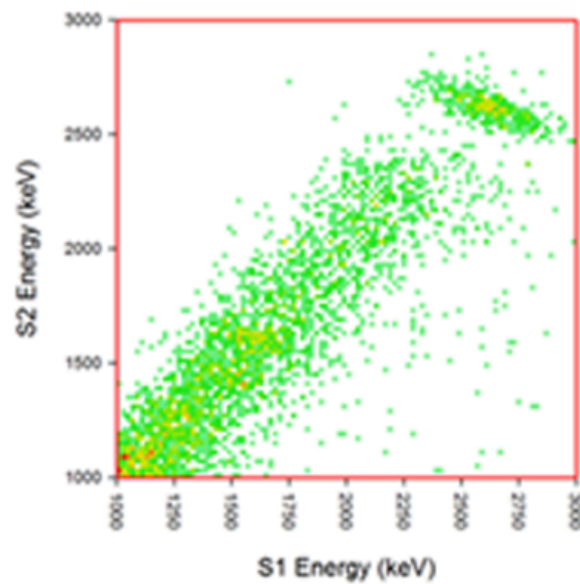


^{137}Cs (662 keV)
2.8% FWHM

Energy resolution measurements in PIXeY, with 1 kV/cm drift field



^{22}Na (1.3 MeV)
2.4% FWHM

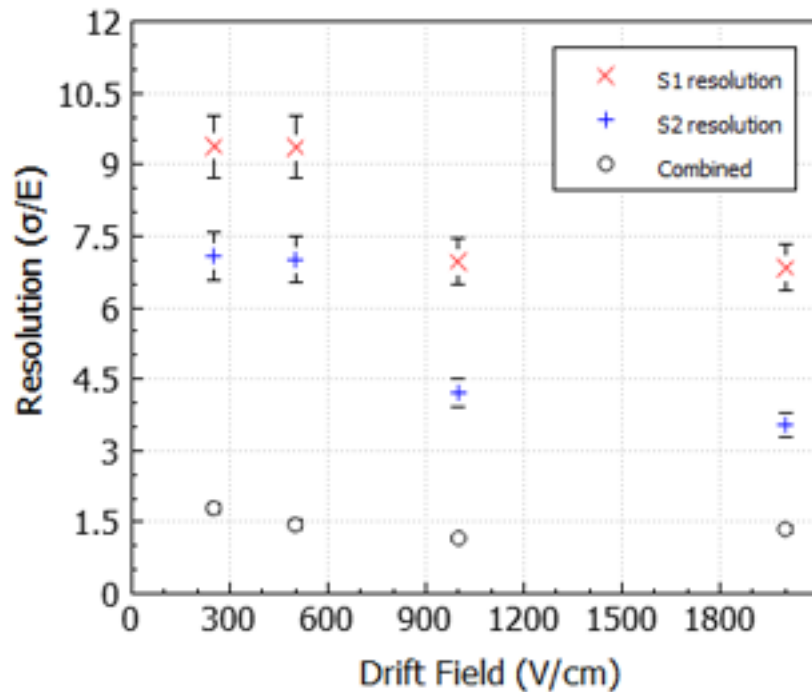


^{228}Th (2.6 MeV)
2.1% FWHM

Gamma-Ray Energy Resolution Measurements with PIXeY

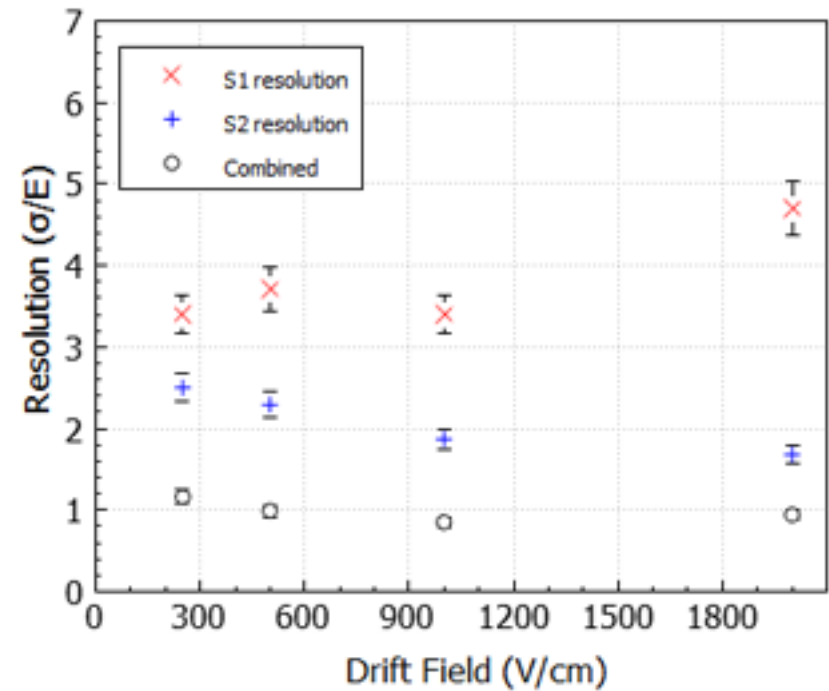
^{137}Cs (662 keV)

2.8% FWHM at 1000 V/cm



^{228}Th (2.6 MeV)

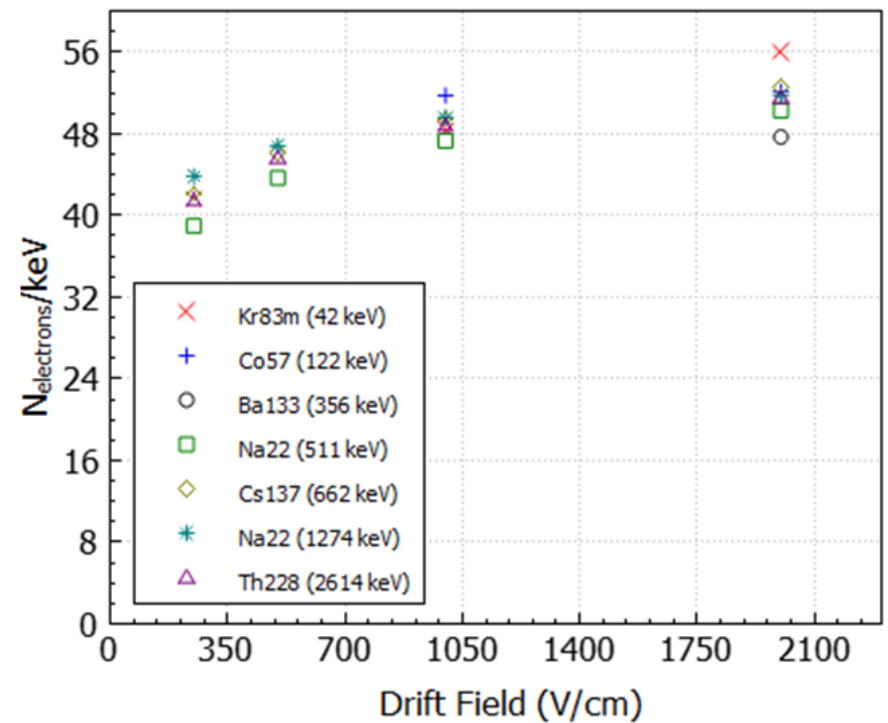
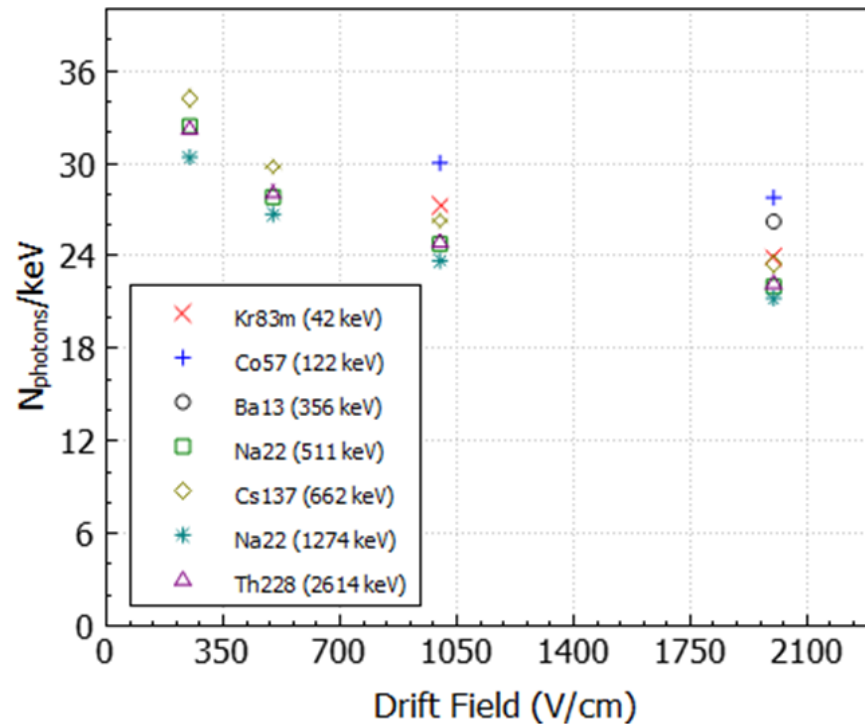
2.1% FWHM at 1000 V/cm



Still have good energy resolution at low drift field!
3.9% FWHM at 250 V/cm, versus 2.8% at 1000 V/cm

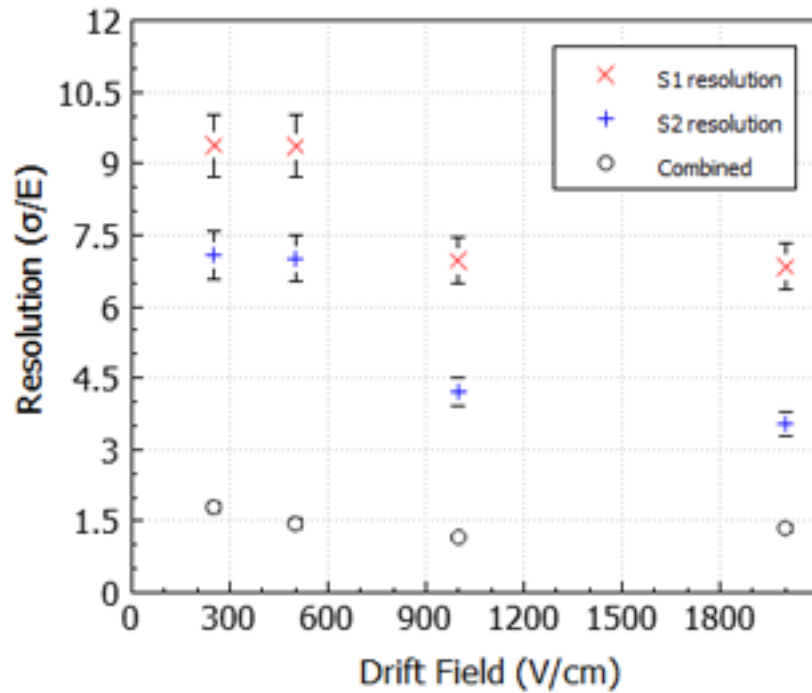
Light and Charge Yield Measurements with PIXeY

Uses known W value of 13.7 eV

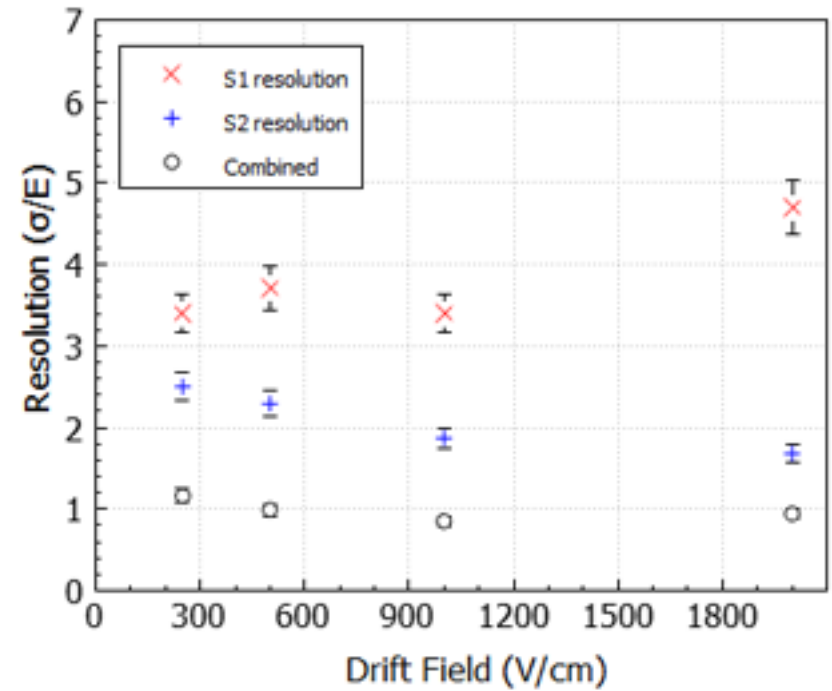


Gamma-Ray Energy Resolution Measurements with PIXeY

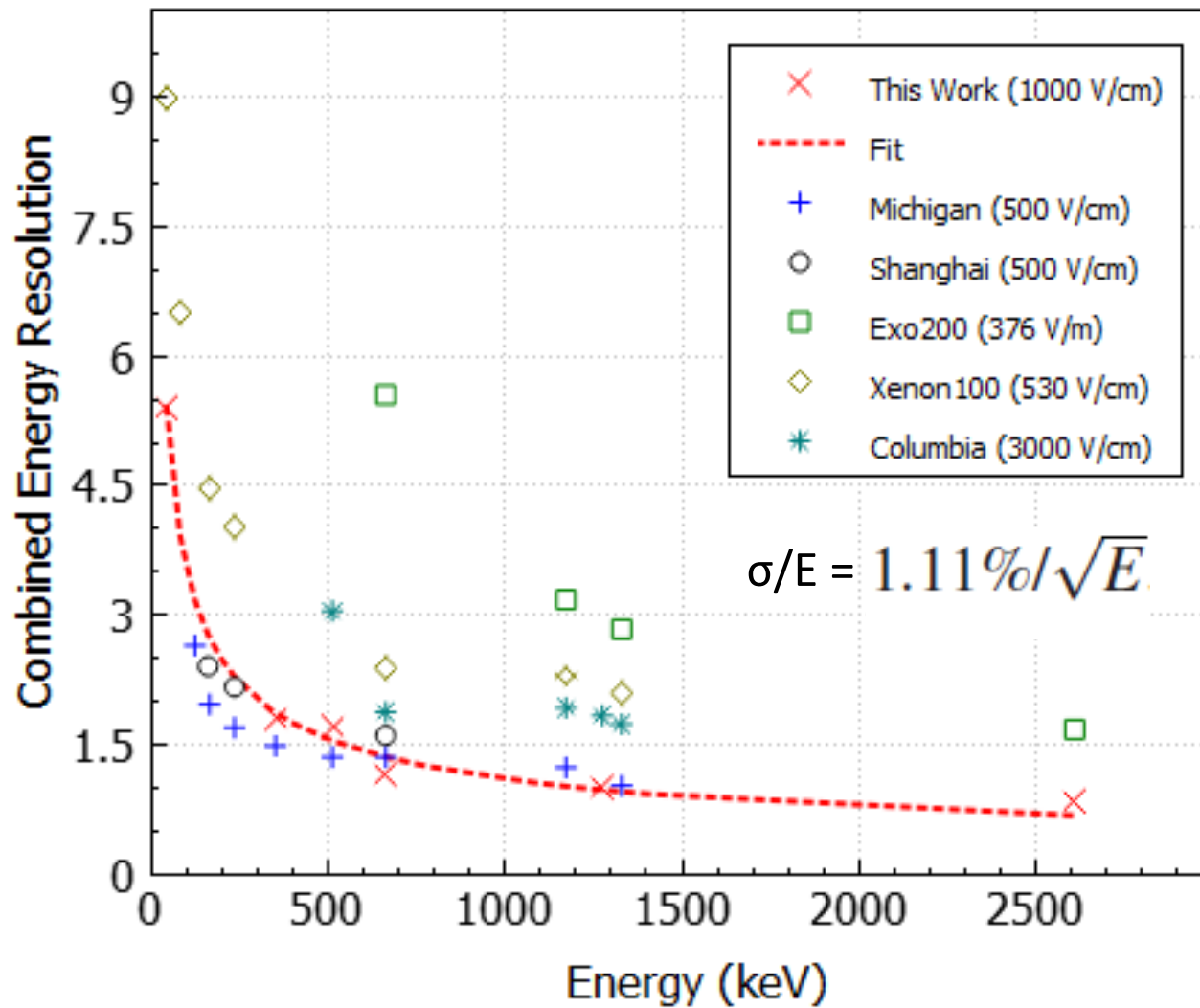
Cs-137 (662 keV)



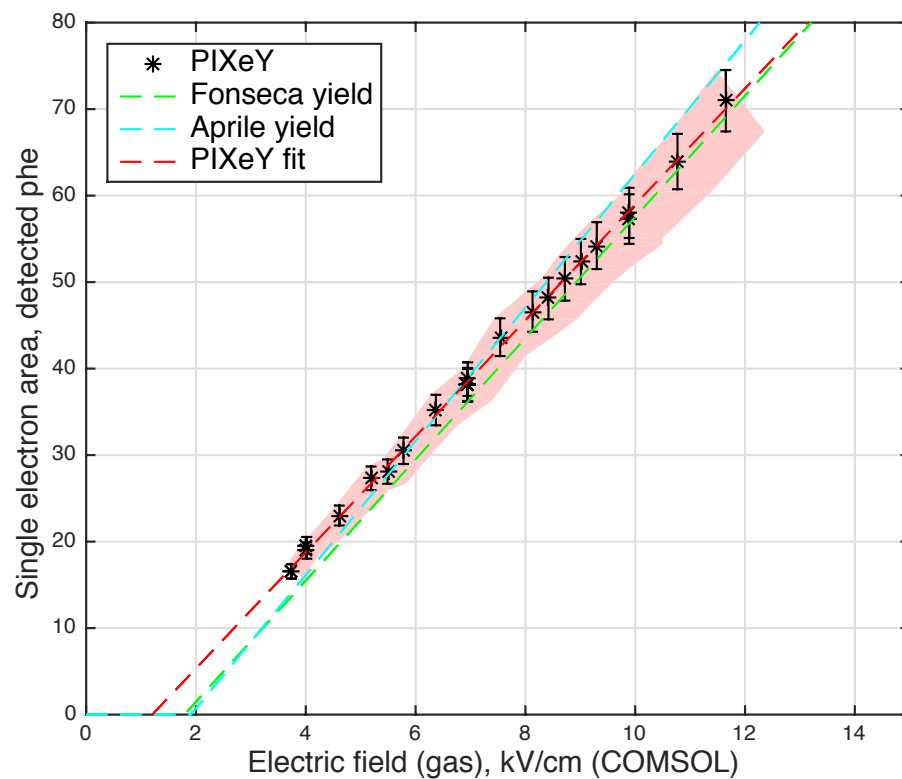
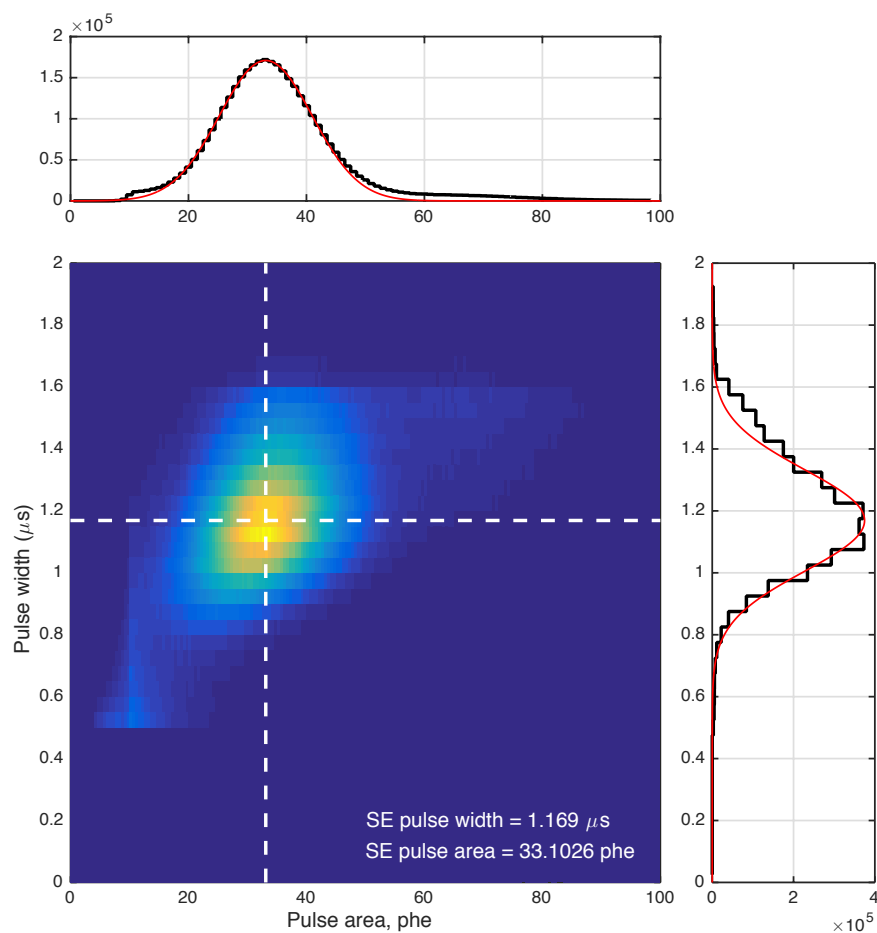
208-Tl (2.6 MeV)



Gamma-Ray Energy Resolution Measurements with PIXeY

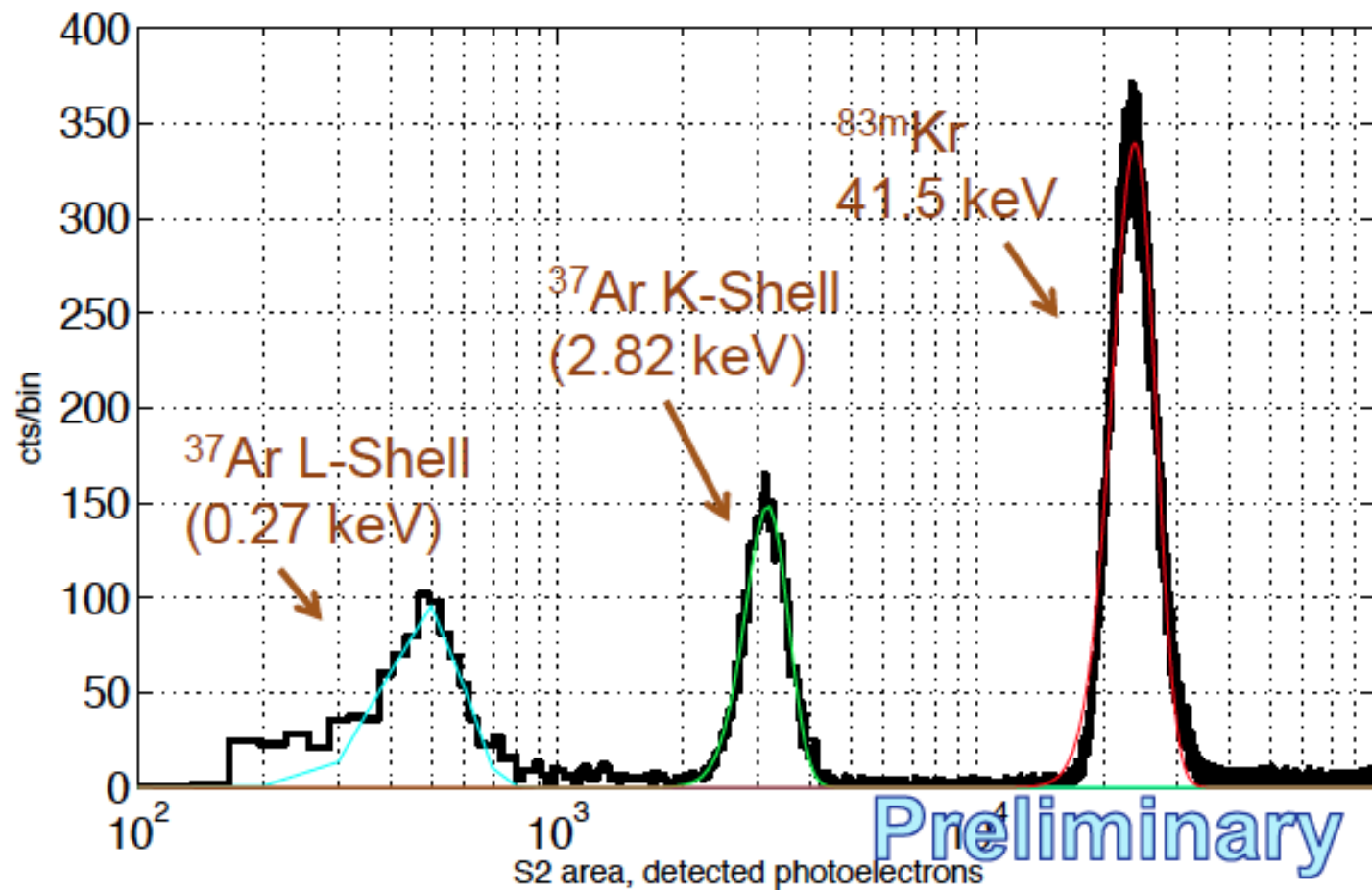


Single electron pulse area, versus electric field in the gas phase



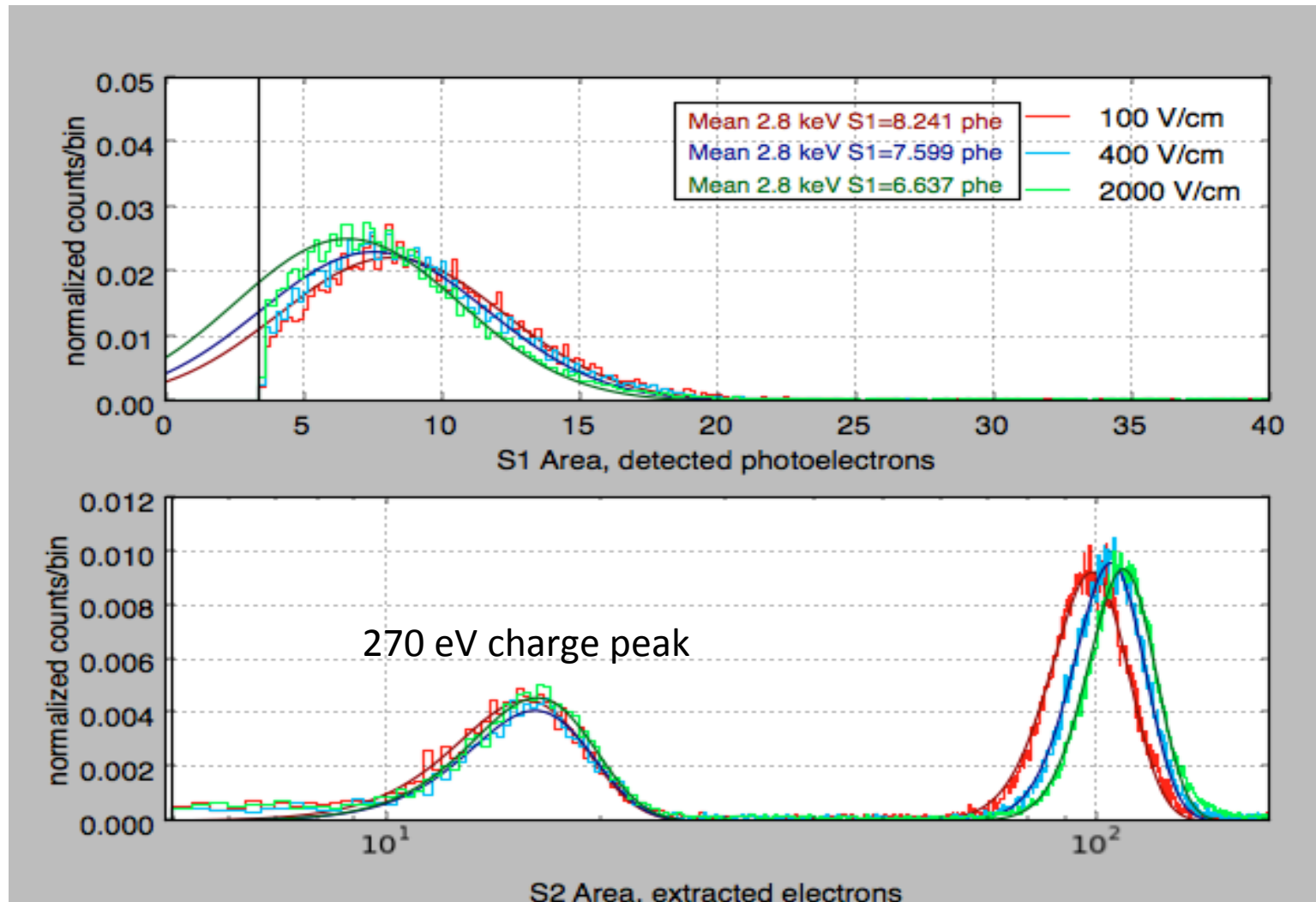
Detector Response Studied Down to Extremely Low Energies

^{37}Ar produced using $^{40}\text{Ca}(n,\alpha)^{37}\text{Ar}$

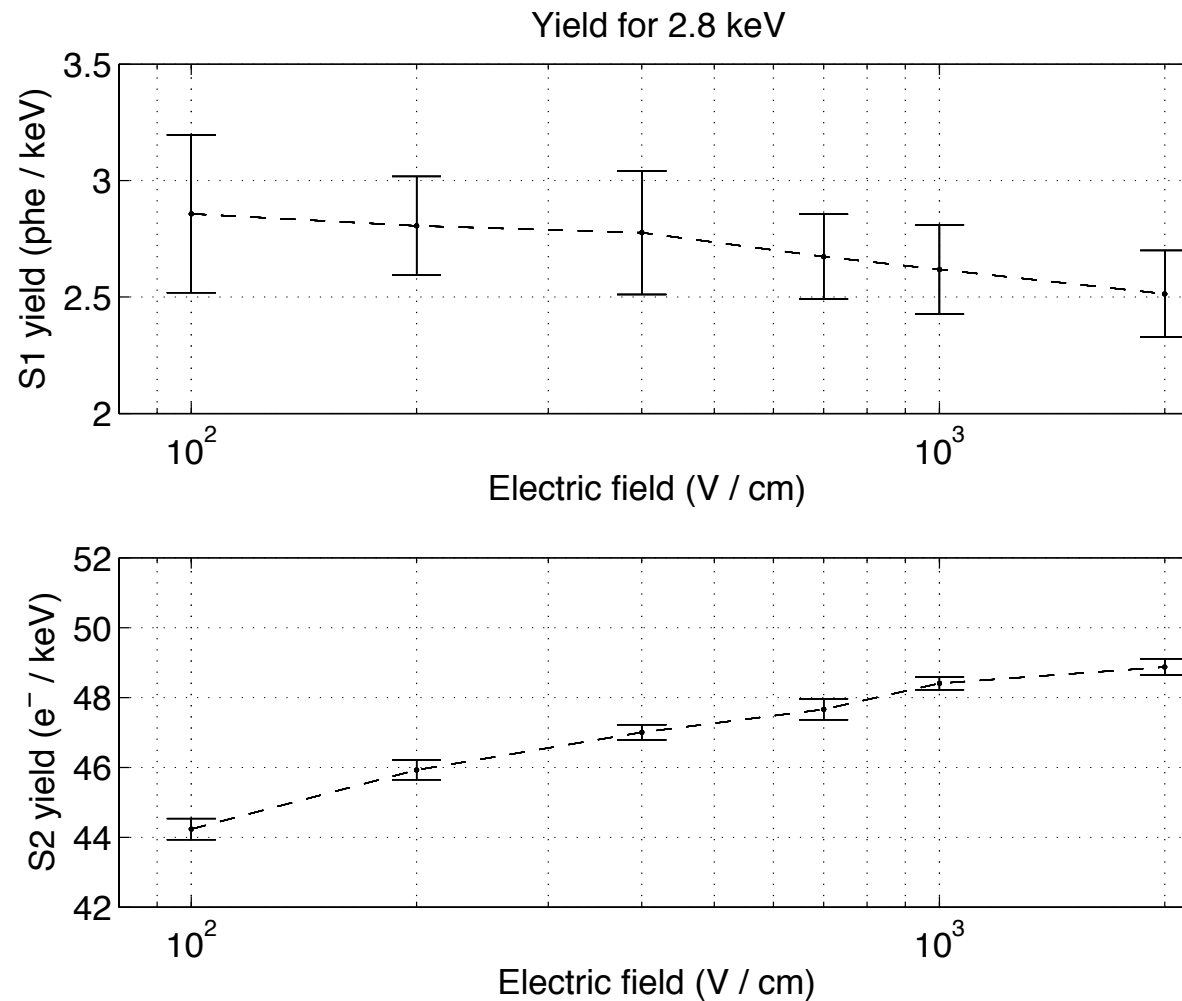


These calibrations use Ar-37 and Kr-83m isotopes, doped into the PIXeY detector

Variation of ^{37}Ar signal with drift field

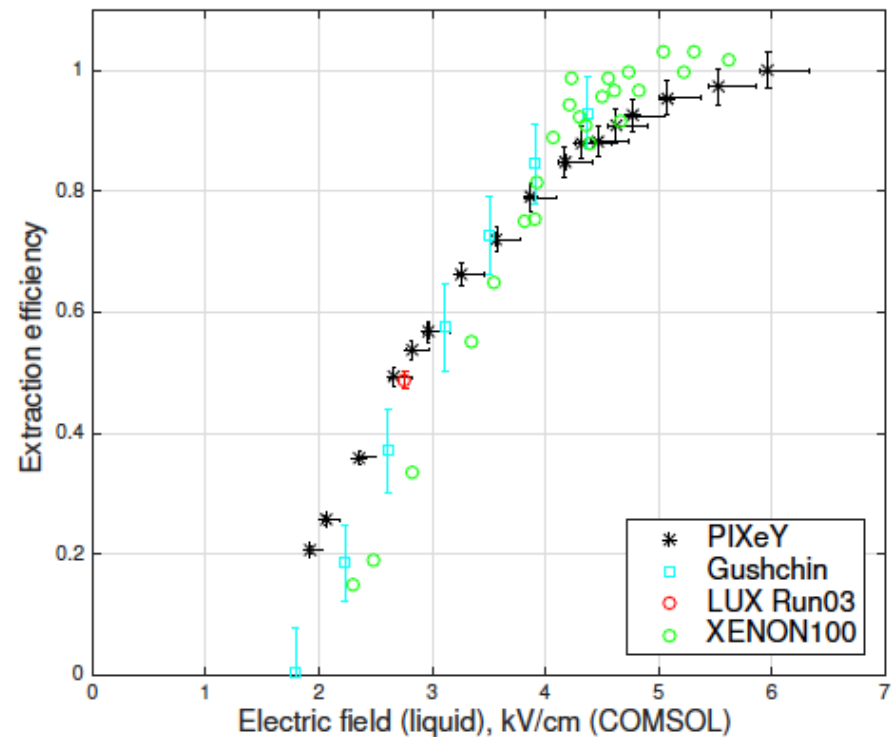
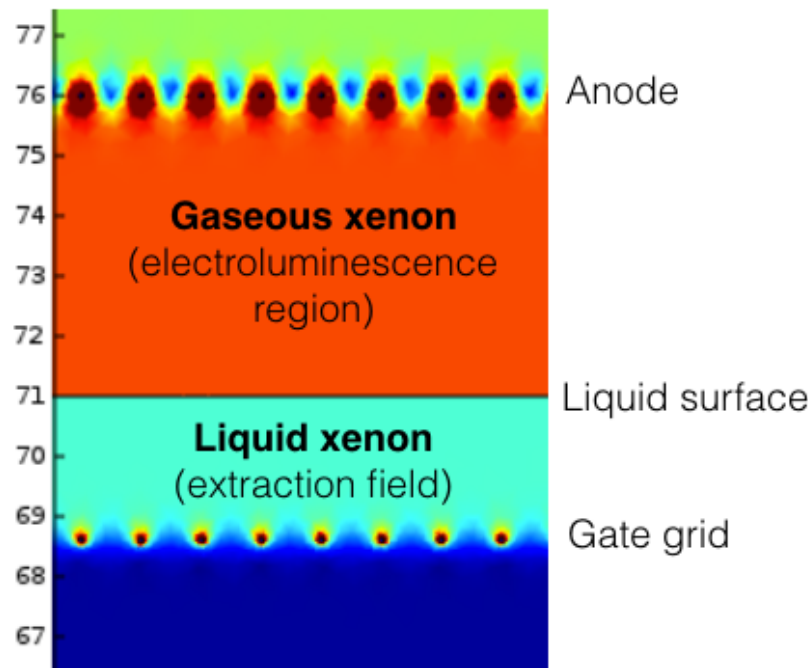


Detector Response Studied Down to Extremely Low Energies



These calibrations use Ar-37 and Kr-83m isotopes, doped into the PIXeY detector

New measurement of electron extraction efficiency



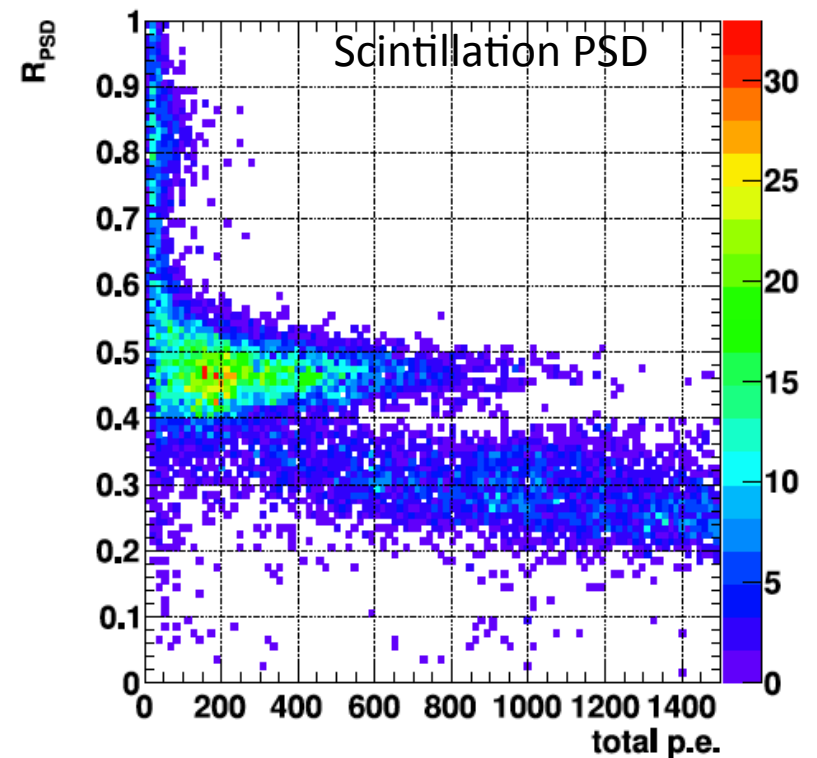
This is the probability that an electron in liquid Xe is extracted into the gaseous Xe, for a given electric field applied across the liquid/gas interface.

Neutron vs Gamma-Ray Discrimination

- Neutron energy deposition is suppressed by a factor of ~ 40 by simple kinematics:

$$E_{Xe} = 2E_n \frac{m_n m_{Xe}}{(m_n + m_{Xe})^2} (1 - \cos \theta)$$

- Charge-to-light ratio is suppressed for neutrons
Standard method for dark matter searches.
- Scintillation pulse-shapes are faster for neutrons, slower for gammas
(K. Ueshima et al, arXiv:1106.2209)

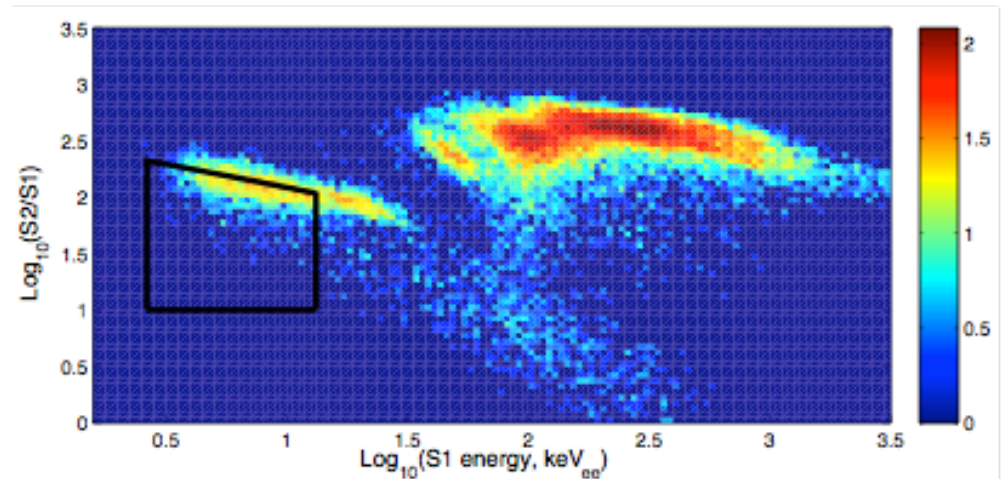


Neutron vs Gamma-Ray Discrimination

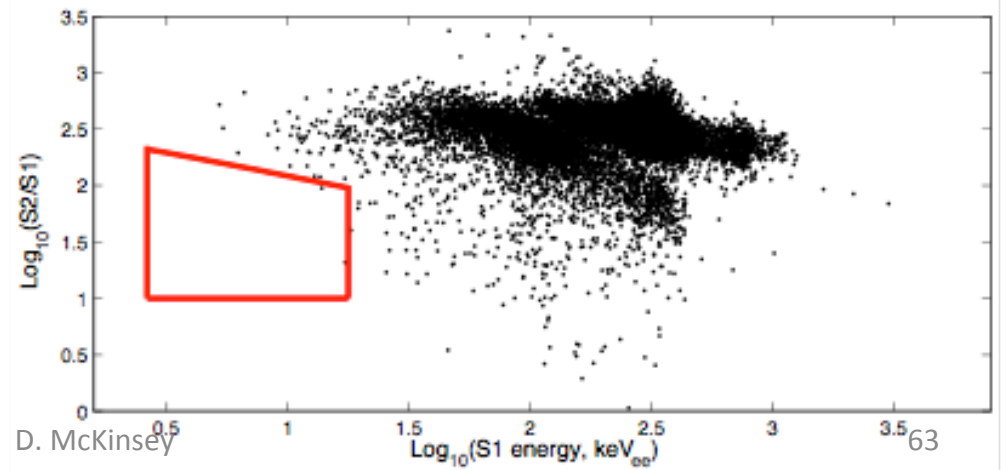
Overall factor of 40,000 gamma-ray rejection

Factor of 40 from kinematics, > 1000 from charge/light ratio.

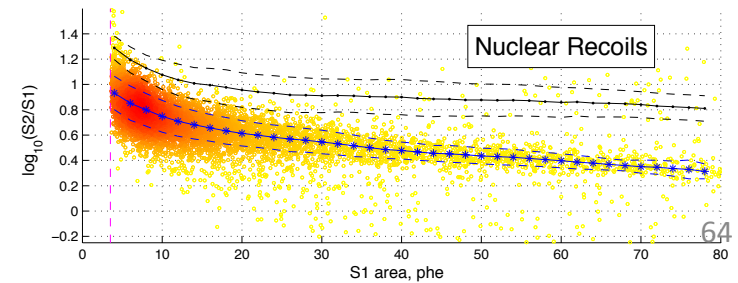
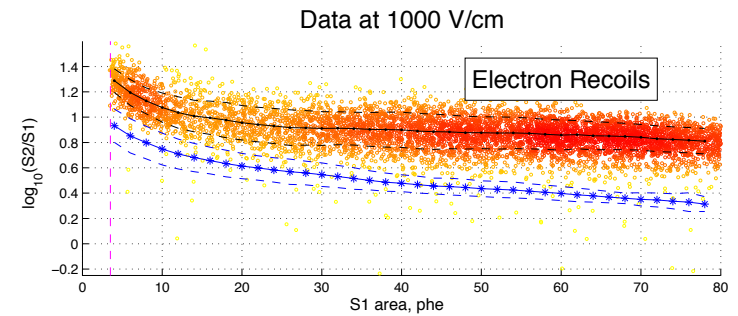
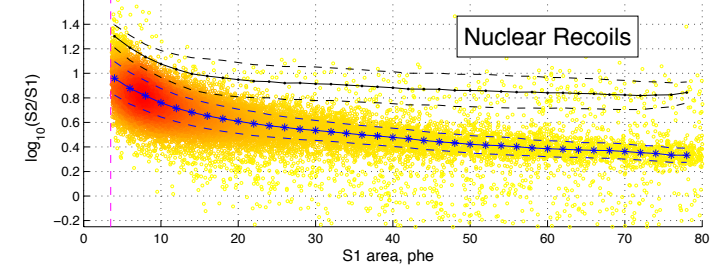
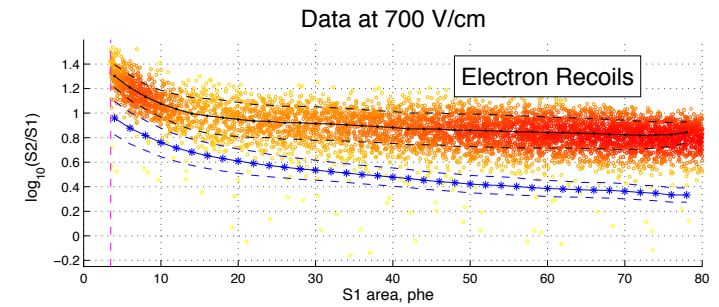
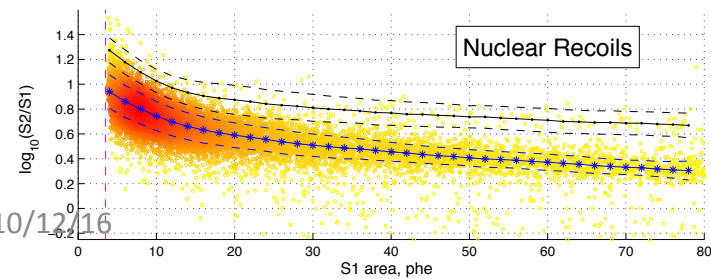
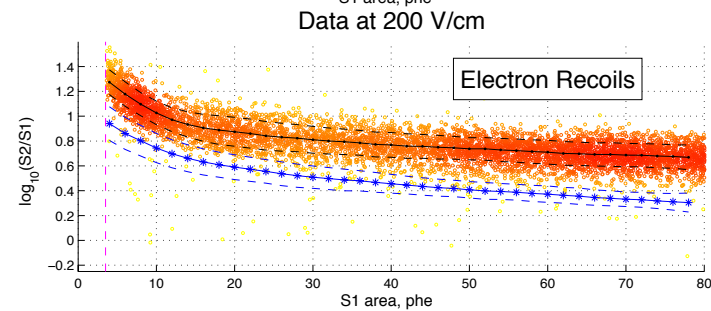
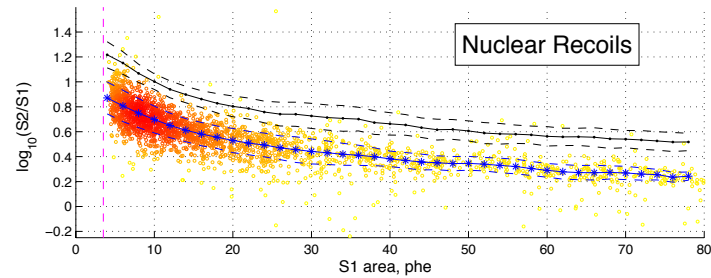
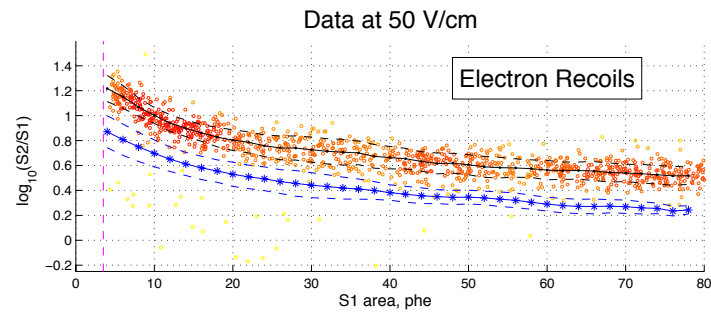
PIXeY neutron irradiation →



PIXeY gamma irradiation →



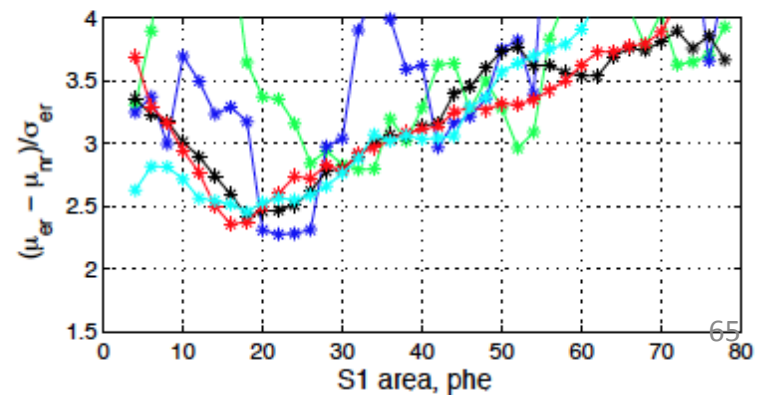
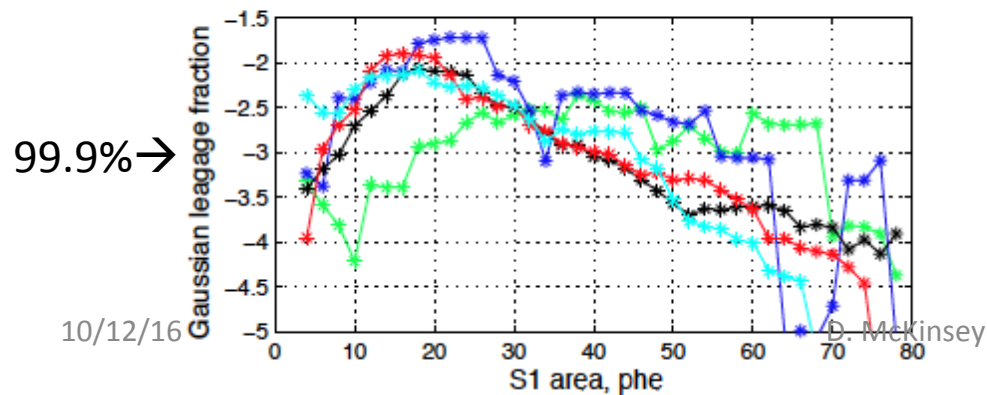
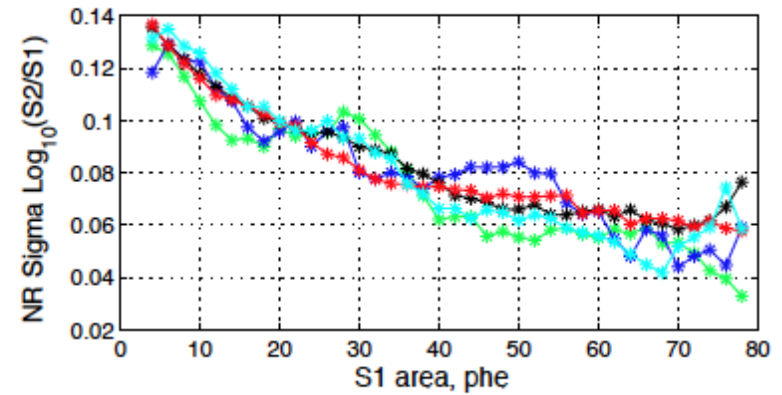
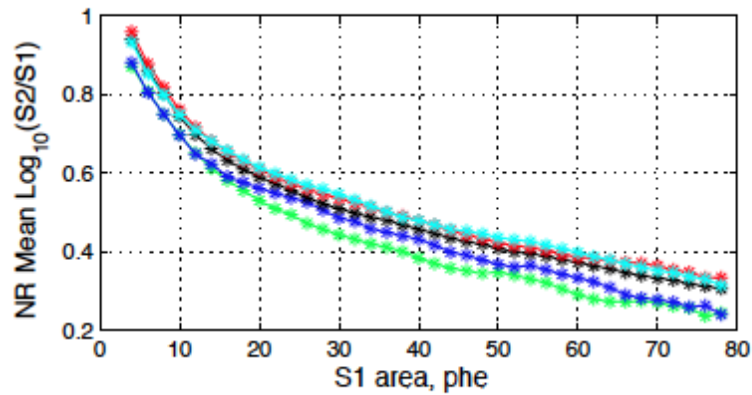
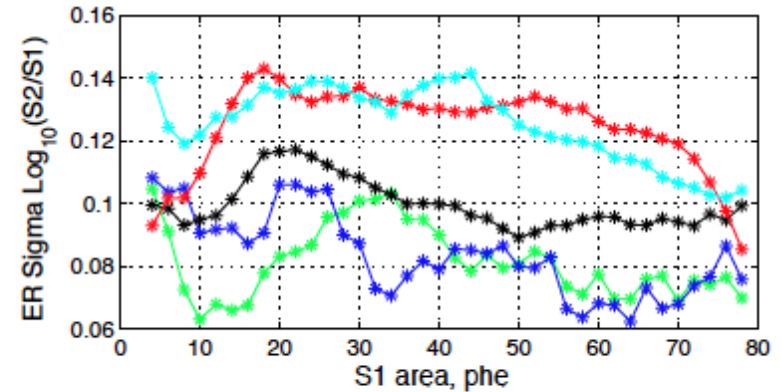
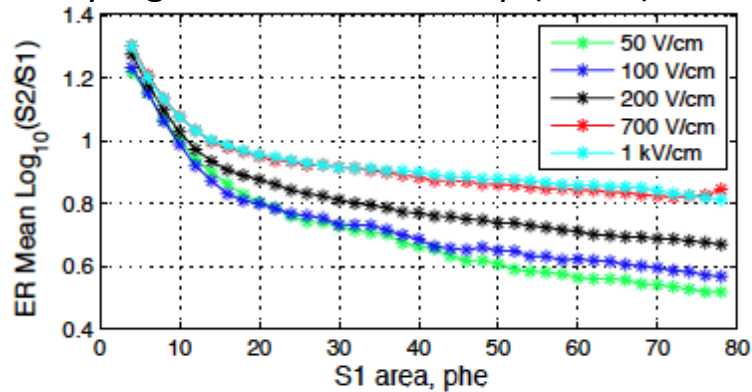
Neutron vs Gamma-Ray Response Studied in PIXeY at a Variety of Electric Fields



Neutron/Gamma Discrimination Through Charge/Light Ratio

Typical discrimination efficiency of 99.9%, varying somewhat with energy

Very high field does not help (much) with discrimination



10/12/16

D. McKinsey

65

Scale Up ≈ 50 in Fiducial Mass

LZ

Total mass – 10 T

WIMP Active Mass – 7 T

WIMP Fiducial Mass – 5.6 T





LZ = LUX + ZEPLIN

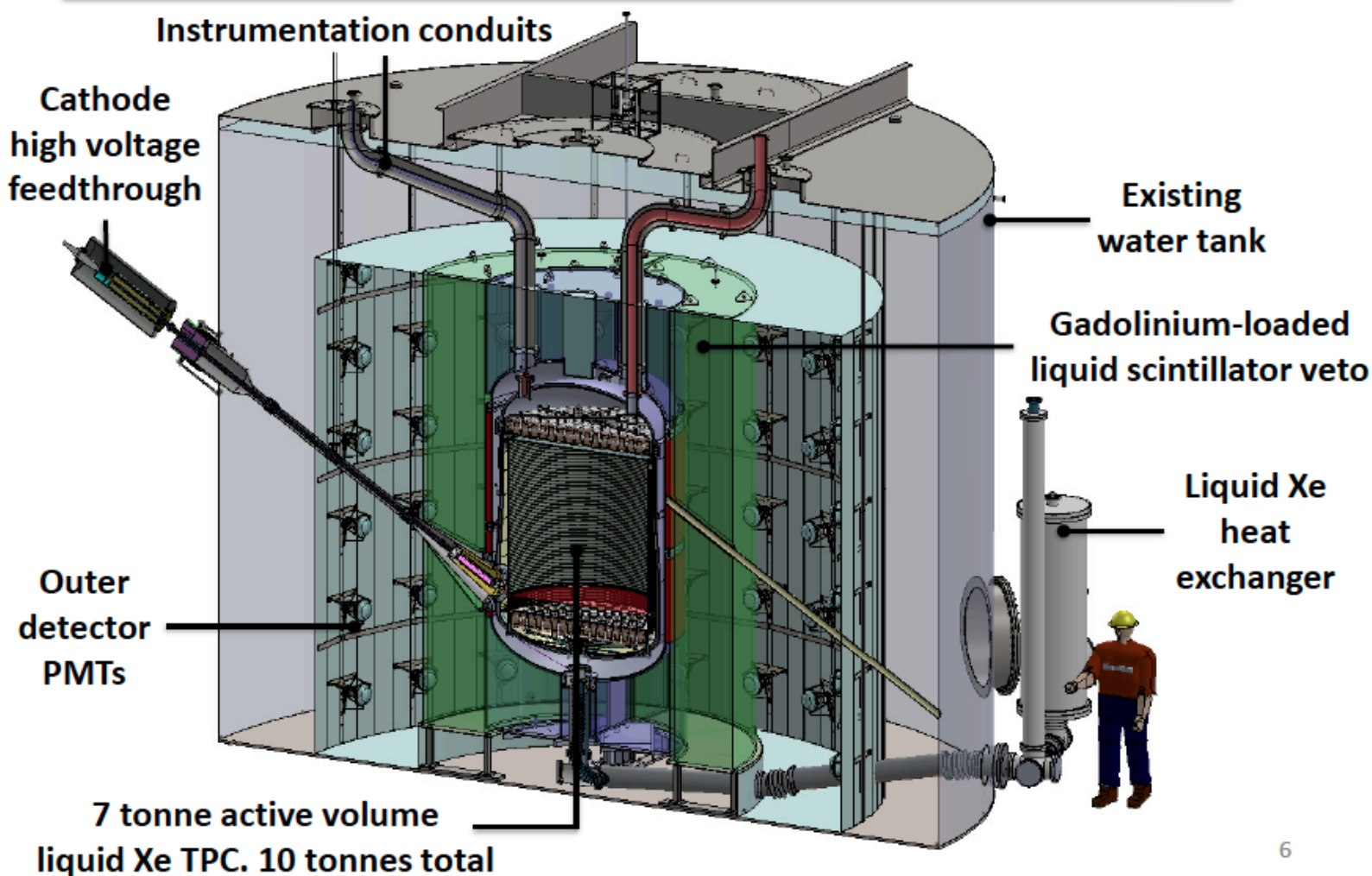
32 institutions currently
About 200 people

LIP Coimbra (Portugal)
MEPhI (Russia)
Edinburgh University (UK)
University of Liverpool (UK)
Imperial College London (UK)
University College London (UK)
University of Oxford (UK)
STFC Rutherford Appleton Laboratories (UK)
University of Sheffield (UK)

University of Alabama
University at Albany SUNY
Berkeley Lab (LBNL)
University of California, Berkeley
Brookhaven National Laboratory
Brown University
University of California, Davis
Fermi National Accelerator Laboratory
Kavli Institute for Particle Astrophysics & Cosmology
Lawrence Livermore National Laboratory
University of Maryland
University of Michigan
Northwestern University
University of Rochester
University of California, Santa Barbara
University of South Dakota
South Dakota School of Mines & Technology
South Dakota Science and Technology Authority
SLAC National Accelerator Laboratory
Texas A&M
Washington University
University of Wisconsin



LZ Detector Overview



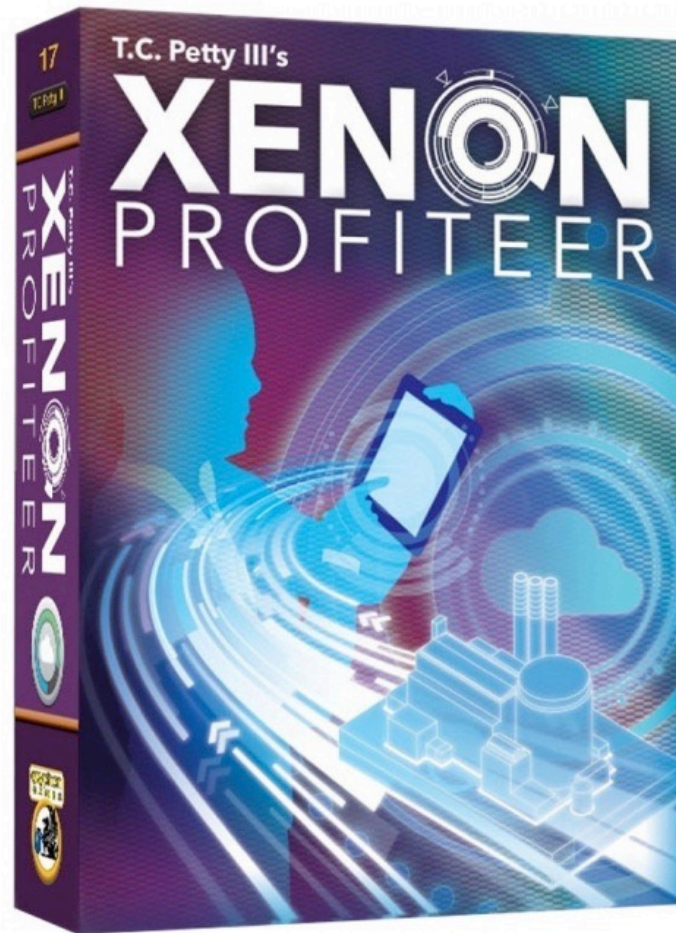
6

LZ Timeline

Year	Month	Activity
2012	March	LZ (LUX-ZEPLIN) collaboration formed
	May	First Collaboration Meeting
	September	DOE CD-0 for G2 dark matter experiments
2013	November	LZ R&D report submitted
2014	July	LZ Project selected in US and UK
2015	April	DOE CD-1/3a approval, similar in UK
		Begin long-lead procurements(Xe, PMT, cryostat)
2016	September	DOE CD-2/3b approval, baseline, all fab starts
2017	June	Begin preparations for surface assembly @ SURF
2018	July	Begin underground installation
2019	Feb	Begin commissioning

“In Xenon Profiteer, you use your entrepreneurial spirit and an Air Separation facility to isolate valuable Xenon and make a profit.”

“***Xenon Profiteer*** is a highly thematic, deck-deconstruction, euro game for 2-4 entrepreneurs in which each player takes control of their own Air Separation Facility and distills Xenon from their Systems to complete lucrative contracts. You will also physically expand your facility by building upgrades, pipelines, and acquiring new contracts and connecting them to your Center Console.”



Gryphon and Eagle Games

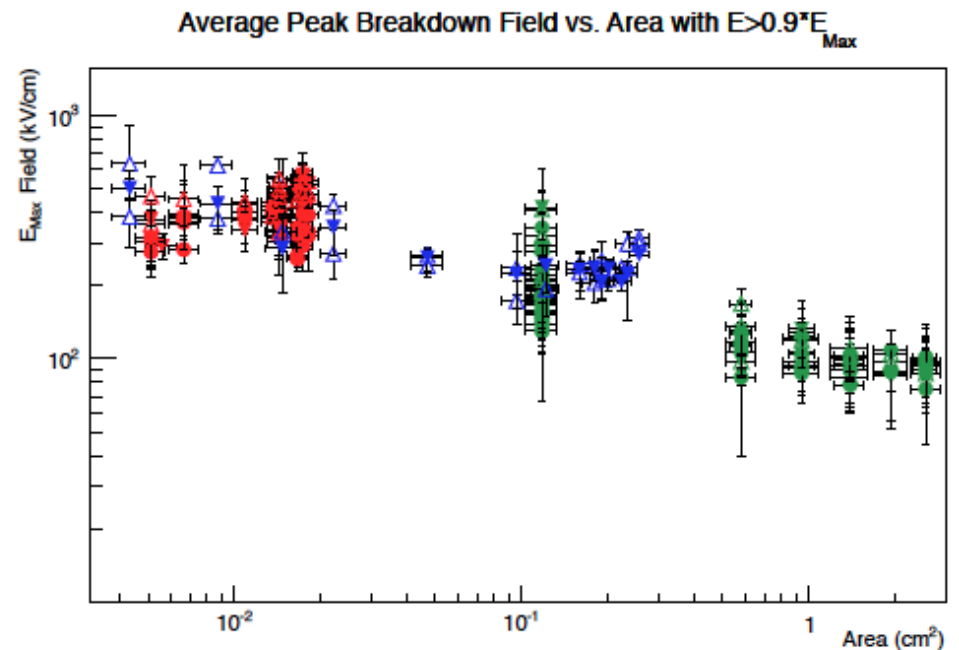
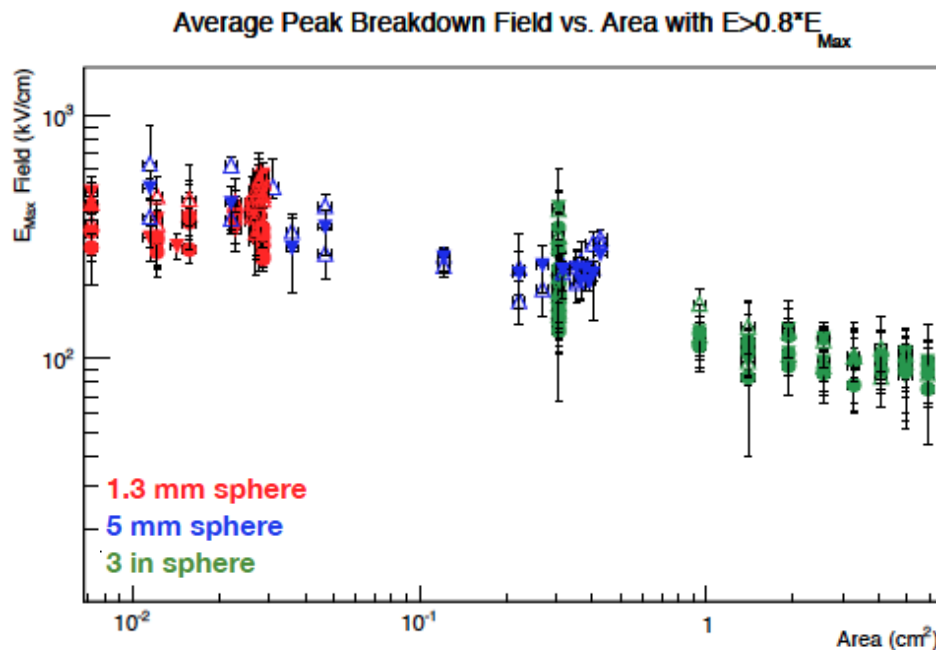
Scaling high voltage

- XENON10: Took data at 13 kV
- Xenon100: Planned for 30 kV cathode operation. Took data at 16 kV.
- LUX: Planned for “up to 100 kV” cathode operation. Took data at 8.5 kV.
- LZ is 2.5 times larger in length scale than LUX

HV Studies for MicroBoone (LAr)

(from S. Lockwitz, LArTPC R&D Workshop, 7/2014)

- E_{\max} vs Area (80% E_{\max} left; 90% right)



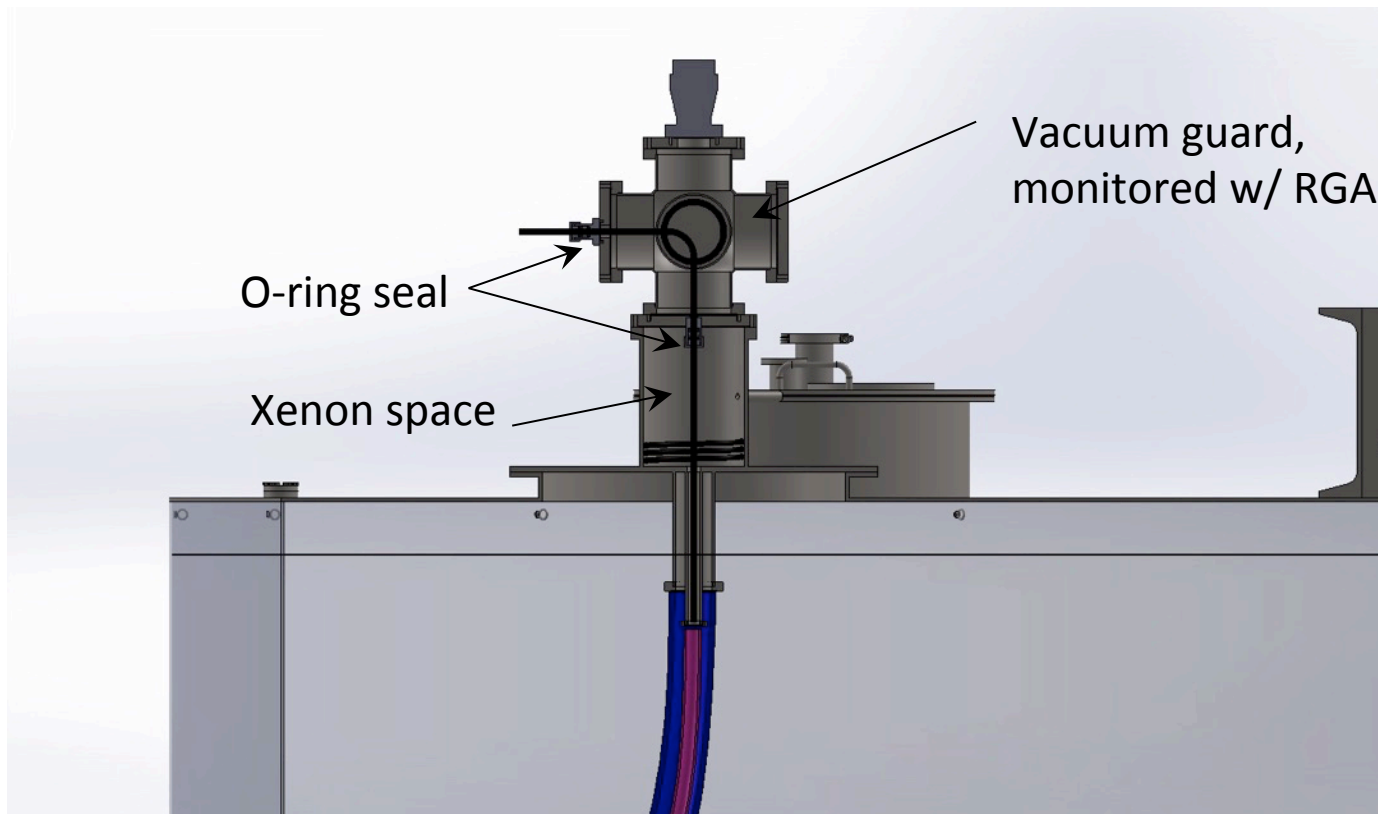
Efforts underway at LBNL to test this field-vs-area relationship in LXe



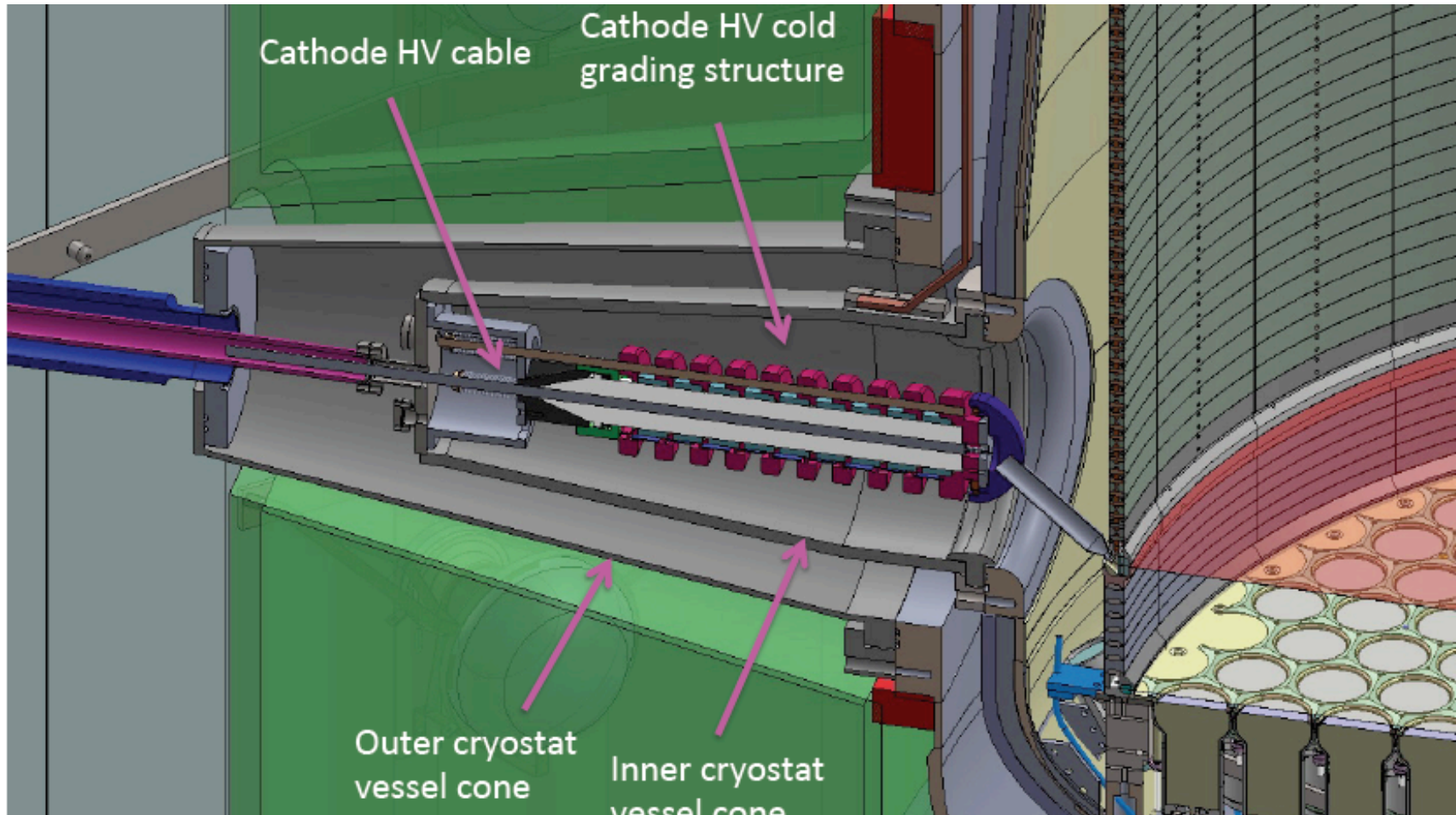
LZ Warm Feedthrough

At the warm end, the cable passes through an o-ring seal into a vacuum space. It then passes through a second o-ring seal into the air.

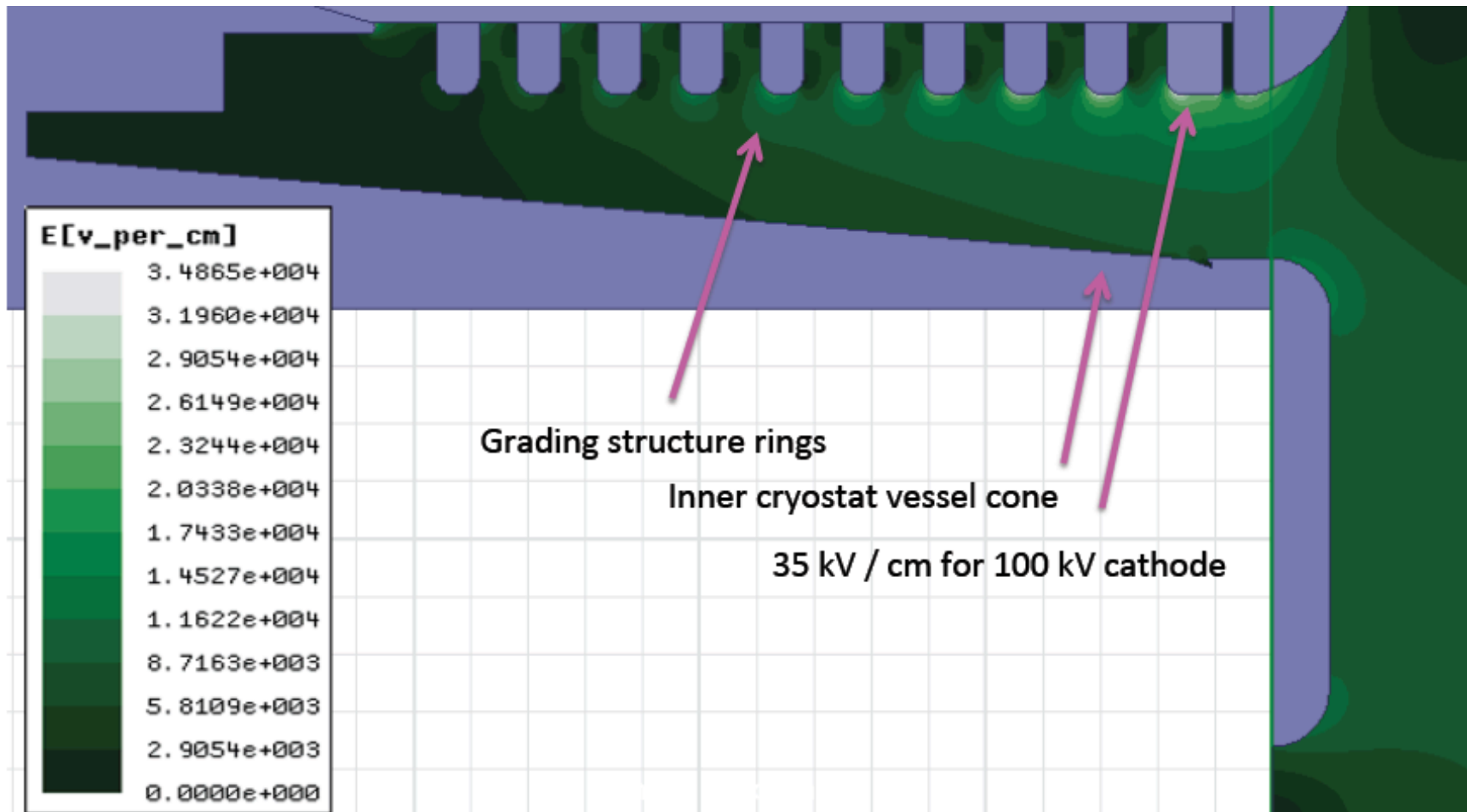
The xenon space and the vacuum space between the bellows terminate. Xe gas is removed from the xenon space from just above the liquid xenon and also from just below the o-ring seal. This forces a slow flow of xenon away from the detector.



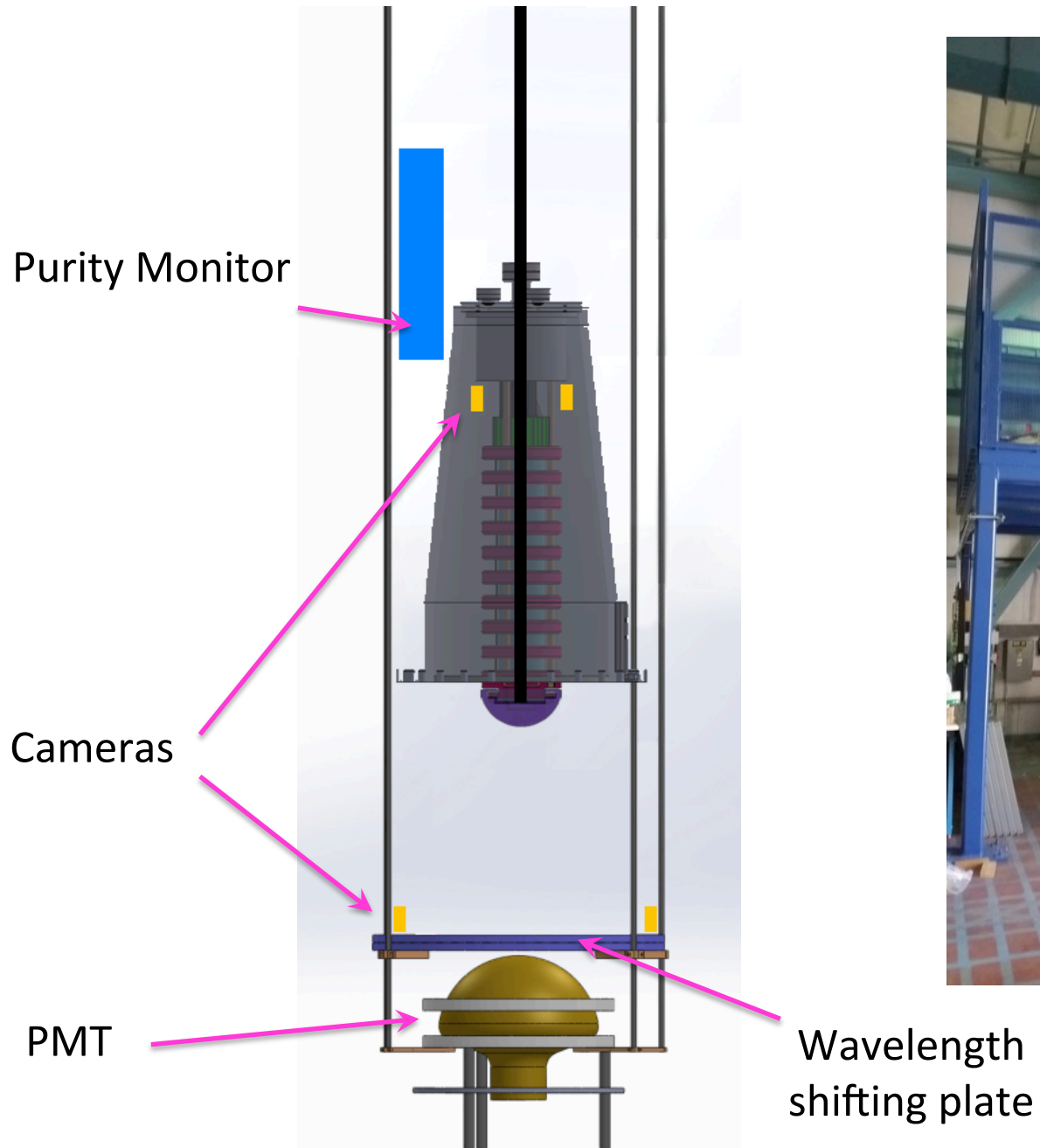
LZ High Voltage Delivery



LZ High Voltage Delivery

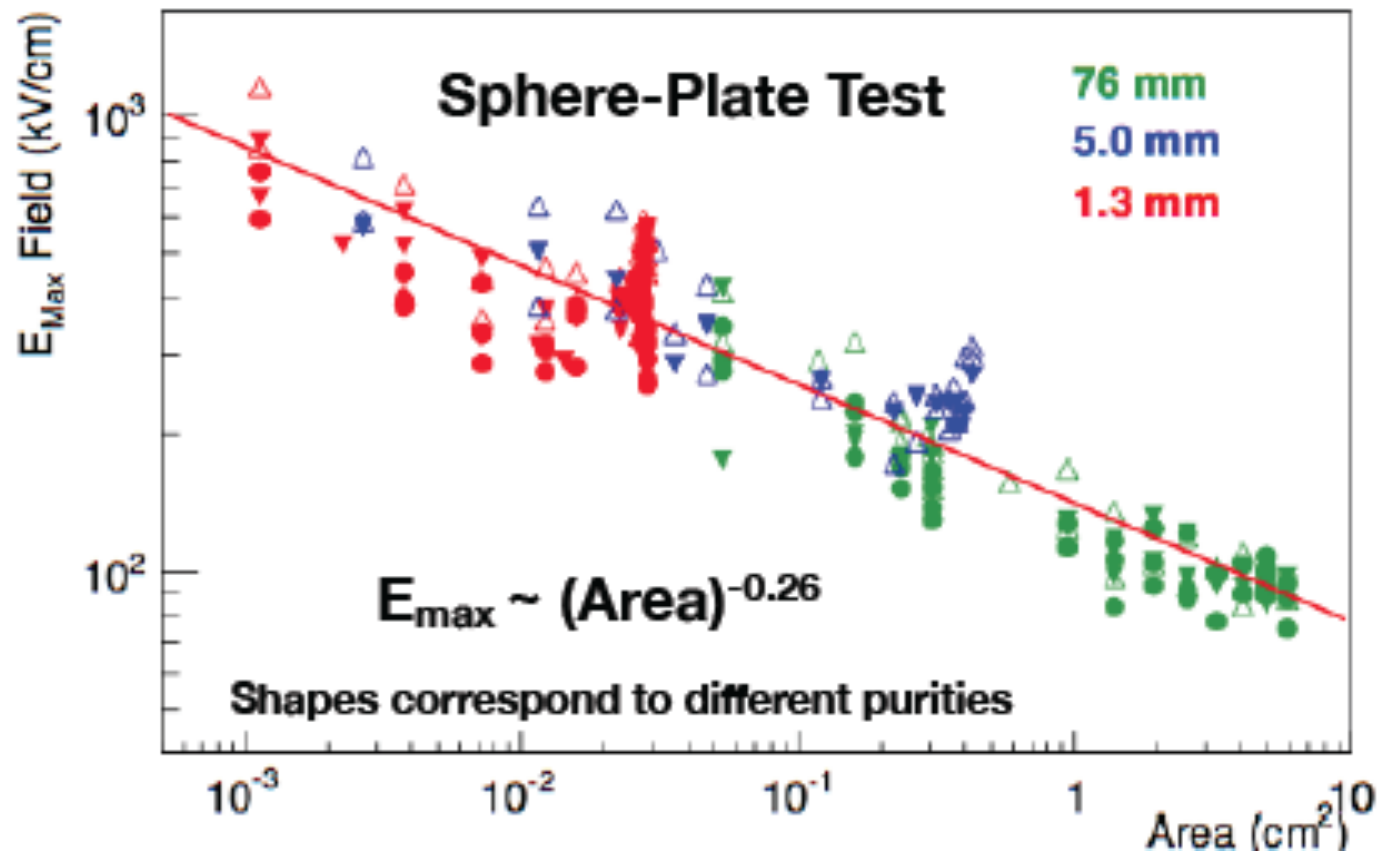


Planned HV testing of LZ Components in B77A



HV Studies for MicroBoone (LAr)

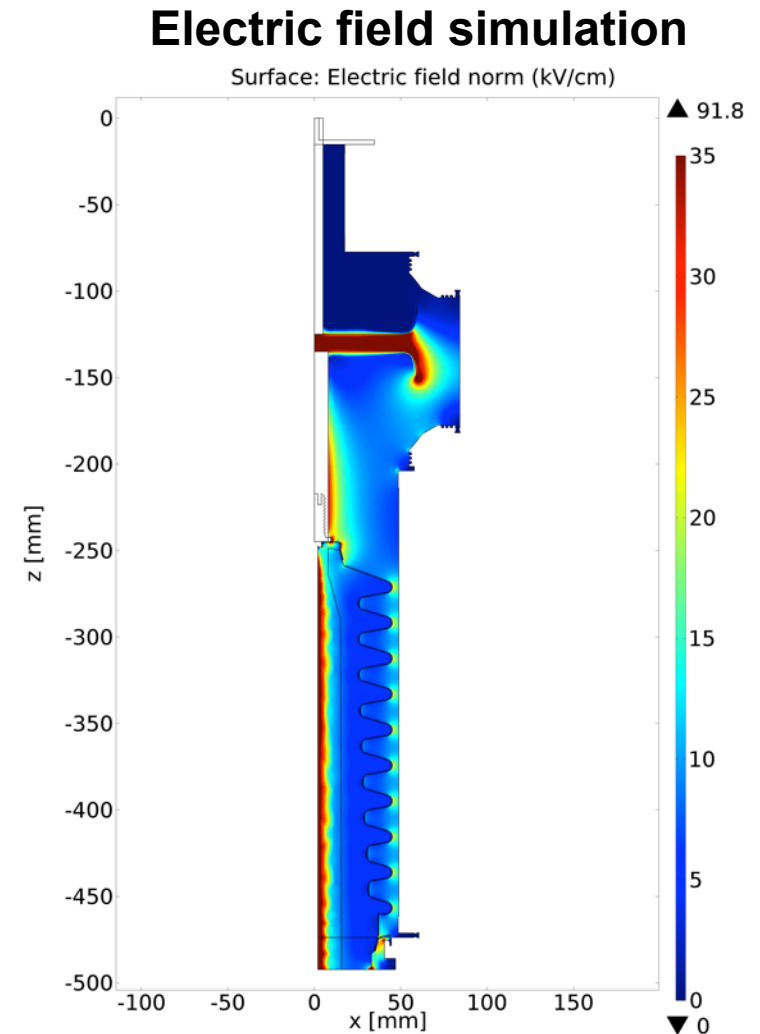
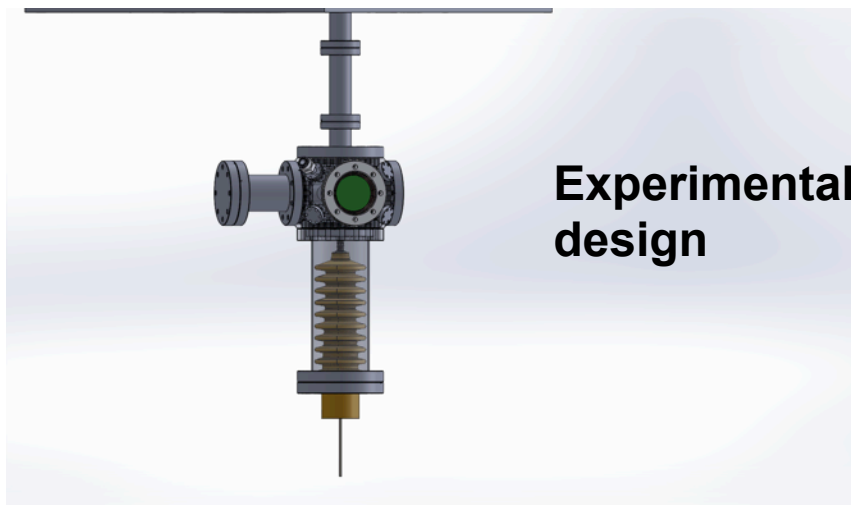
(from S. Lockwitz, CPAD 2016)



Does a similar relationship hold in LXe?

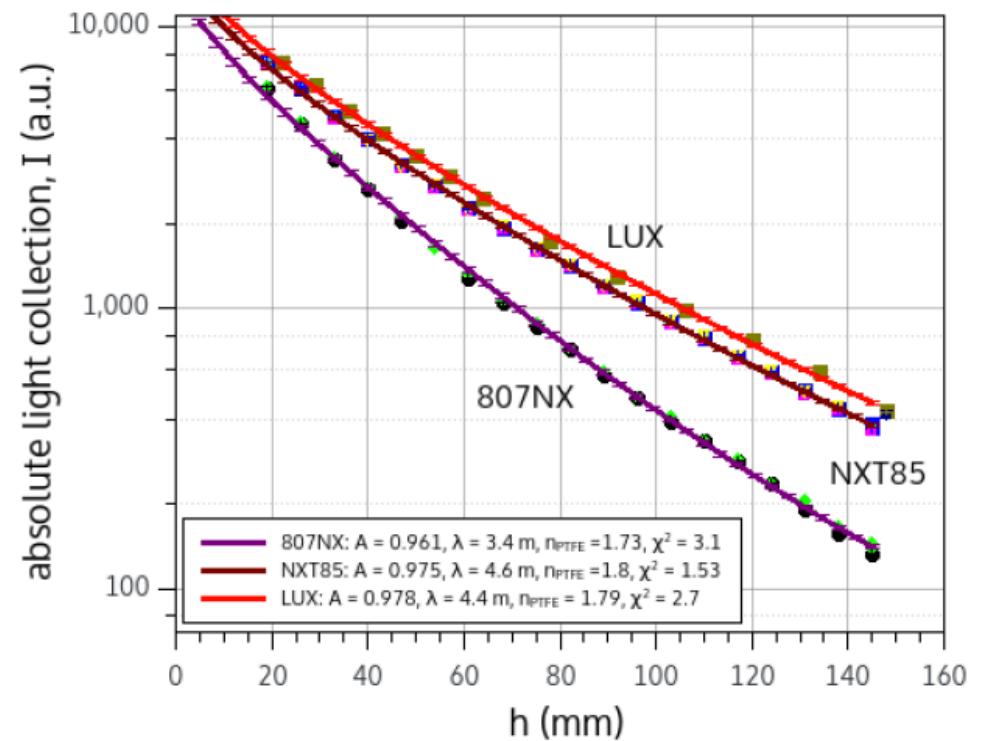
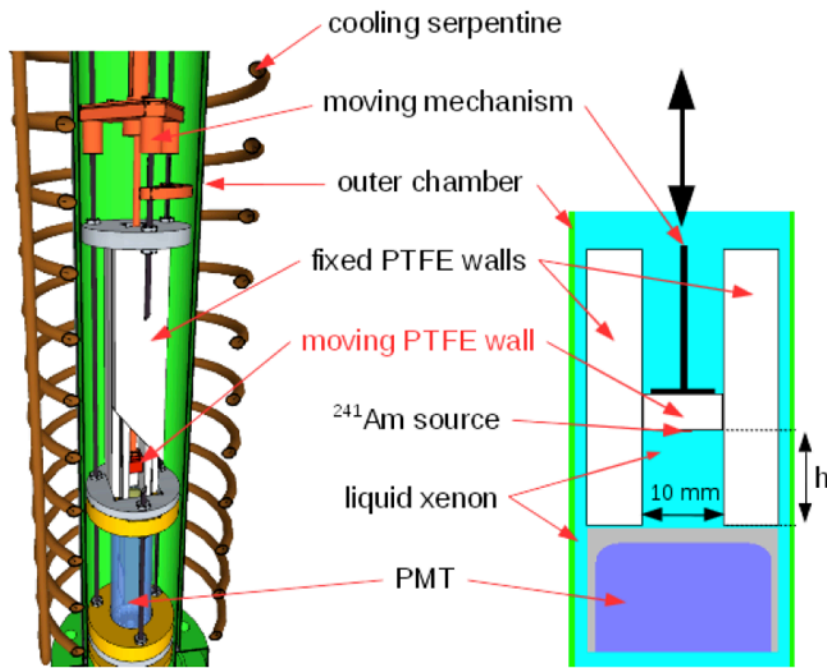
High Voltage Studies (LDRD-supported)

- The processes that determine high-voltage breakdown and electroluminescence in LXe and LAr are not well understood, but limit the voltages that may be applied to conductors immersed in these liquids.
- A dedicated study will be performed, varying voltages, electrode areas, gap sizes, and electrode surface preparation.
- The experimental apparatus includes a LXe or LAr-filled experimental chamber, with a movable electrode. Optical access allows viewing of breakdown events.



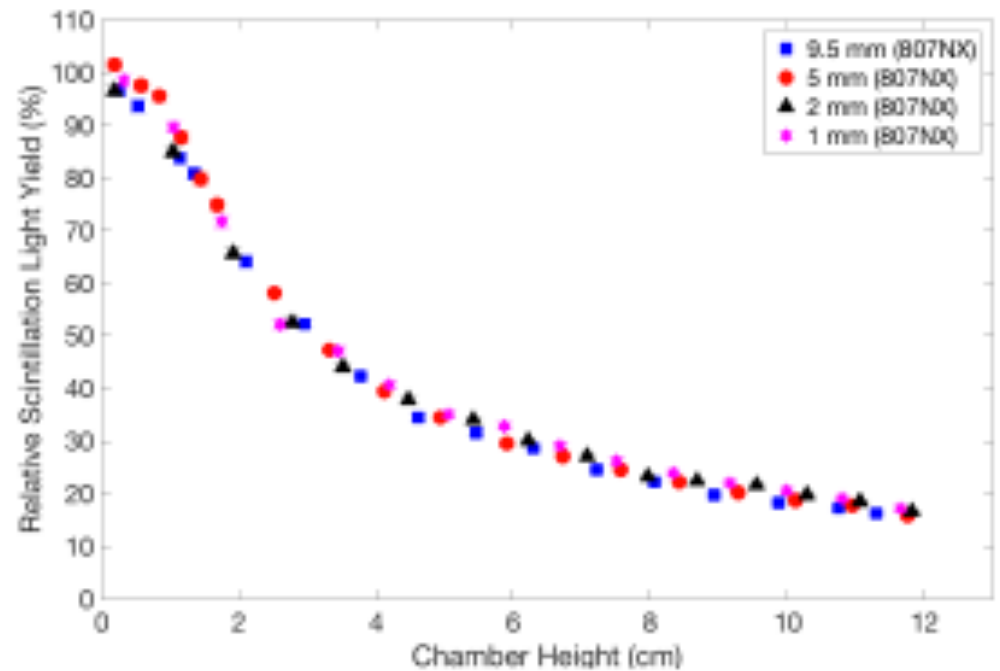
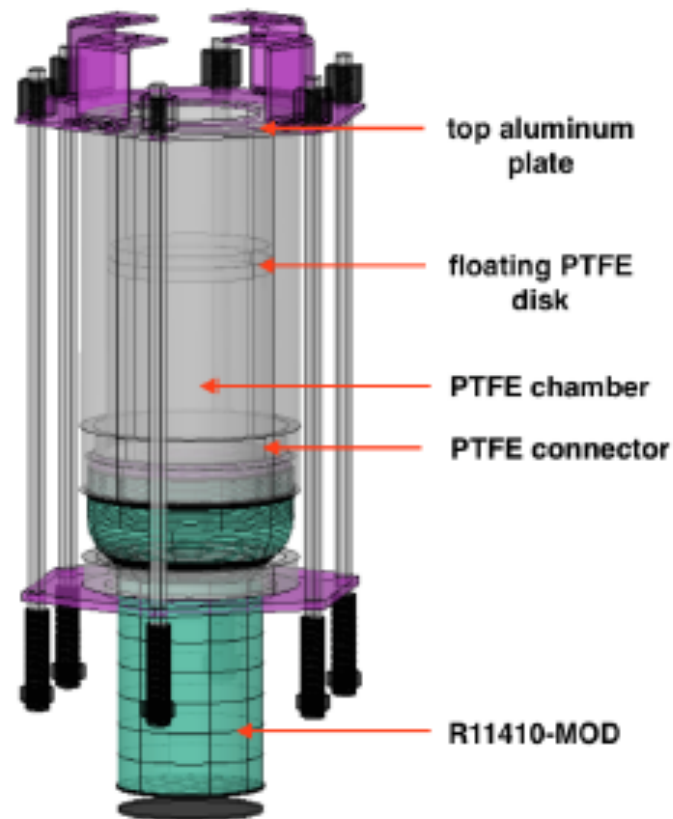
PTFE reflectance has been measured to be 50-70% for xenon scintillation light in vacuum and room temperature and is known to be much higher when immersed in LXe.

(F. Neves et al, Identification of Dark matter 2016)



PTFE	BHR	
	Best Fit	95% CL
807NX	0.961	>0.955
NXT85	0.975	>0.973
LUX	0.978	>0.975

Even very thin PTFE gives high reflectivity for LXe scintillation light
(J. Haefner et al., arxiv:1608.01717)



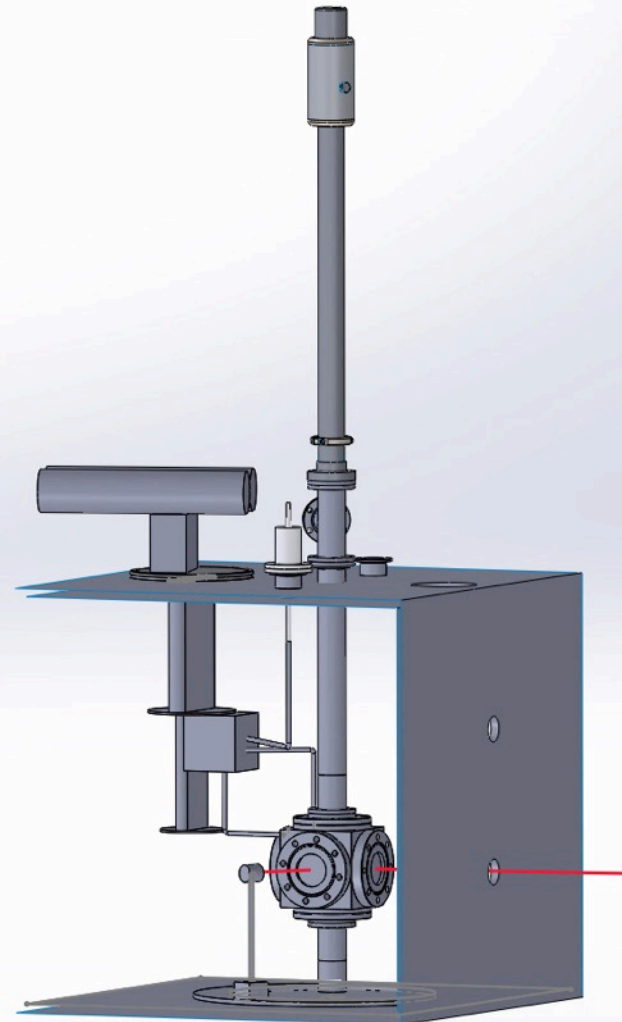
Light collection and reflectivity

Current and future LXe-based dark matter experiments rely on high reflectivity of PTFE in the vacuum ultraviolet.

- PTFE covers the inside wall of the time projection chamber.
- Current LXe experiments see a surprisingly high reflectivity ($> 95\%$).
- The origin of this high reflectivity is not physically understood.
- The ratio of specular versus diffuse reflection is unknown.

Goal: Develop a physical model for PTFE reflectivity in LXe.

- Dedicated, controlled optical measurements, varying wavelength, incident angle, and reflection angle, with and without LXe surrounding the PTFE.
- Measurements will use an ultraviolet lamp, monochromator and LXe-filled optical cell.



Materials for Gamma Detection

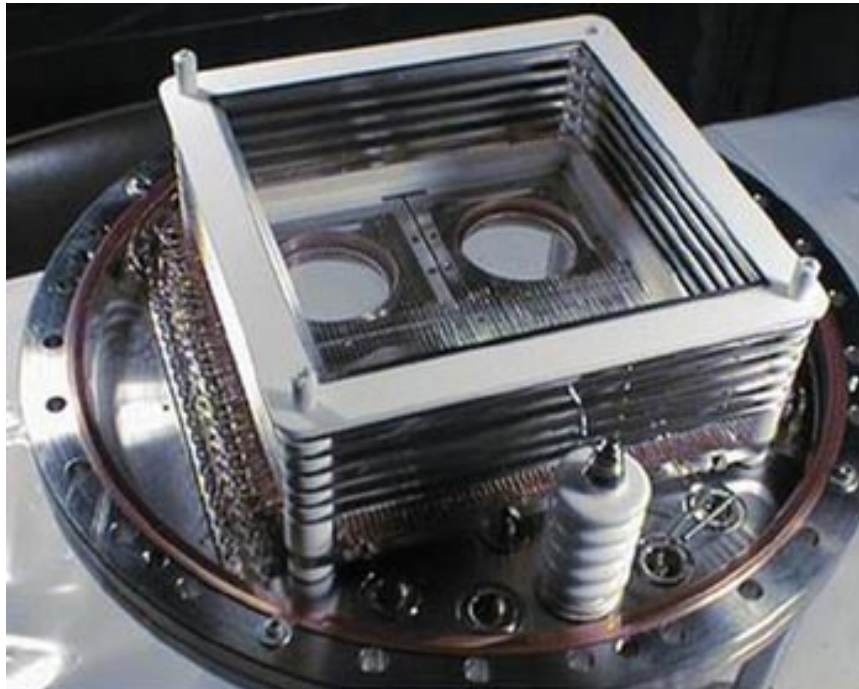
	Energy resolution (662 keV)	Position resolution	Density	Cost	Detector element thickness	n/gamma discrimination
Plastic scintillator	Poor	~ 10 cm	1.0 g/cc	~\$30/kg	~ 20 cm	No
Liquid scintillator	20%	~ 10 cm	0.9 g/cc	~\$30/kg	~ 20 cm	Yes
Sodium Iodide	6%	~ few cm	3.7 g/cc	~\$800/kg	~ 10 cm	No
CZT	1%	~ 1 mm	5.8 g/cc	~\$30,000/kg	~ 1 cm	No
Germanium	0.2%	~ 3 mm	5.3 g/cc	~\$20,000/kg	~ 5 cm	No
Liquid Xenon	3-6%	~ 1 mm	3.0 g/cc	\$1,200/kg	~ 20 cm	Yes

Liquid Xenon combines:

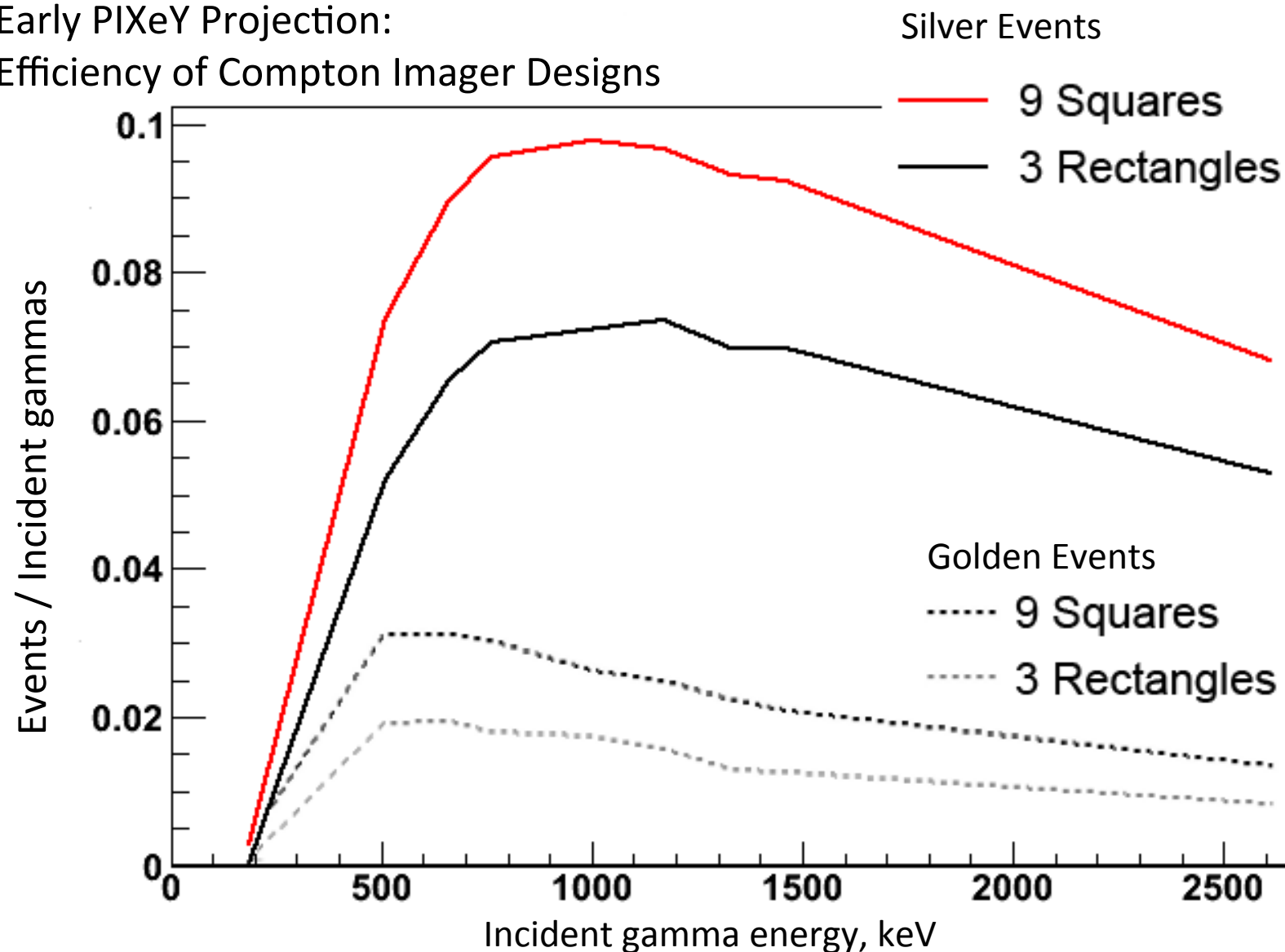
- Energy resolution between CZT and sodium iodide
- Cost of sodium iodide
- Position resolution of CZT
- Scalability of organic scintillator.

LXeGRIT Gamma Astronomy Telescope

- Single-phase, all-liquid xenon TPC. Energy readout by charge only.
- Durable, balloon borne for operation in the upper atmosphere.
- 5.9% FWHM energy resolution at 1 MeV
- 4.7 degree FWHM angular resolution



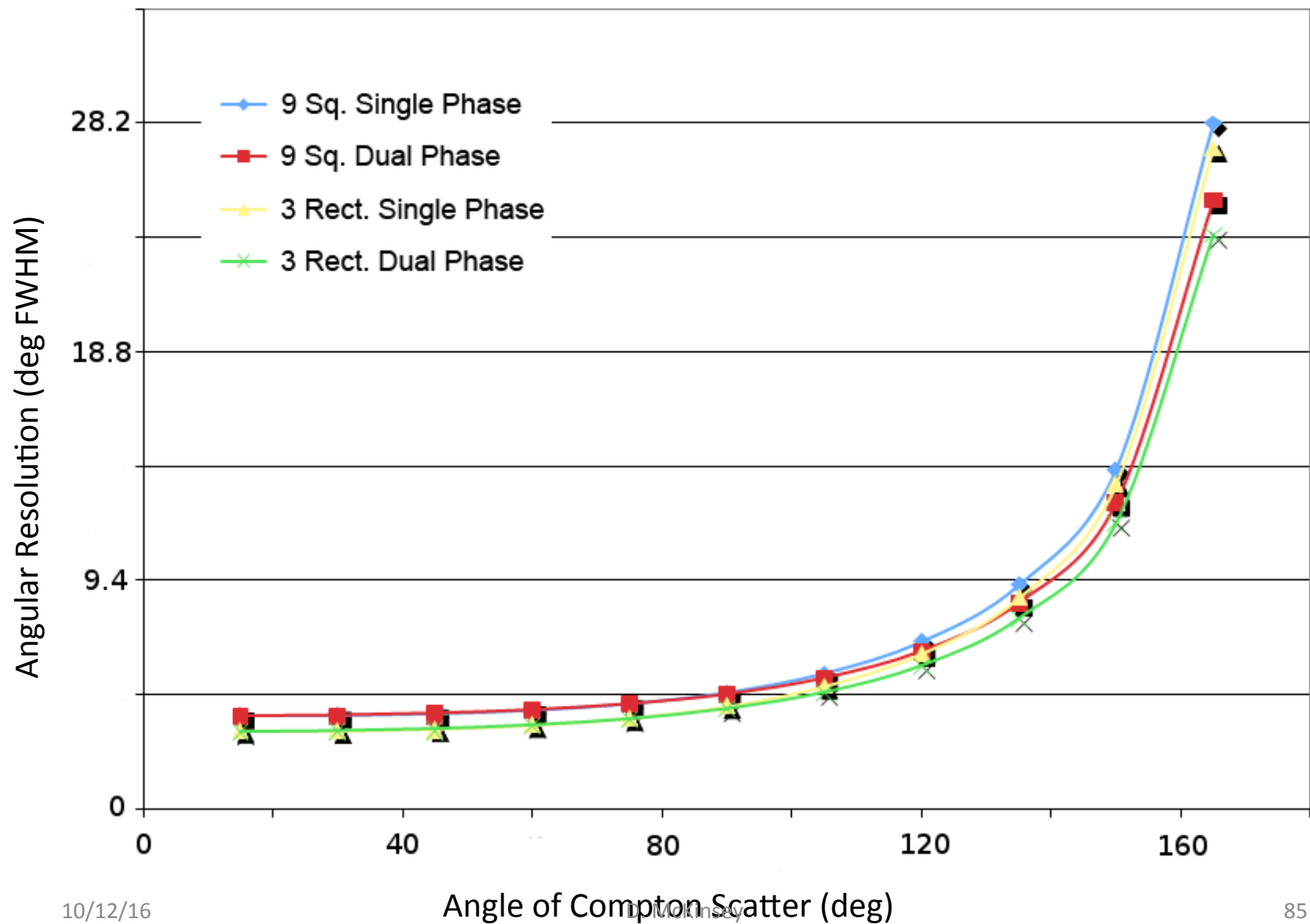
Early PIXeY Projection: Efficiency of Compton Imager Designs



Golden events: Single isolated Compton scatter followed by photoabsorption.

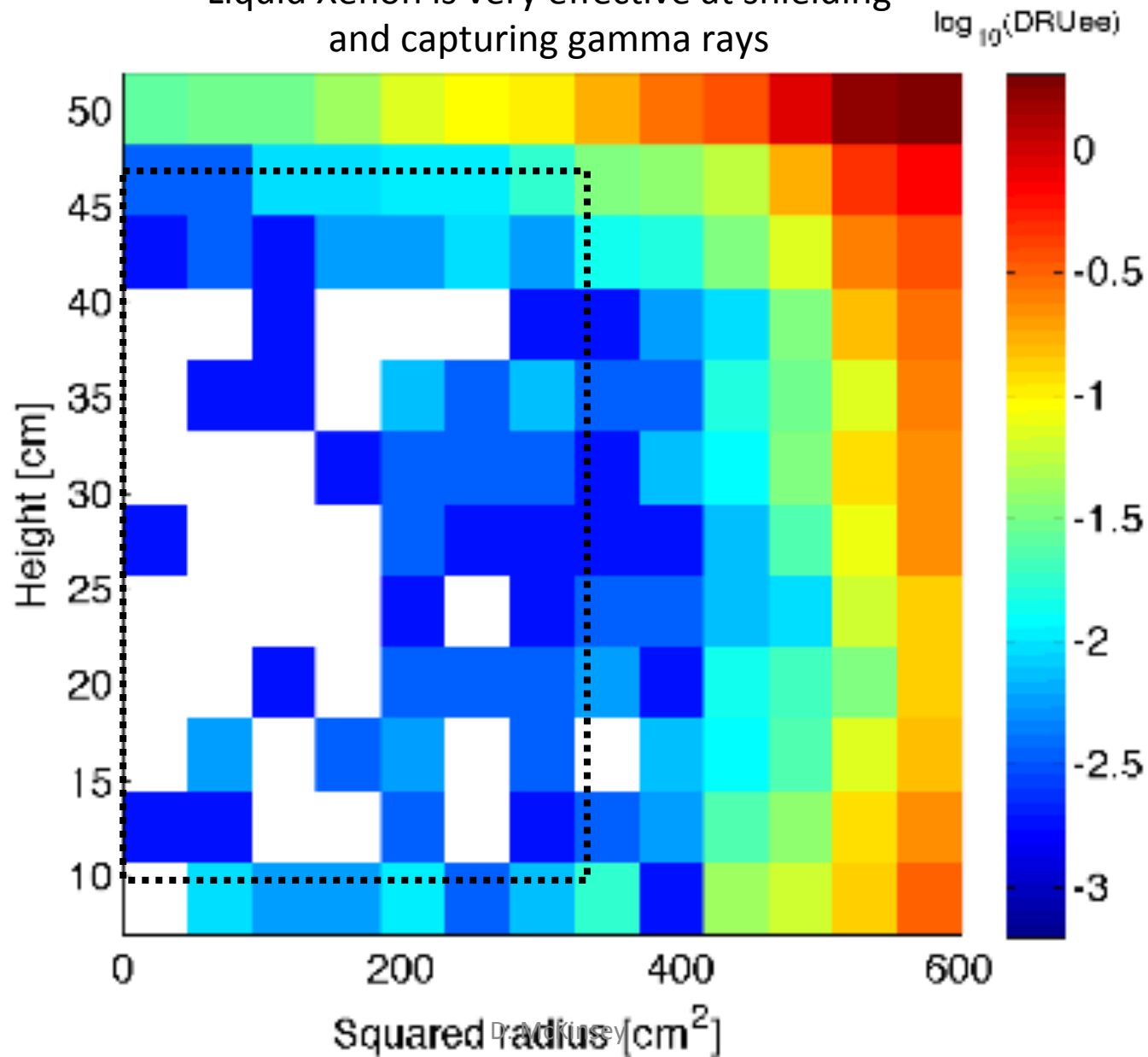
Silver events: Single isolated Compton scatter followed by capture of the remaining energy within the active xenon.

Projected Angular Resolution of Golden Events from 1.001 MeV gamma



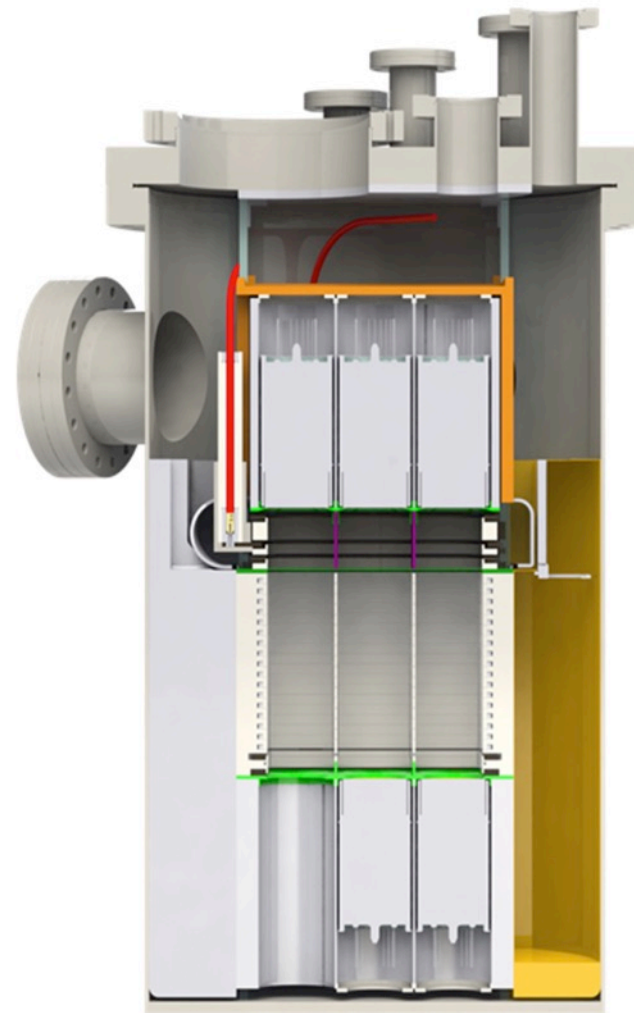
Self-Shielding of Gamma Rays in LUX

Liquid Xenon is very effective at shielding and capturing gamma rays



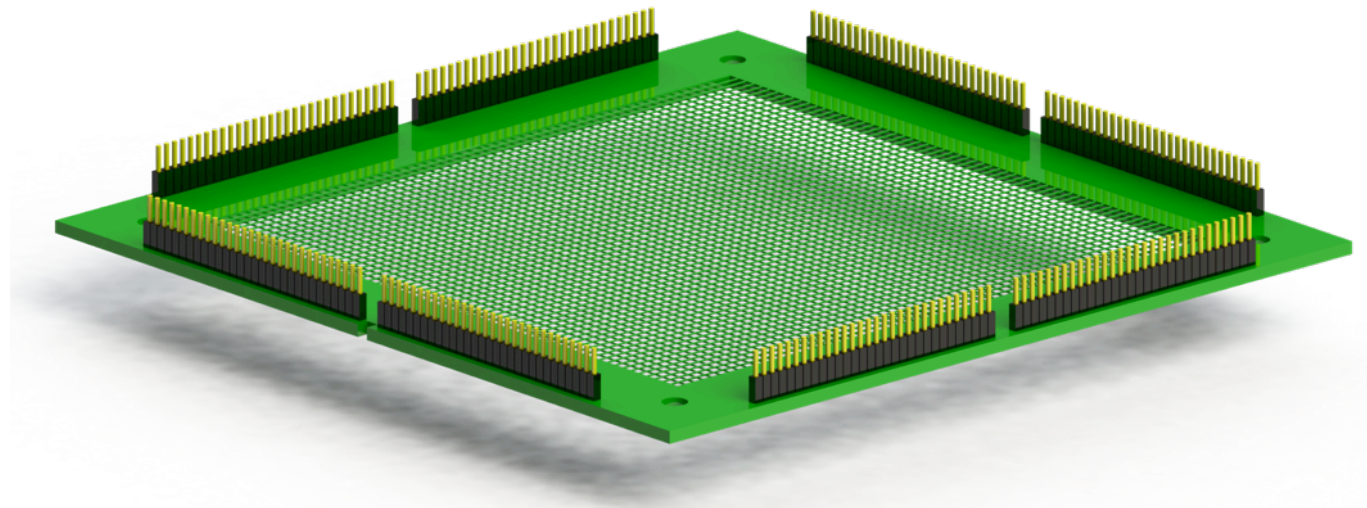
The CoDeX Detector

- Compton Detection in Xenon
- R&D detector built to demonstrate Compton Imaging:
 - Two-phase LXe TPC (18 kg active)
 - Teflon walls
 - 18 R8778 PMTS
 - 120 charge readout channels
 - Operates under existing PIXeY cryogenic and circulation platform



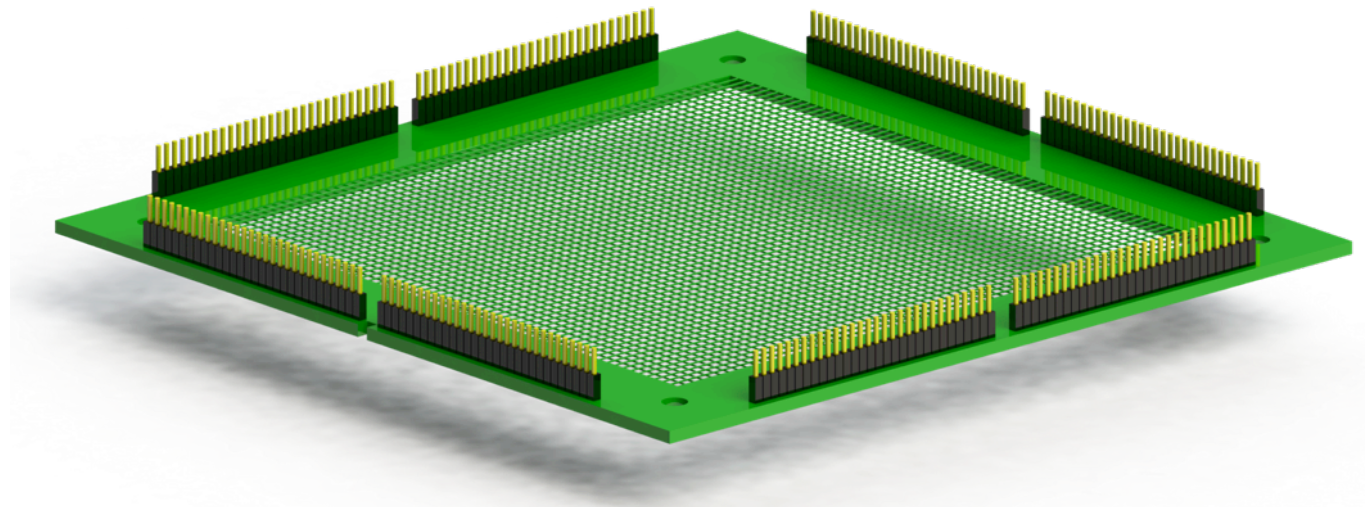
The CoDeX Detector

PIXeY + Wire Readout = CoDeX



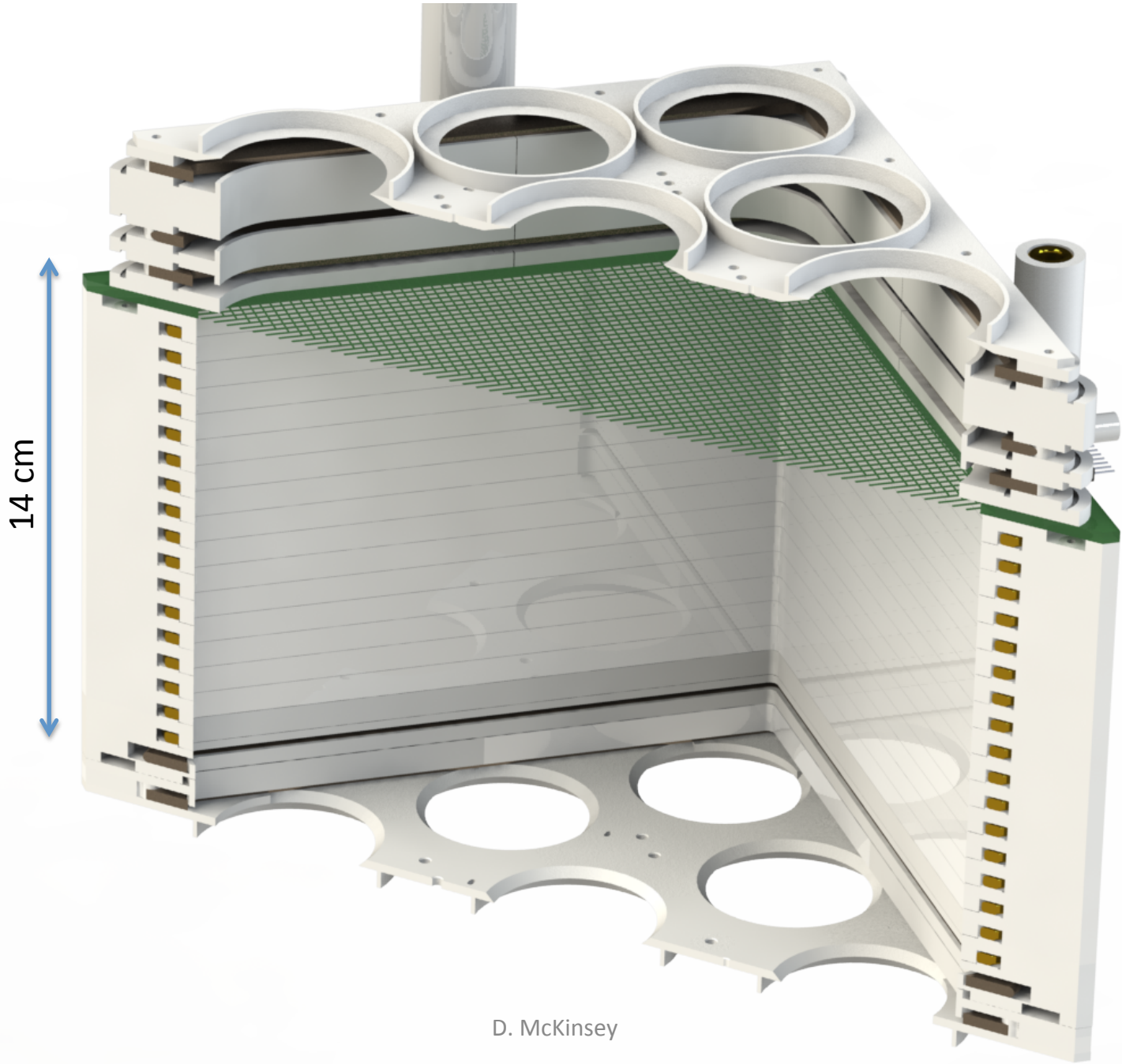
The CoDeX Detector

PIXeY + Wire Readout = CoDeX

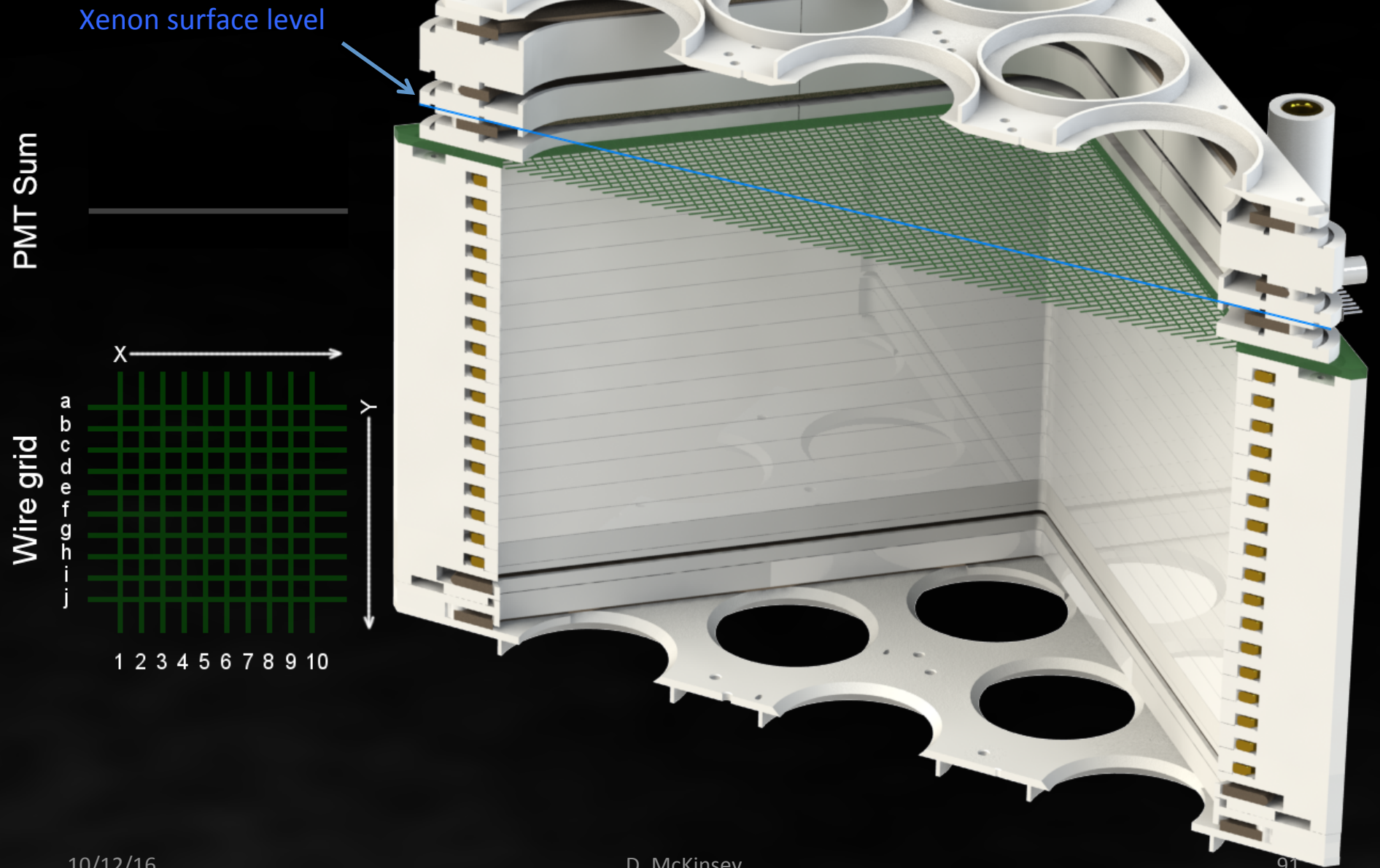


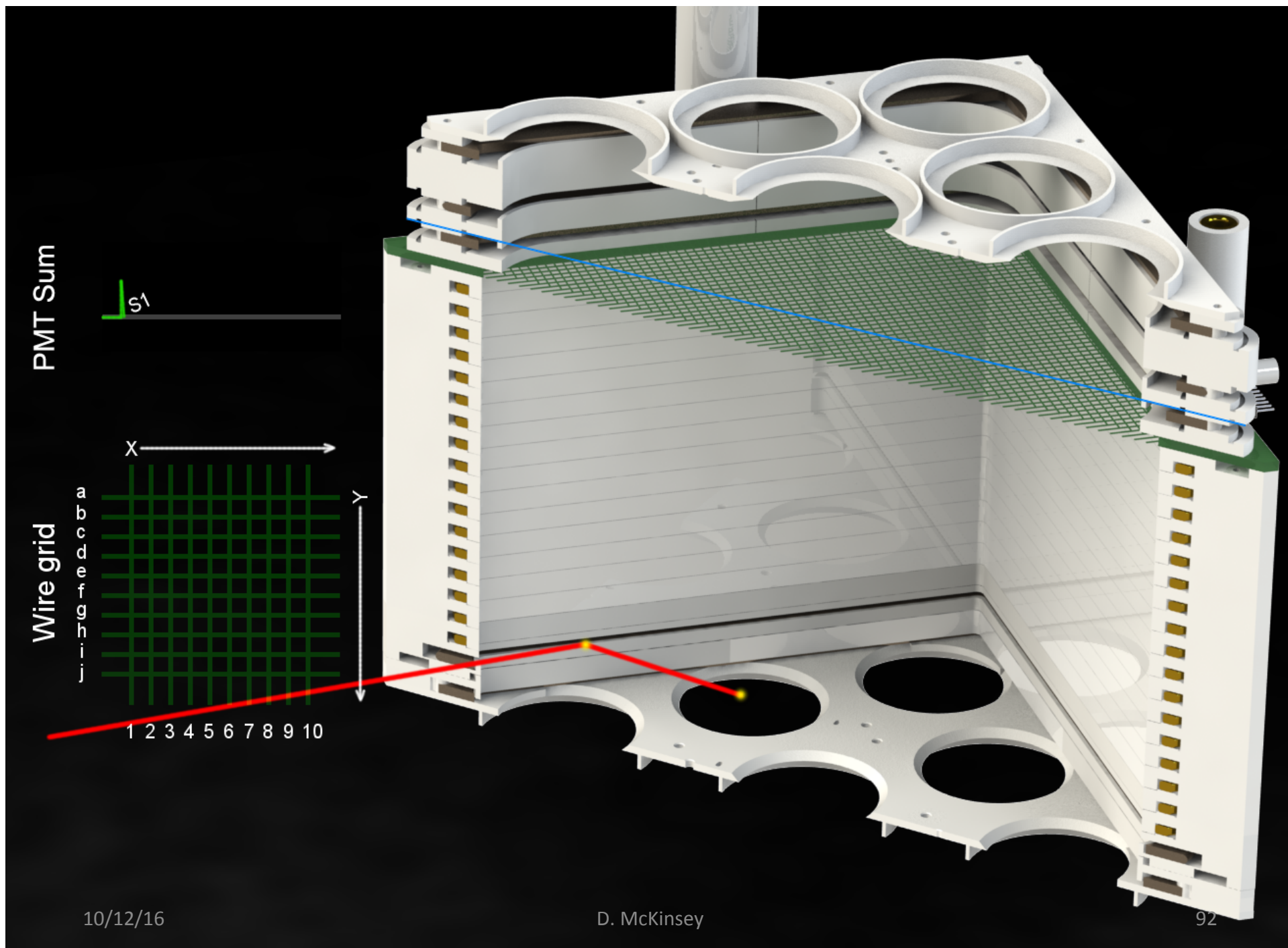
(+ 4 PMTs, 12 kg Xe, and make it square)

Liquid Xenon TPC Cutaway



Two-Phase Xenon Compton Imaging Upgrade





PMT Sum

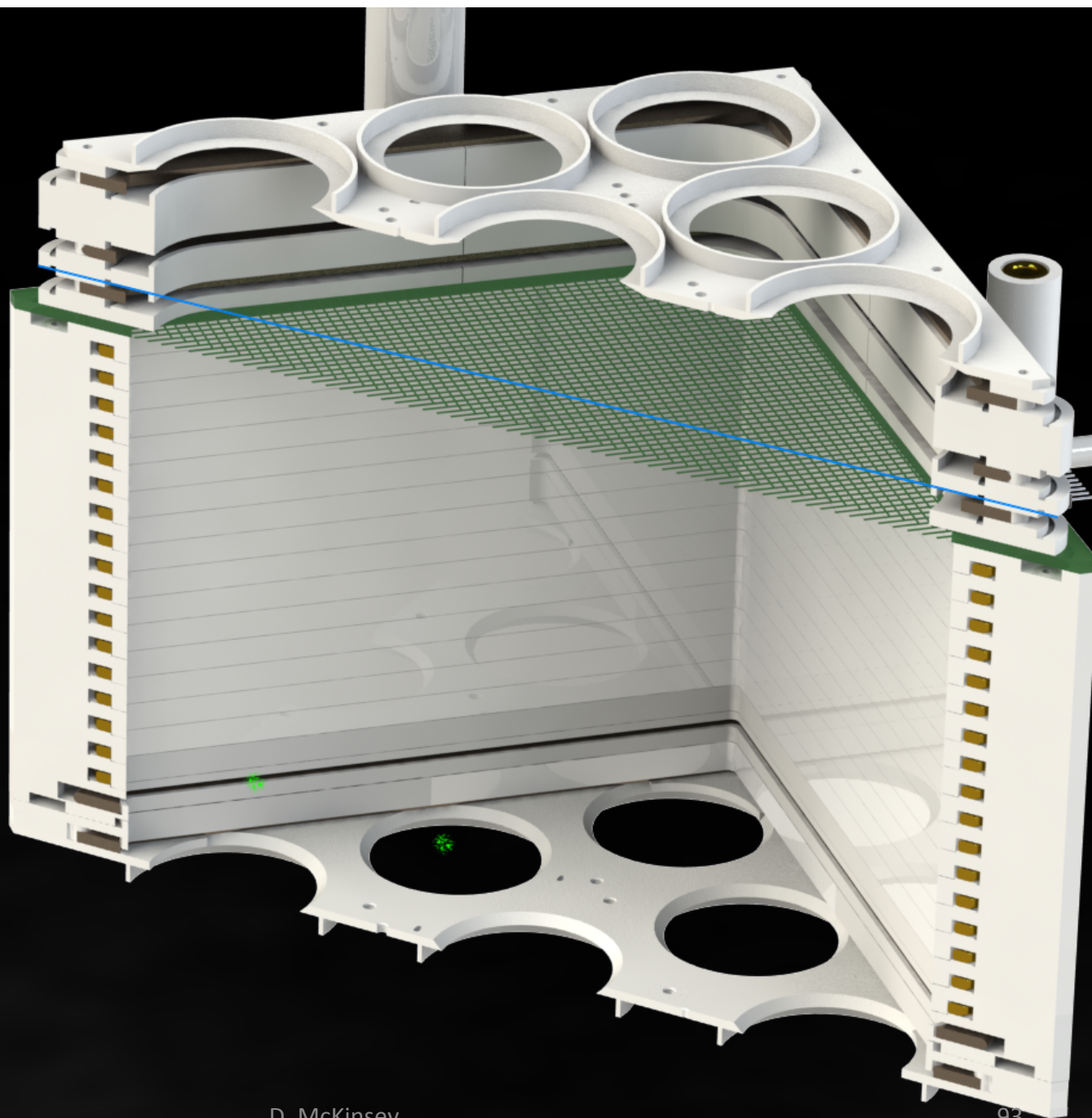
Wire grid

S₁

X

Y

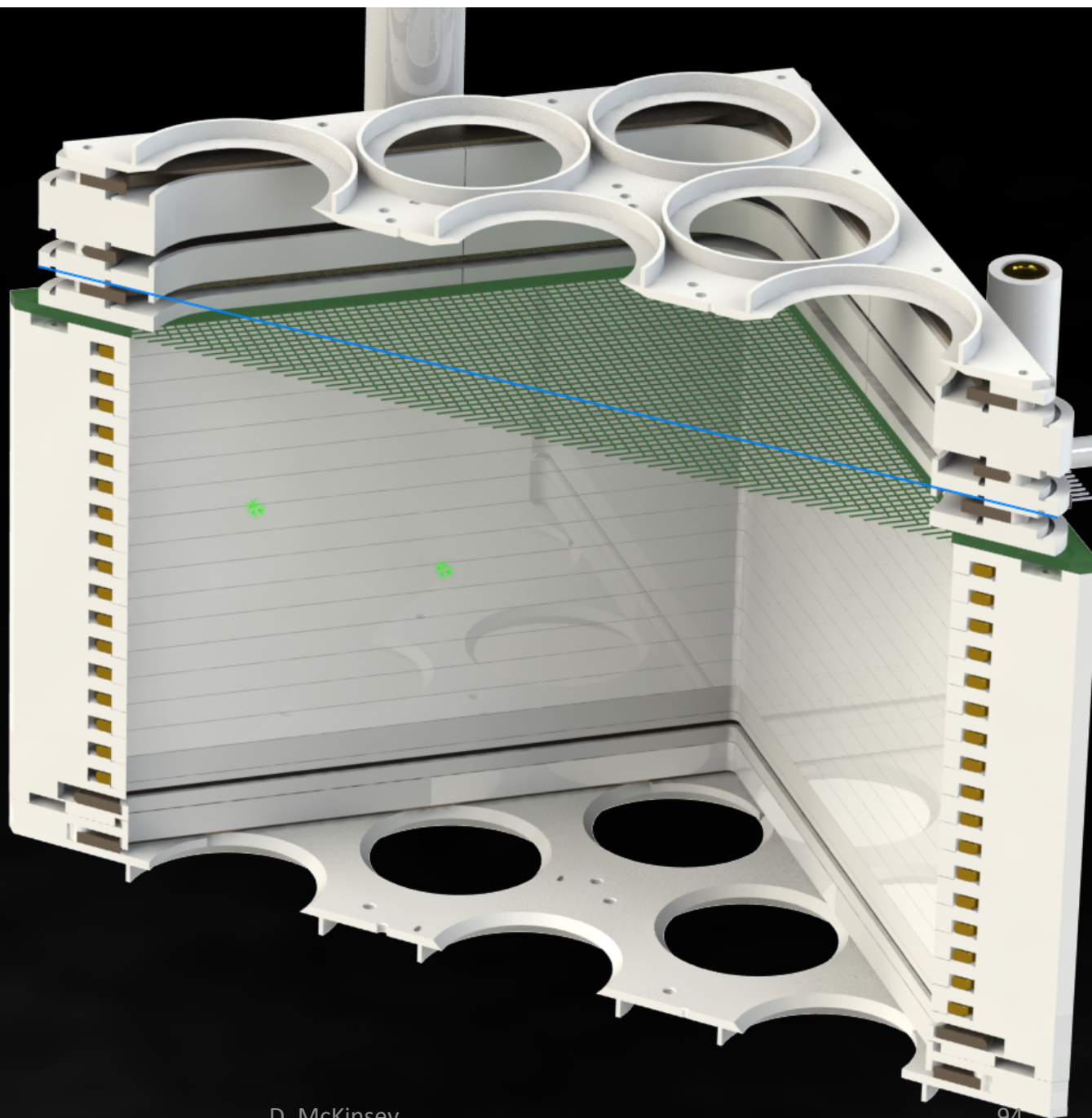
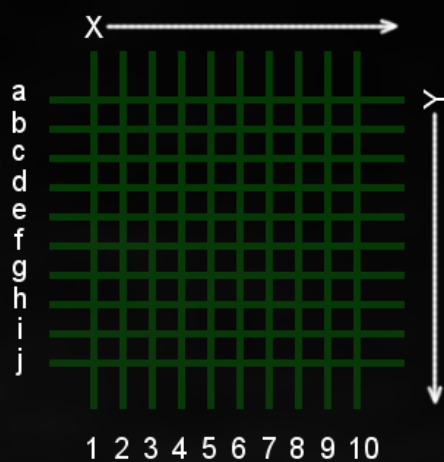
1 2 3 4 5 6 7 8 9 10



PMT Sum



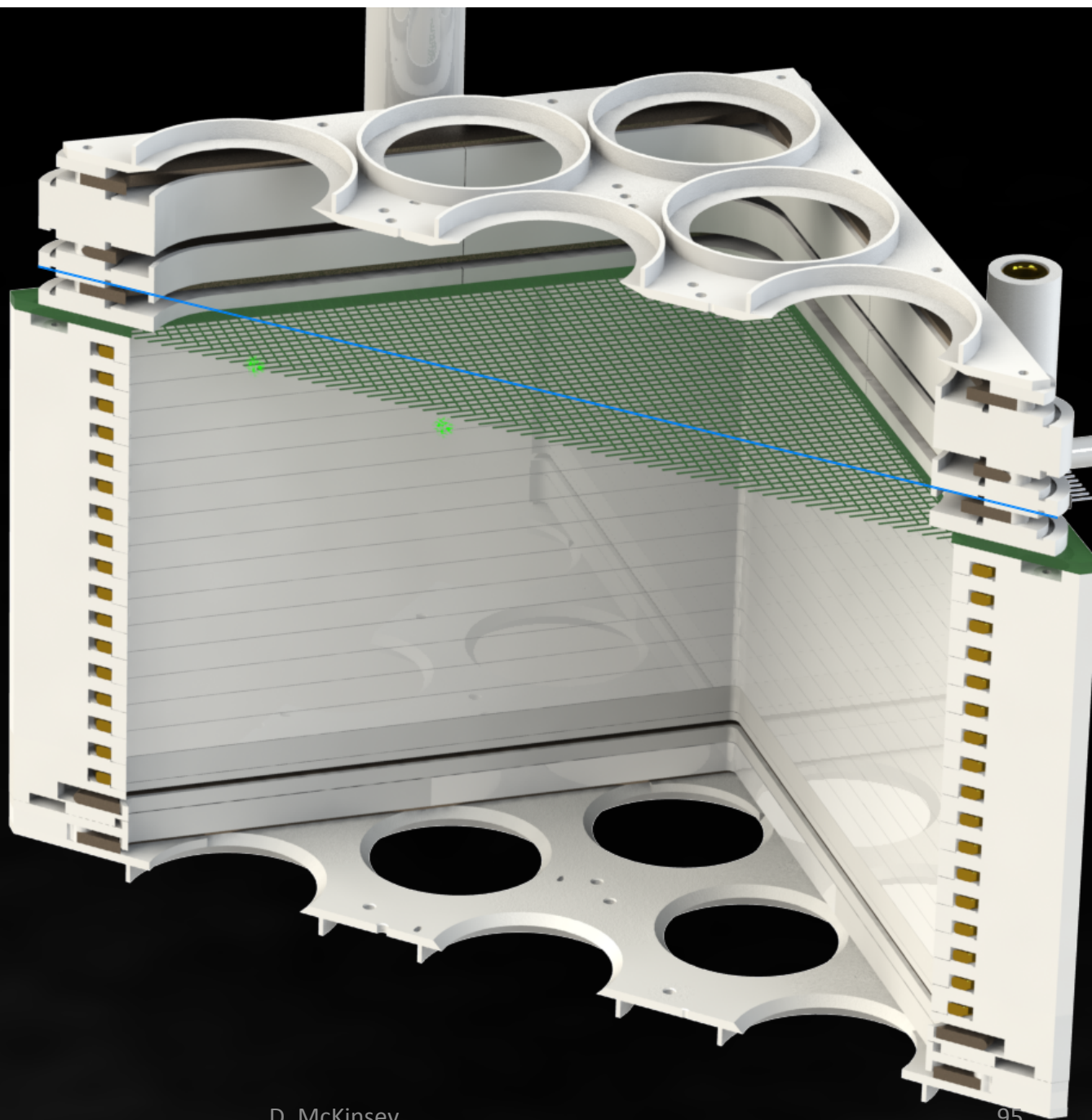
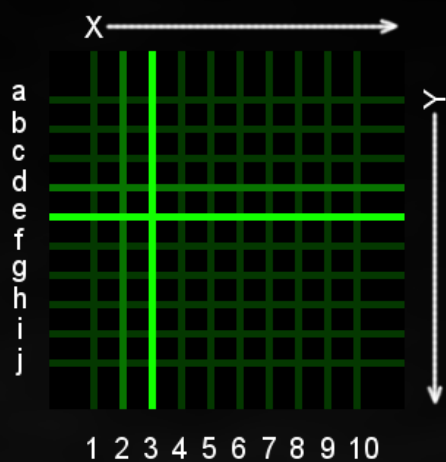
Wire grid



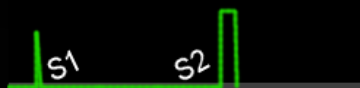
PMT Sum



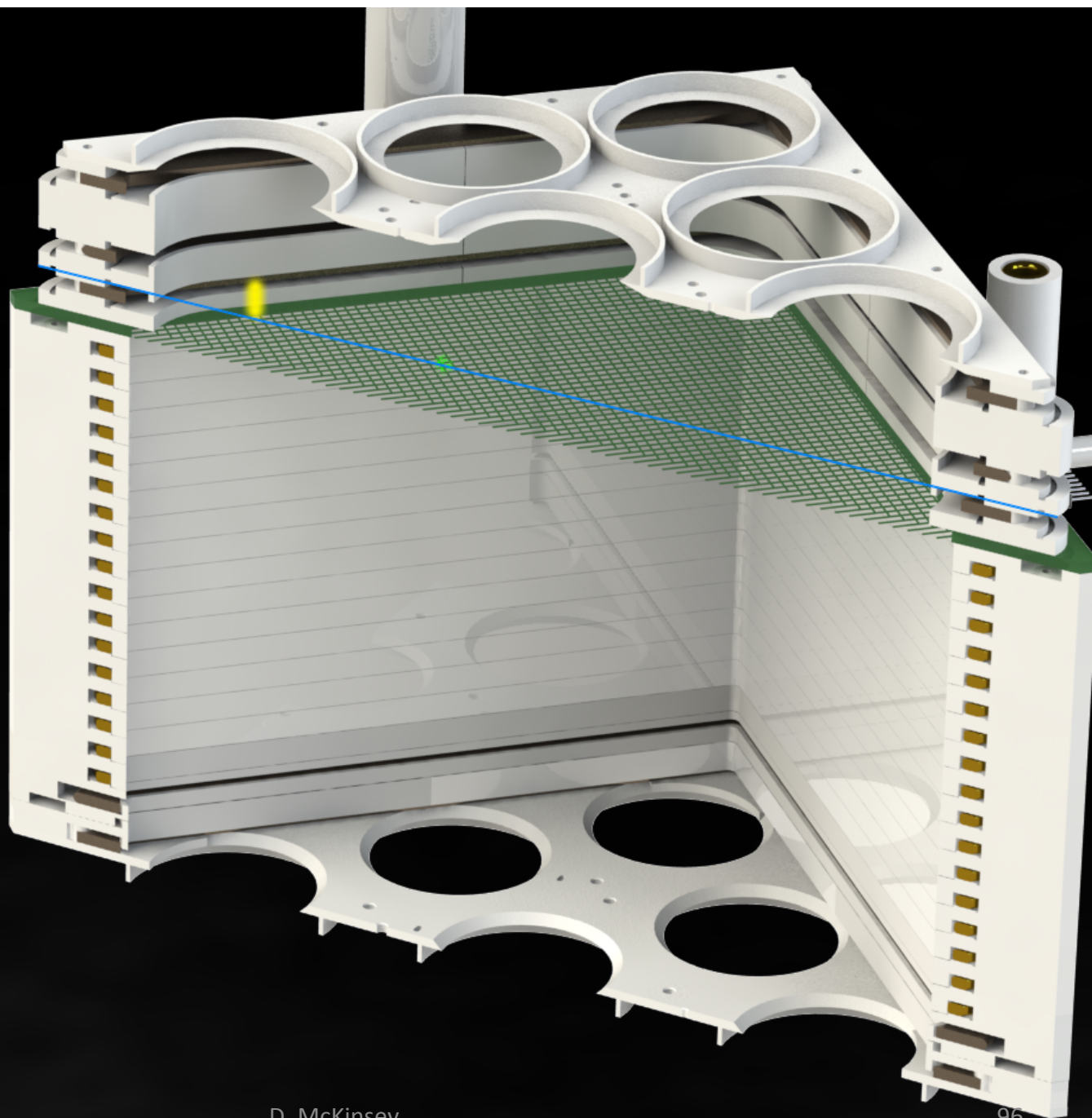
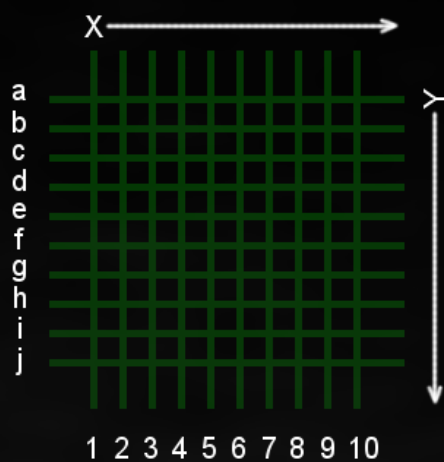
Wire grid



PMT Sum



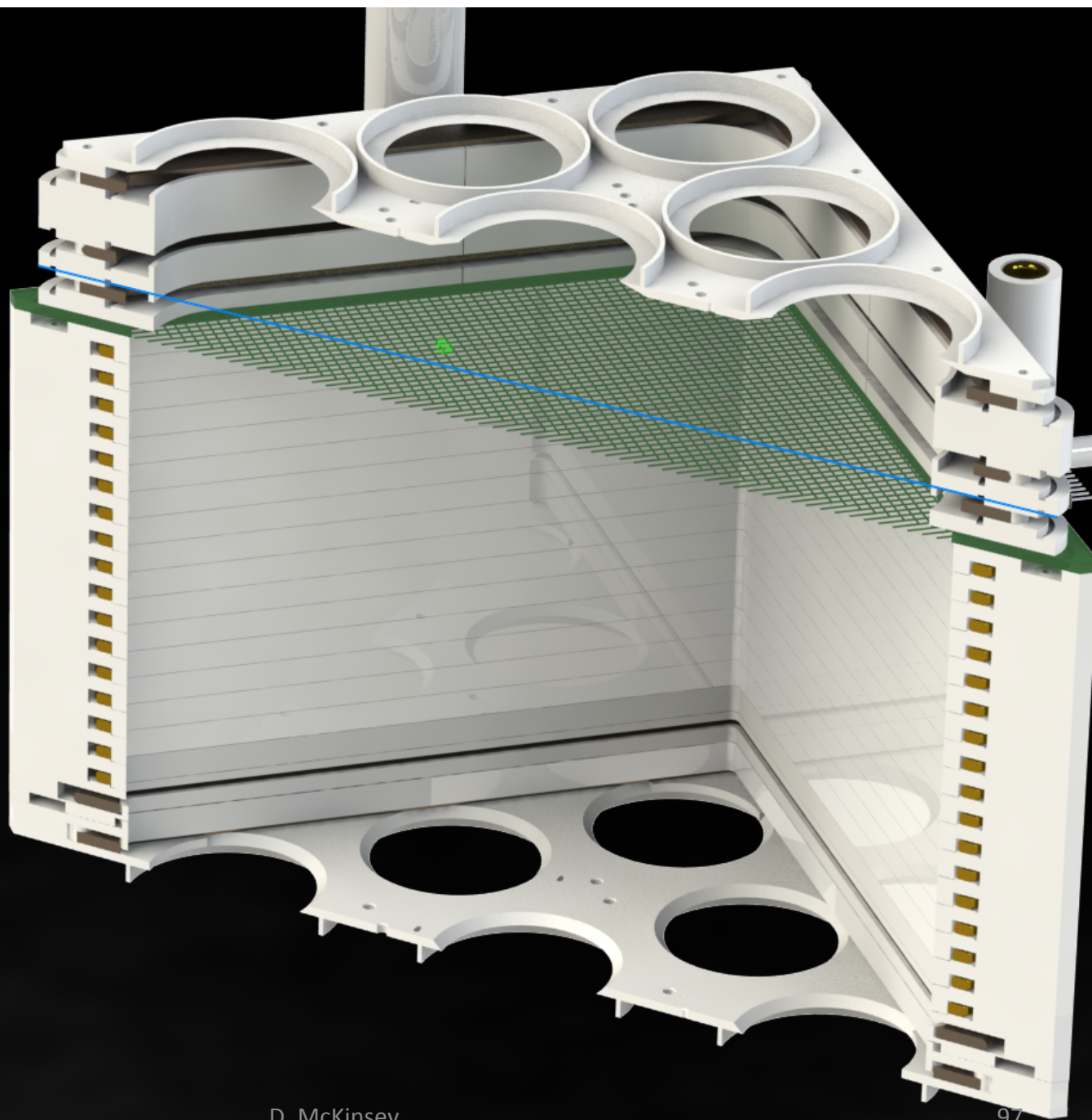
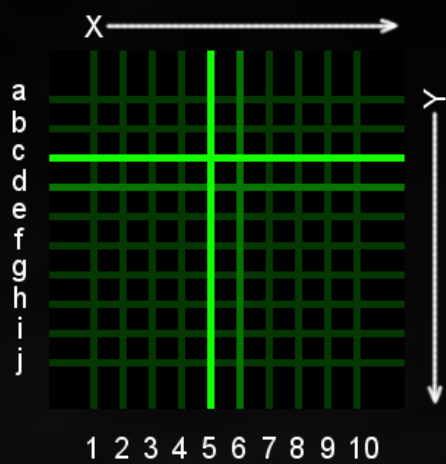
Wire grid



PMT Sum



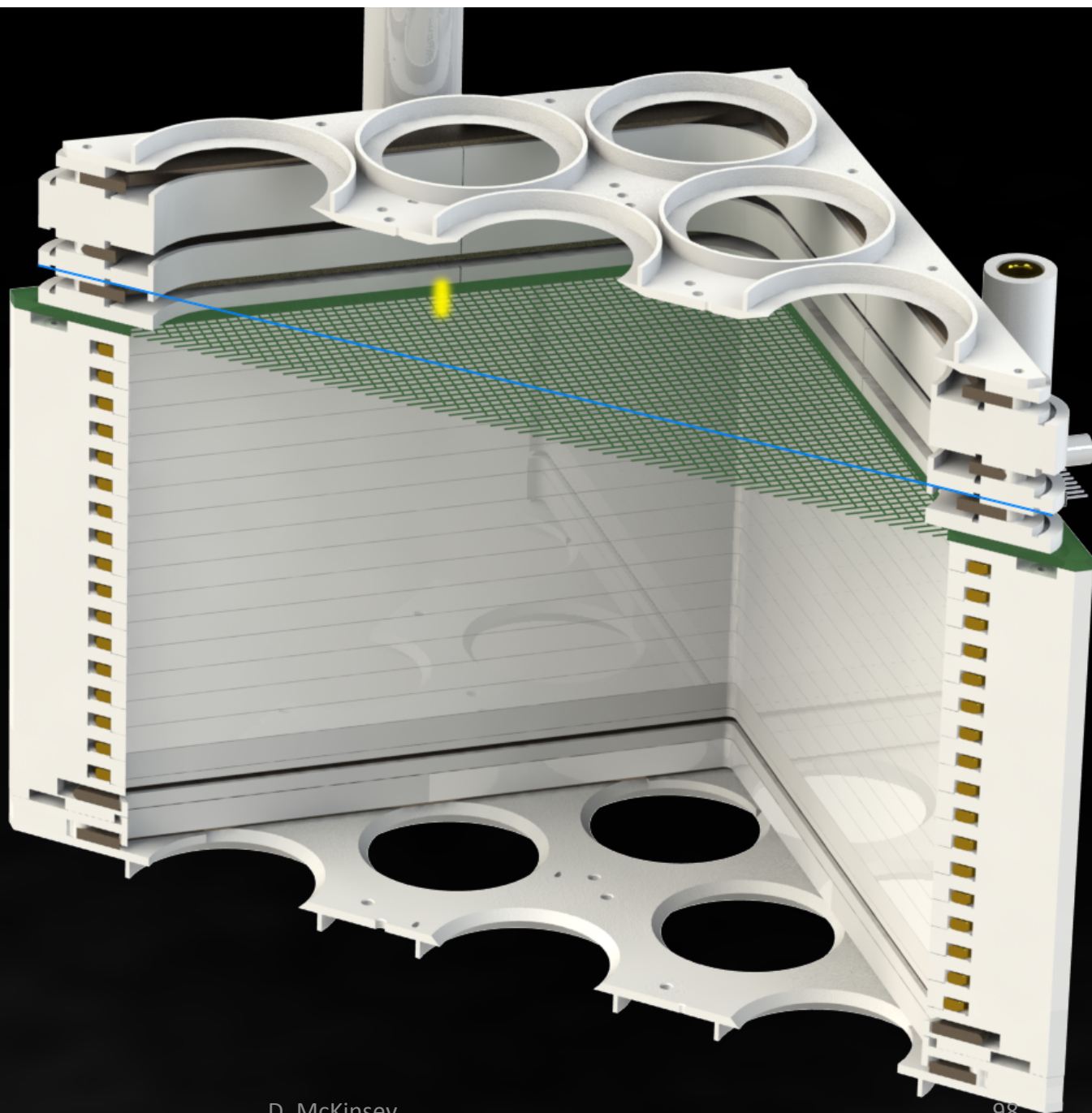
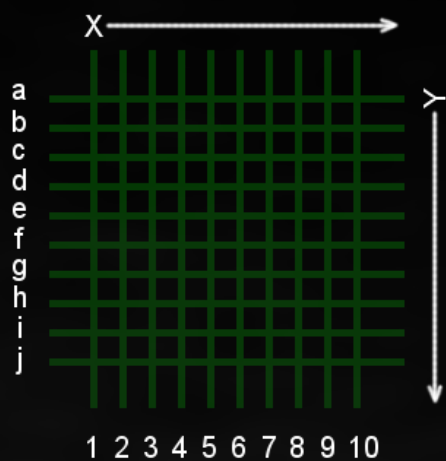
Wire grid



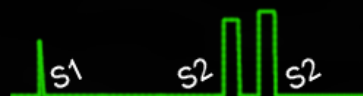
PMT Sum



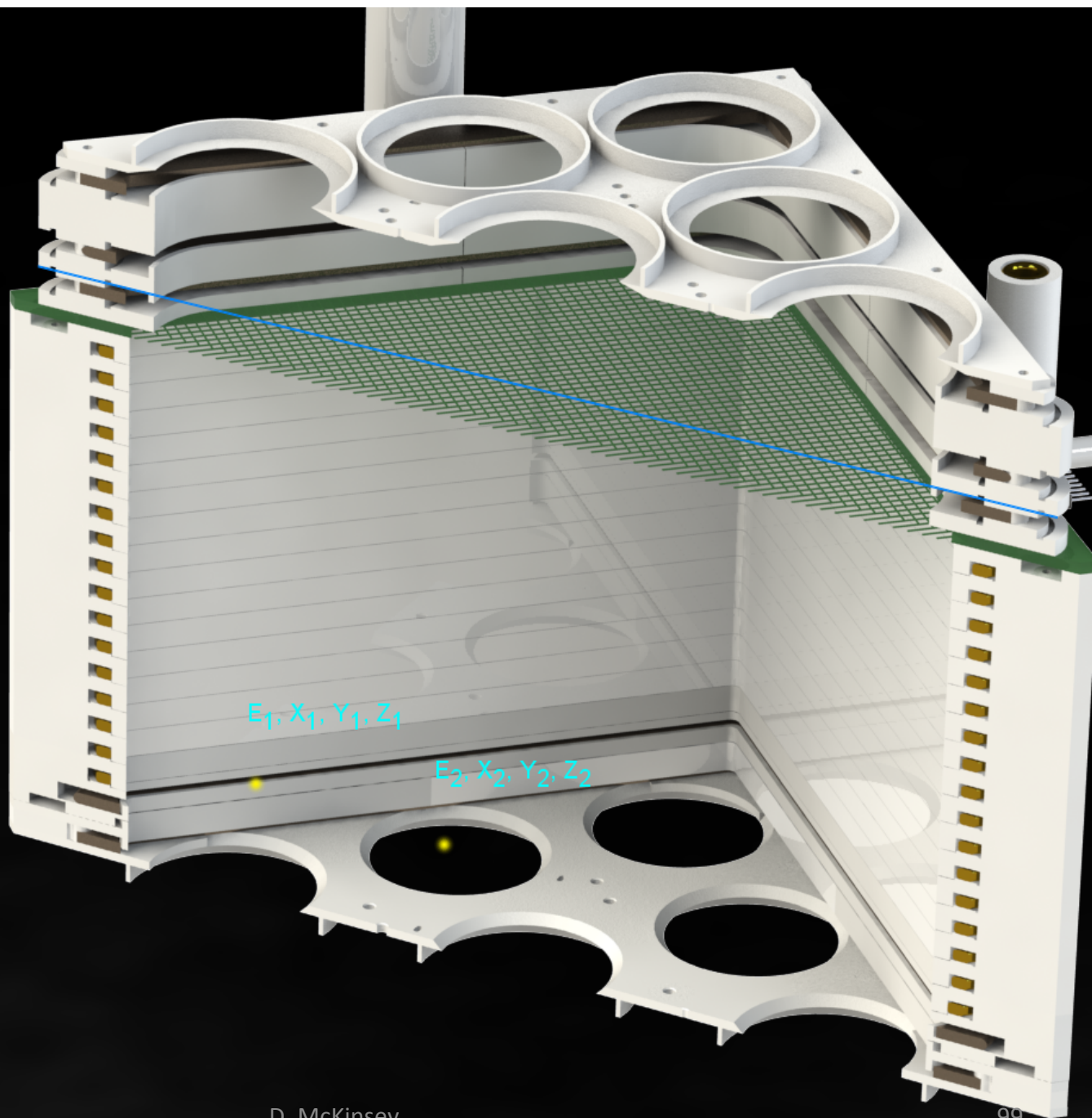
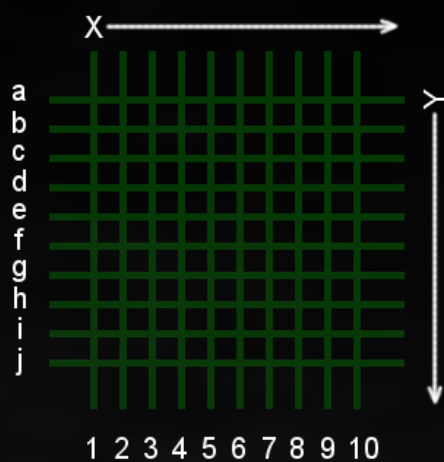
Wire grid

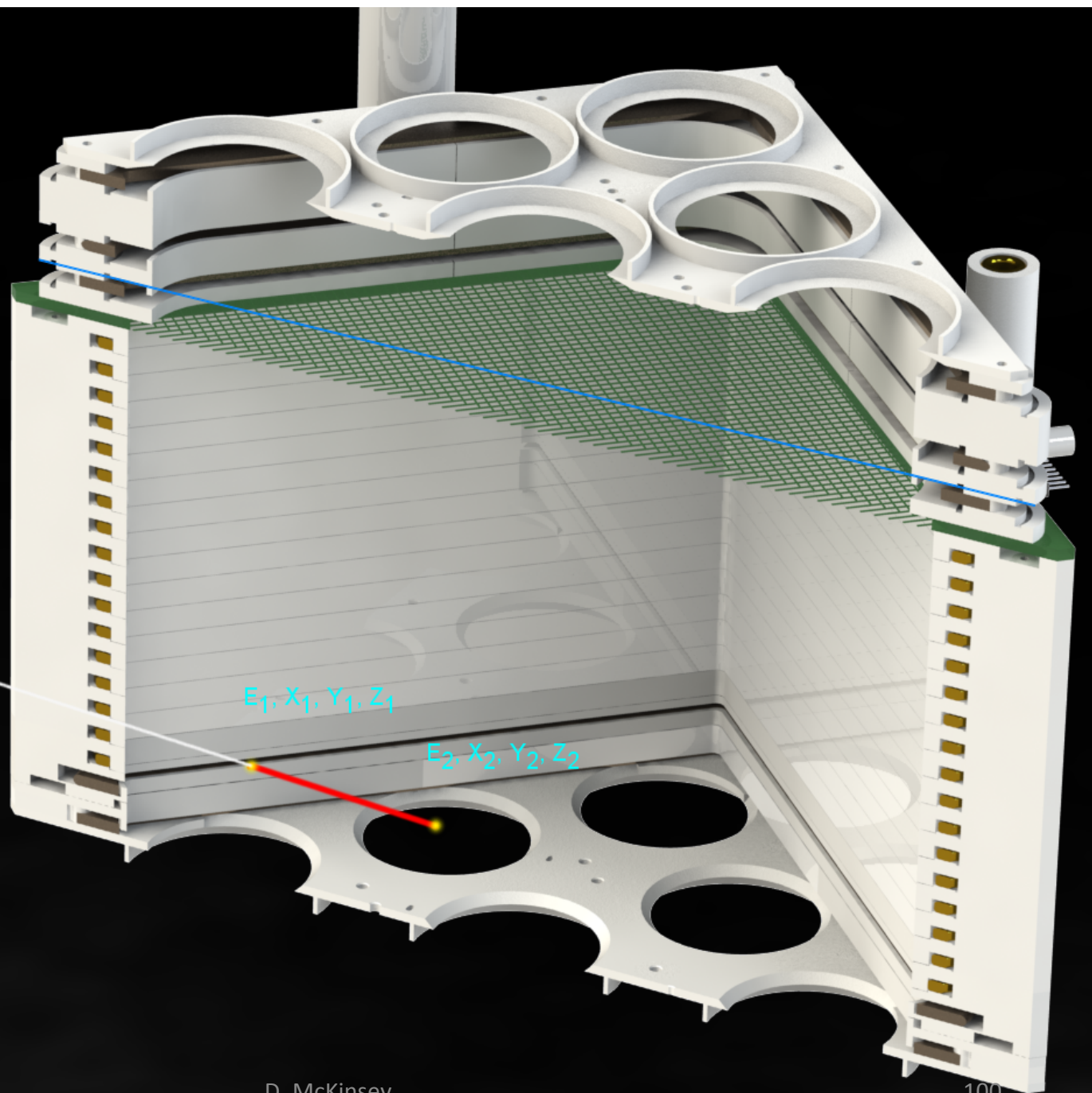


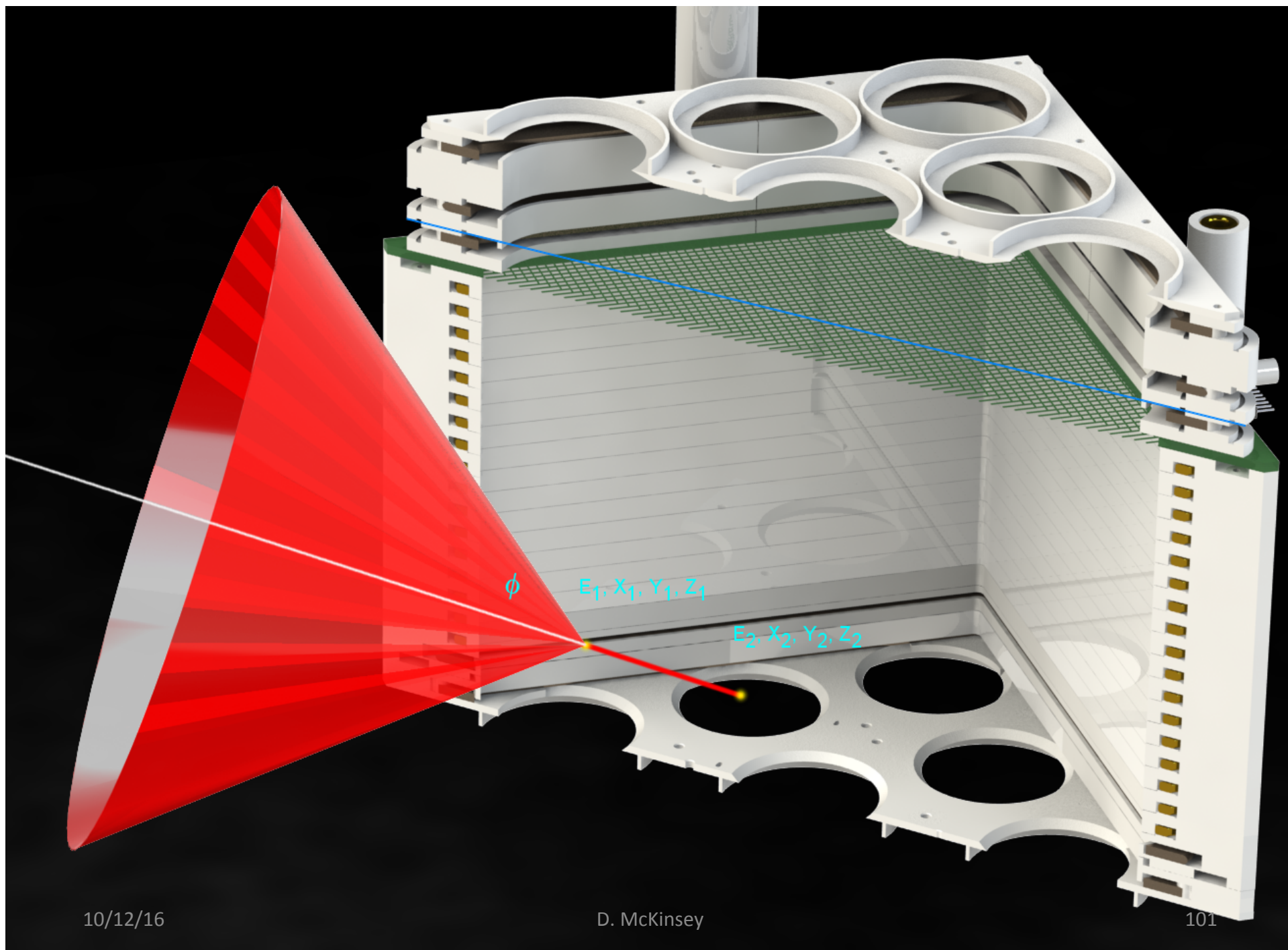
PMT Sum



Wire grid







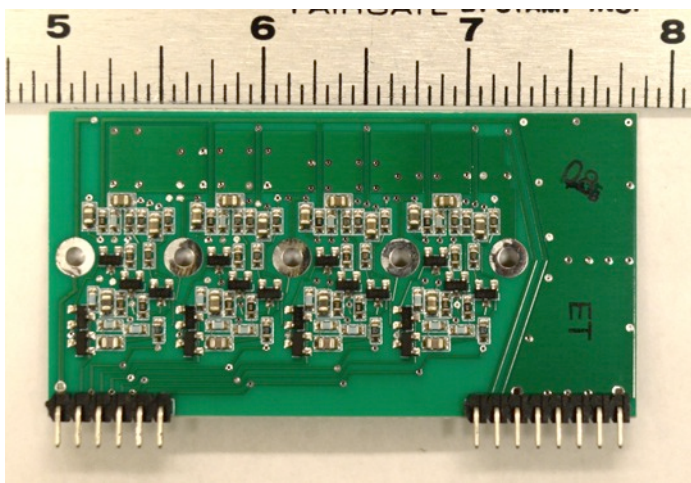


10/12/16

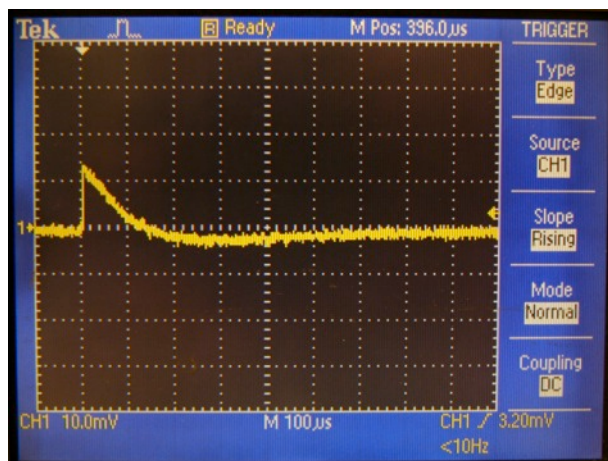
D. McKinsey

102

Crossed Wire Readout: Amplification and Sampling

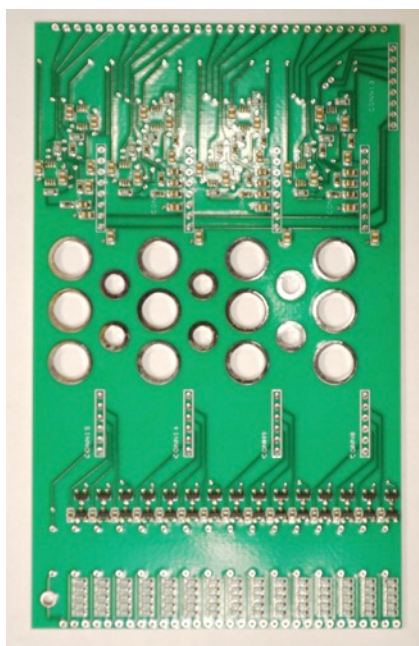


4-channel charge-sensitive preamplifiers



Discrete all-JFET design operates at 170 K
Dissipated power is 110 mW / channel
RMS Noise $< 3 \text{ nV} / \text{Hz}^{1/2}$ referred to input.
50 pF total capacitance, 200 kHz bandwidth

→ 419 electrons RMS charge noise, equivalent to $\sim 10 \text{ keV}$



4 preamplifier boards mount to each motherboard



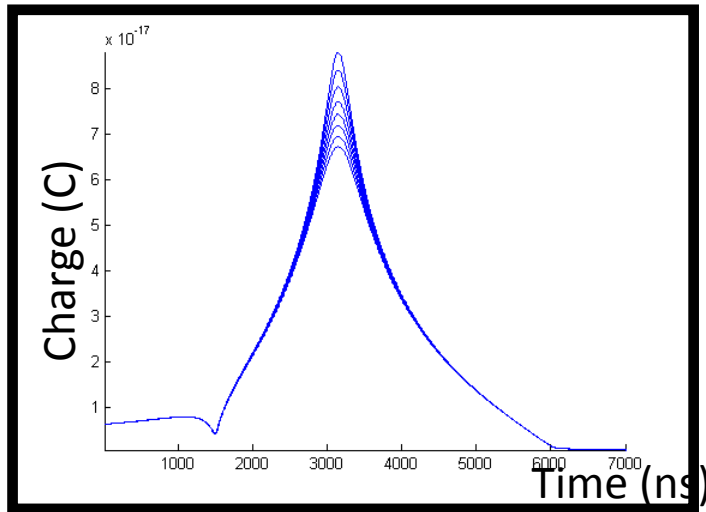
8 motherboards each decouple and amplify 15 channels.



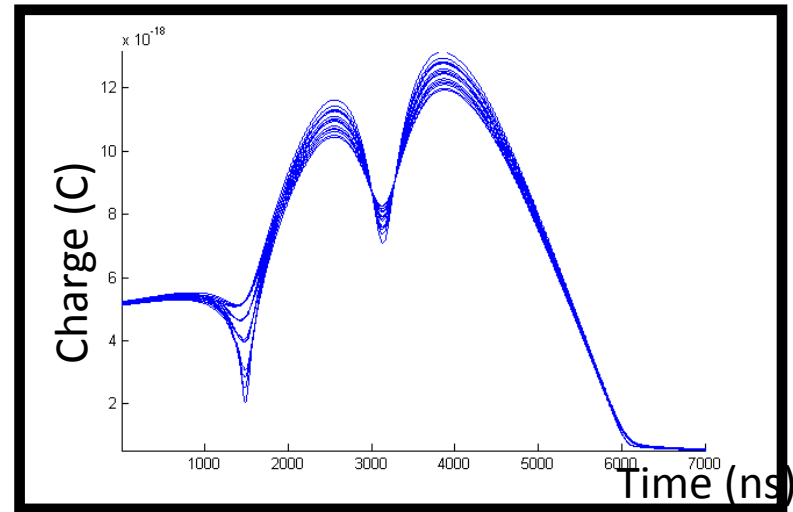
CAEN liquid argon TPC readout
128 channels, 12 bit, 2.5 MS/sec

Simulated Wire Grid Response

Adjacent Wire

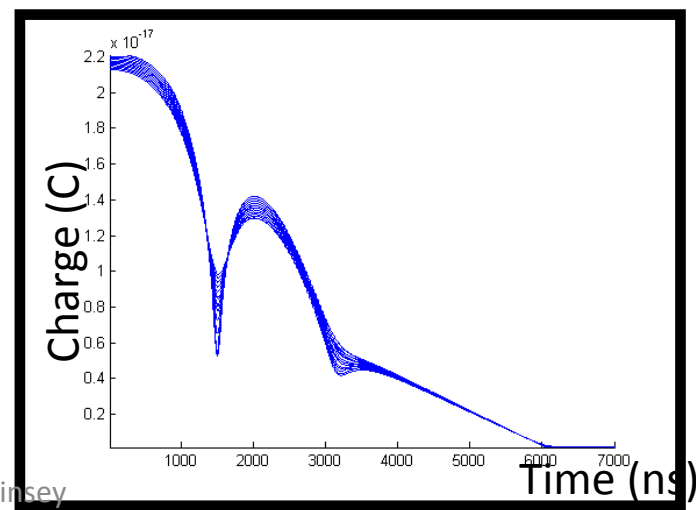
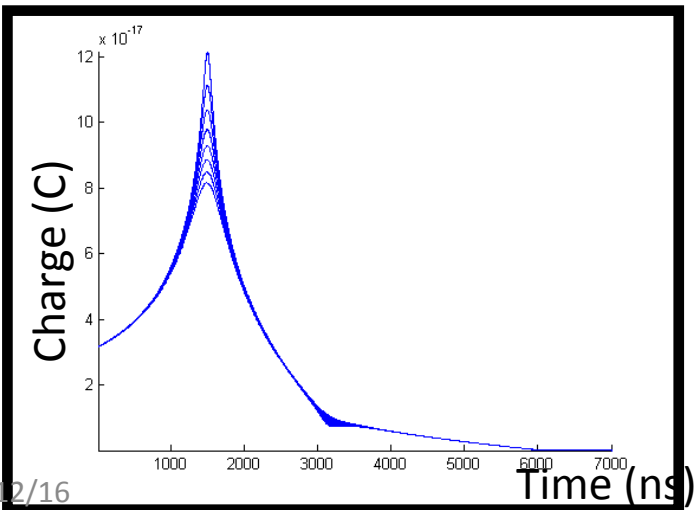


2nd Wire Away



X

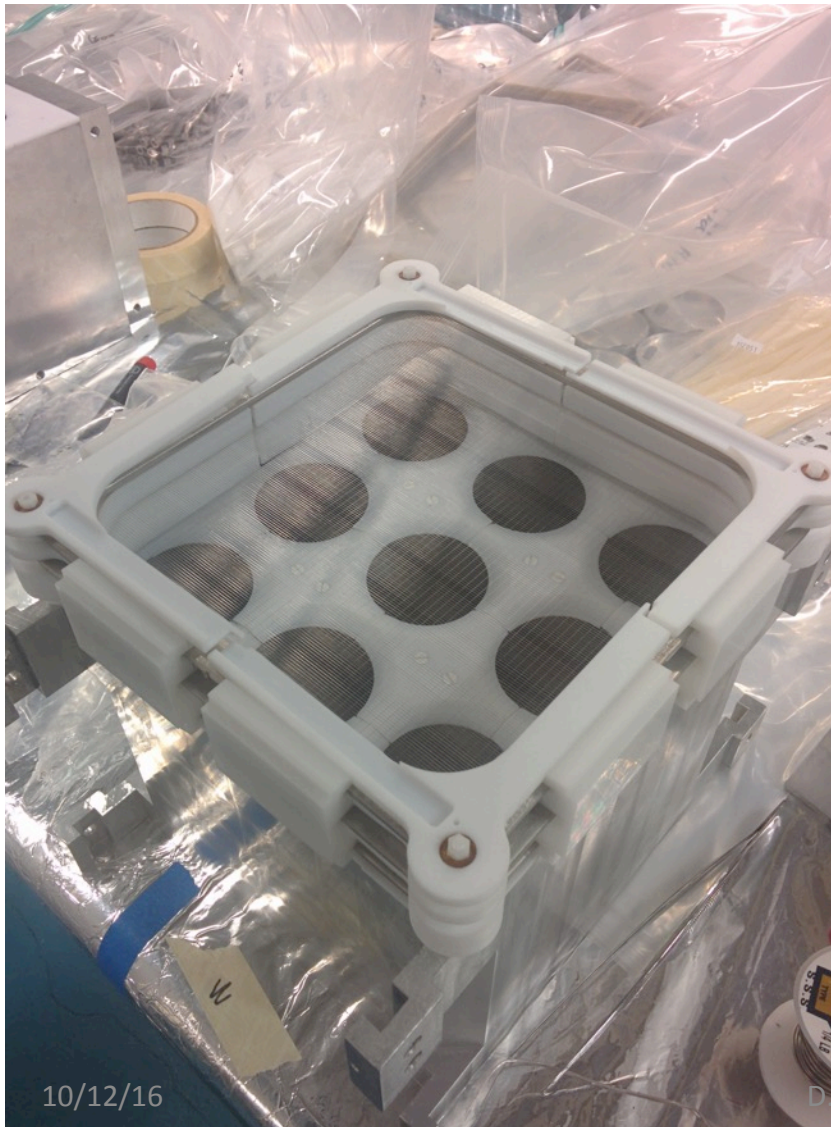
Y



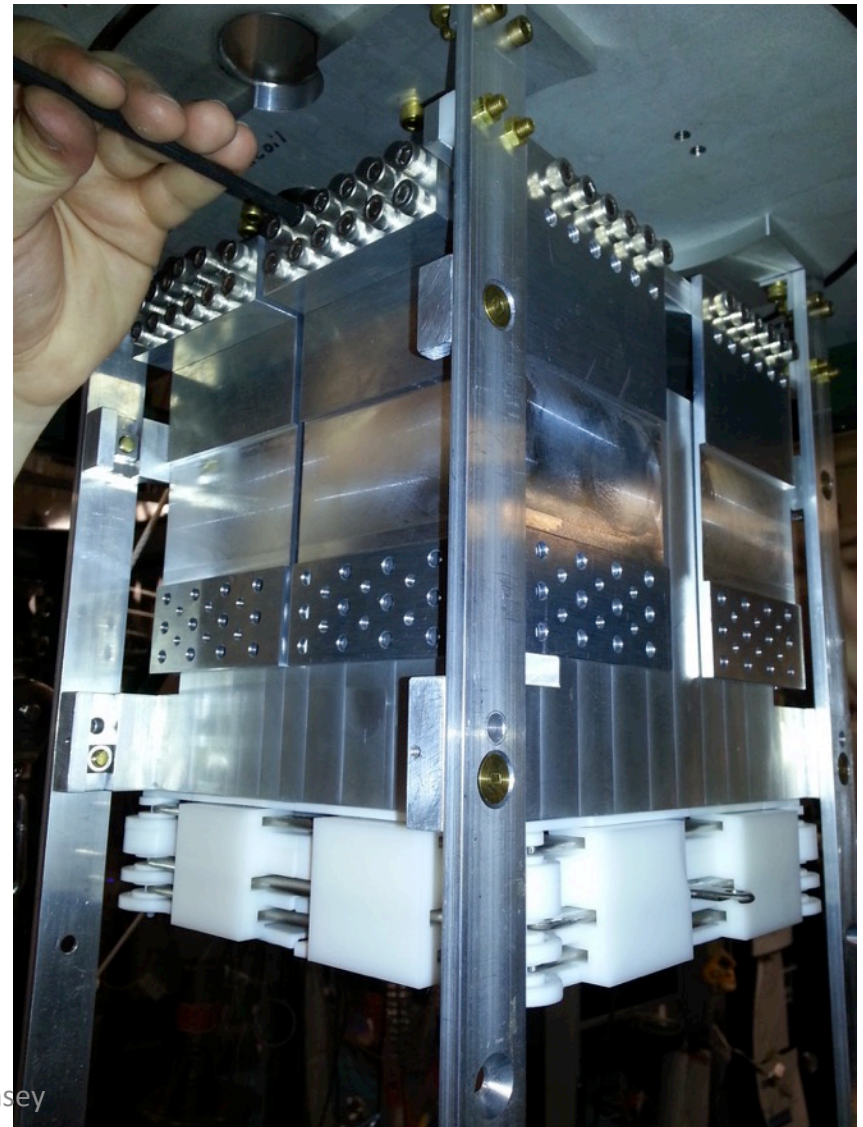
10/12/16

D. McKinsey

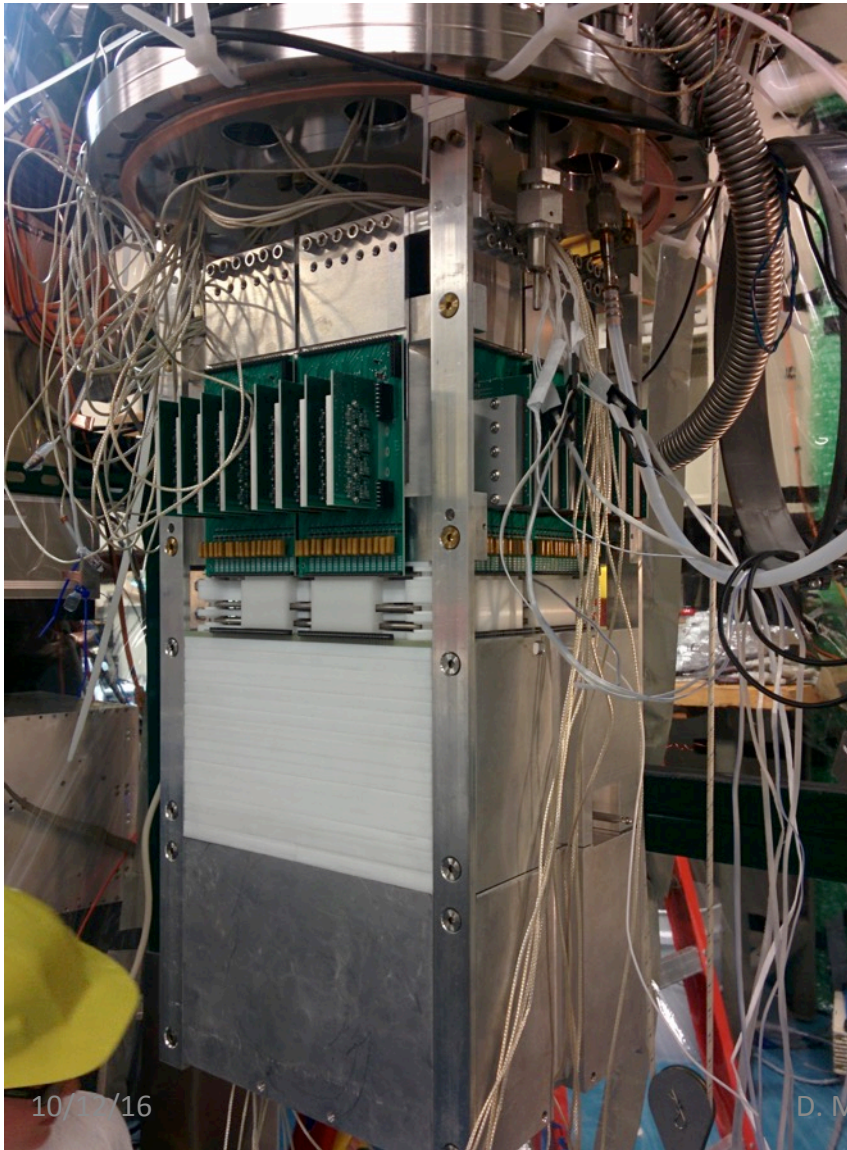
Photos of CoDeX Construction



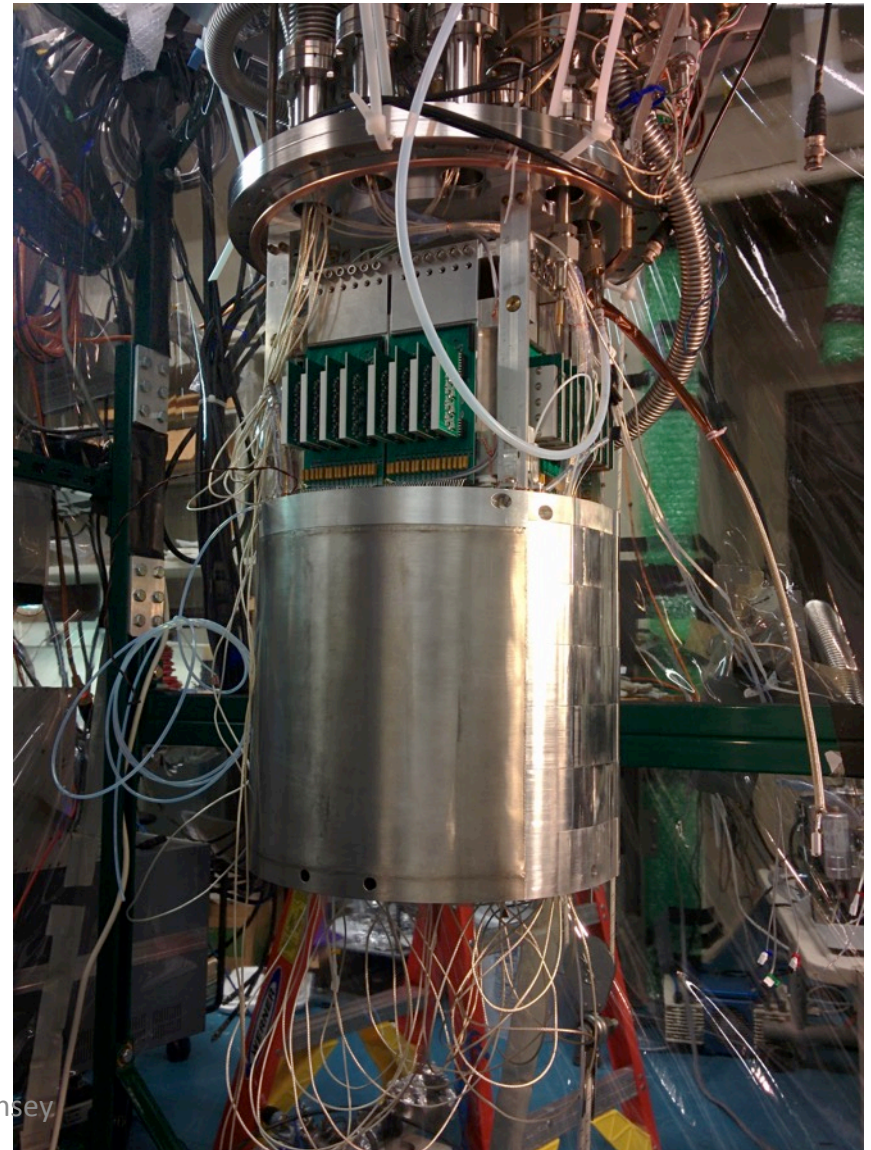
D. McKinsey



Photos of CoDeX Construction

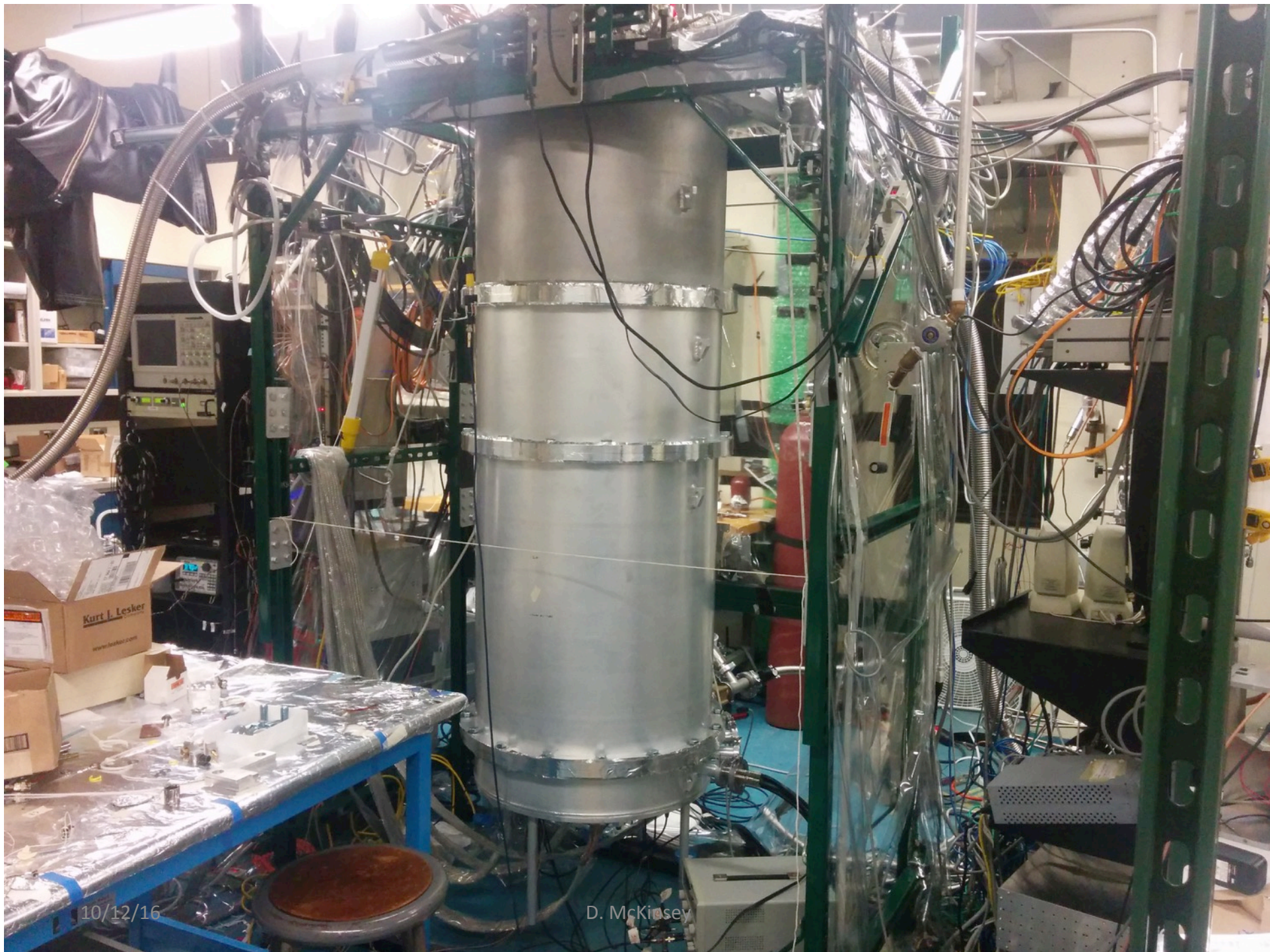


D. McKinsey



Photos of CoDeX Construction





10/12/16

D. McKinsey

CoDeX Current Status

- Initial successful cool-down in December 2015 at Yale University
- First xenon fill at the beginning of January 2016
- Stable operation through mid March 2016
- Warmed up while wire grid problems were addressed
- Second xenon fill May 2016
- Operation through end of May 2016
- PMT and wire grid data taken during second run:
 - Background data
 - Cs137 source in two positions ~30 cm from detector
 - Na22 source in two positions ~30 cm from detector
- Detector transported from Yale University to University of California Berkeley at the beginning of June 2016
- Data analysis from initial run is ongoing
- Further operation of CoDeX detector is planned at UC Berkeley

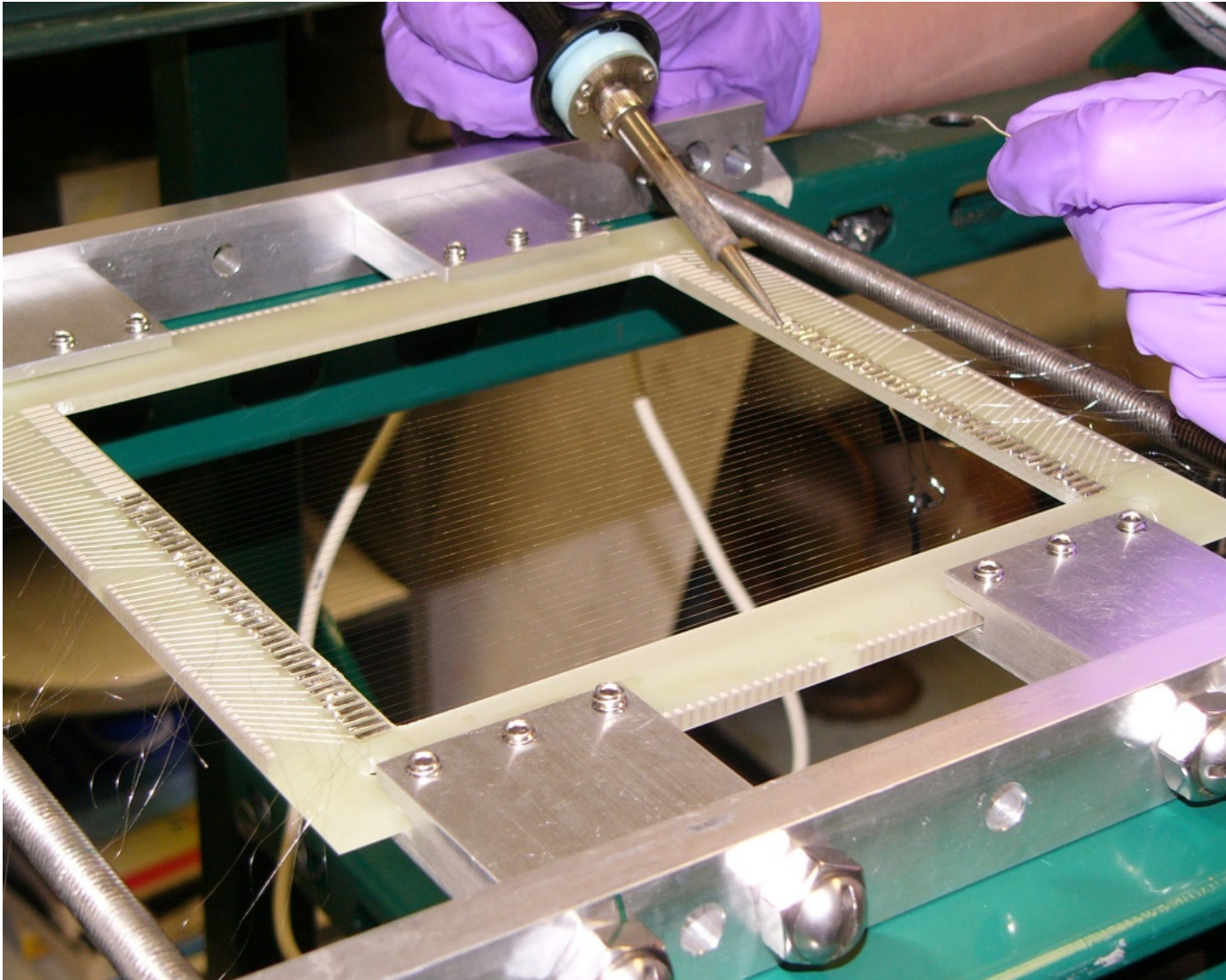
Summary

- Lots of progress on two-phase Xe technology
 - Calibration techniques
 - Quantification of charge and light yields, recombination
 - Electron recoil/nuclear recoil discrimination
 - High electric fields, breakdown
 - Light collection

.... And more progress to come!

Backup

Crossed Wire Readout: The Grids



SI WIMP-nucleon exclusion

- Brazil bands show the 1- and 2-sigma range of expected sensitivities, based on random BG-only experiments.
- **Factor of 4 improvement** over the previous LUX result in the high WIMP masses
- Minimum exclusion of $2.2 \times 10^{-46} \text{ cm}^2$ at 50 GeV

